Recent progress in bound-state QED: from light elements to super-heavy ones

Paul Indelicato

Mathematical models of Quantum Field Theory

Centre de Mathématiques Appliquées, École Polytechnique

décembre 2010 (Palaiseau)

Topics

- Introduction
- Principe of Bound-state QED
  - Dirac equation
  - Field operators
  - Gell-Mann and Low theorem and perturbation expansion
  - Two-time green function
  - Mixing QED and relativistic perturbation theory
  - Renormalisation
- Numerical methods
  - Exact coulomb Green function
  - Integration techniques
- Recent experimental results
- The hydrogen/muonic hydrogen puzzle
- Super-Heavy elements
- Conclusion

What do we want to know?

- One-electron QED corrections
  - One electron ions: nl→1s transitions are the most sensitive
  - Two-loop effects checked only in light elements and lithium-like systems
- Two-electron QED corrections
  - Much more difficult to evaluate (same as one-electron, plus two-electron correlation and combined QED-correlation)
  - Most advanced on the experimental and theoretical side are three-electron ions (Storage rings, dielectronic resonance, free electron lasers…)
  - Helium fine structure is now better understood

LKB

Non-perturbative bound-states QED

Principles

Starting point

Dirac Equation

Relativistic Wave Equation for one Fermion in an electro-magnetic potential $(\phi, \vec{A})$:

$$i\hbar\frac{\partial}{\partial t}\psi = [c\vec{\alpha}(\vec{p} - q\vec{A}) + q\phi + \beta mc^2]\psi$$

where

$$\beta = \begin{pmatrix} I & 0 \\ 0 & -I \end{pmatrix}, \quad \vec{\alpha} = \begin{pmatrix} 0 & \vec{\sigma} \\ \vec{\sigma} & 0 \end{pmatrix}$$

are called Dirac matrices.

They obey anti-commutation relations

$$\beta\alpha^i + \alpha^i\beta = 0, \quad \beta^2 = 1, \quad \alpha^i\alpha^j + \alpha^j\alpha^i = -2\delta_{ij}$$

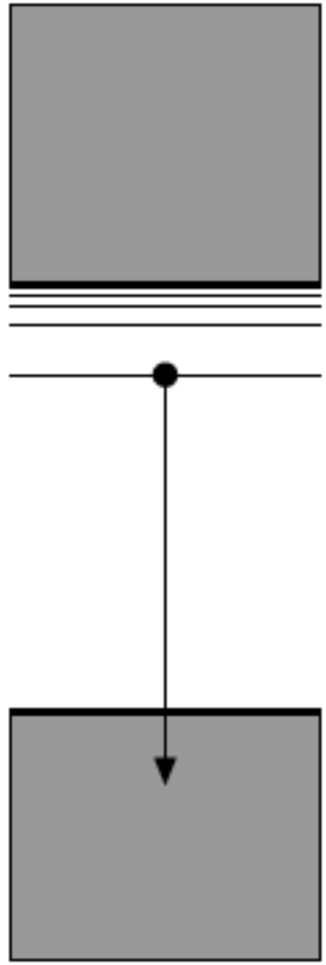

Fields operators (second quantization)

$$\psi(x) \;=\; \sum_{E_n>0} a_n e^{-iE_n t}\phi_n(\vec{x}) + \sum_{E_m<0} b_m^\dagger e^{iE_n t}\phi_m(\vec{x})$$

- ϕ_n are solutions of the Dirac equation $h_0\phi_n = E_n\phi_n$
- a_n is the electron annihilation operator for an electron in state n $(E_n > 0)$
- $b_n^\dagger$ is the positron creation operator for a positron in state m $(E_m < 0)$
- Because we are dealing with fermions, these operators anti-commute $\{a_n, a_m^\dagger\} = \delta_{nm}$; $\{a_n, a_m\} = 0, \ldots$
- An unperturbed state is obtained by having a creation operator acting on the vacuum: $|n\rangle = a_n^\dagger |0\rangle$ while annihilation operators destroy the vacuum: $a_n |0\rangle = 0$

S-matrix theory

Perturbation potential switched off at $t = \pm\infty$.

$$V_{\epsilon,g} = gH_I e^{-\epsilon|t|},$$

and

$$H_I = j^\mu A_\mu - \delta M(x),$$

- $j^\mu = -e\bar{\psi}(x)\gamma^\mu\psi(x)$ is the 4-current
- $\delta M(x) = \delta m\bar{\psi}(x)\psi(x)$ is the mass counter-term
- A_μ is the photon 4-vector potential

The adiabatic evolution operator transform the wave function at t_1 into one at t_2

$$U_{\epsilon,g}(t_1, t_2) = Te^{-i\int_{t_1}^{t_2} dt V_{\epsilon,g}(t)}.$$

where T is the time ordering operator.

Energy shifts

- The adiabatic S-matrix is defined as $S_{\epsilon,g} = \lim_{t\to\infty} U_{\epsilon,g}(-t,t)$
- The energy shift is given by the Gell-Mann and Low theorem

$$\Delta E_{N_p} = \lim_{\substack{\epsilon\to 0\\ g\to 1}} \frac{i\epsilon g}{2}\frac{\partial}{\partial g} \log \langle N_p;0|\, S_{\epsilon,g}\, |N_p;0\rangle$$

for a p-electron state with no real photons

- the logarithmic derivative diverges as $1/\epsilon$ as do the norm of the exact wave function
- Gell-Mann and Low say that the energy shift is still well defined

Perturbation theory

The S-matrix can be expanded in power of g.

$$g\frac{\partial}{\partial g}\log\langle S_{\epsilon,g}\rangle\Big|_{g=1} = \frac{\left\langle S^{(1)}_{\epsilon,1}\right\rangle + 2\left\langle S^{(2)}_{\epsilon,1}\right\rangle + 3\left\langle S^{(3)}_{\epsilon,1}\right\rangle + \cdots}{1 + \left\langle S^{(1)}_{\epsilon,1}\right\rangle + \left\langle S^{(2)}_{\epsilon,1}\right\rangle + \left\langle S^{(3)}_{\epsilon,1}\right\rangle + \cdots}$$

$$= \left\langle S^{(1)}_{\epsilon,1}\right\rangle + 2\left\langle S^{(2)}_{\epsilon,1}\right\rangle - \left\langle S^{(1)}_{\epsilon,1}\right\rangle^2 + 3\left\langle S^{(3)}_{\epsilon,1}\right\rangle - 3\left\langle S^{(1)}_{\epsilon,1}\right\rangle\left\langle S^{(2)}_{\epsilon,1}\right\rangle + \left\langle S^{(1)}_{\epsilon,1}\right\rangle^3$$
$$+ 4\left\langle S^{(4)}_{\epsilon,1}\right\rangle - 4\left\langle S^{(1)}_{\epsilon,1}\right\rangle\left\langle S^{(3)}_{\epsilon,1}\right\rangle - 2\left\langle S^{(2)}_{\epsilon,1}\right\rangle^2 + 4\left\langle S^{(1)}_{\epsilon,1}\right\rangle^2\left\langle S^{(2)}_{\epsilon,1}\right\rangle - \left\langle S^{(1)}_{\epsilon,1}\right\rangle^4$$

where

$$\begin{aligned}\left\langle S^{(j)}_{\epsilon,1}\right\rangle &= \langle N_p;0|\, S^{(j)}_{\epsilon,1}\, |N_p;0\rangle \\ \langle S_{\epsilon,g}\rangle &= \langle N_p;0|\, S_{\epsilon,g}\, |N_p;0\rangle\end{aligned}$$

Perturbation theory 2

From the definition of the S-matrix and of the evolution operator one obtains

$$S^{(j)}_{\epsilon,g} = \frac{(-ig)^j}{j!} \int d^4x_j \ldots \int d^4x_1 e^{-\epsilon|t_j|} \ldots e^{-\epsilon|t_1|} T\left[H_I(x_j)\ldots H_I(x_1)\right]$$

Using Wick's theorem it is possible to re-express all contributions in term of Vacuum expectation values

$$\begin{aligned}
T\left[\psi(x)\psi(y)\right] &= :\psi(x)\psi(y): + \langle 0| T\left[\psi(x)\psi(y)\right]|0\rangle =: \psi(x)\psi(y):, \\
T\left[\bar{\psi}(x)\bar{\psi}(y)\right] &= :\bar{\psi}(x)\bar{\psi}(y): + \langle 0| T\left[\bar{\psi}(x)\bar{\psi}(y)\right]|0\rangle =: \bar{\psi}(x)\bar{\psi}(y):, \\
T\left[\psi(x)\bar{\psi}(y)\right] &= :\psi(x)\bar{\psi}(y): + \langle 0| T\left[\psi(x)\bar{\psi}(y)\right]|0\rangle, \\
T\left[\bar{\psi}(x)\psi(y)\right] &= :\bar{\psi}(x)\psi(y): + \langle 0| T\left[\bar{\psi}(x) r\psi(y)\right]|0\rangle.
\end{aligned}$$

The propagator is expressed in term of vacuum expectation value of $T\left[\psi(x)\bar{\psi}(y)\right]$ as

$$S_F(x,y) = \langle 0| T\left[\psi(x)\bar{\psi}(y)\right]|0\rangle$$

QED at order α and α^2

Self Energy

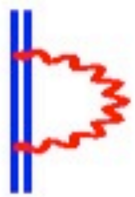

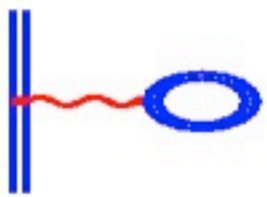

Vacuum Polarization

H-like "One Photon" order (α/π)

QED at order α and α^2

Self Energy

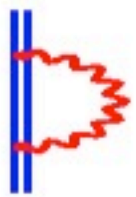

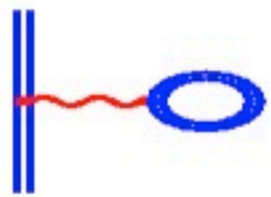

Vacuum Polarization

H-like "One Photon" order (α/π)

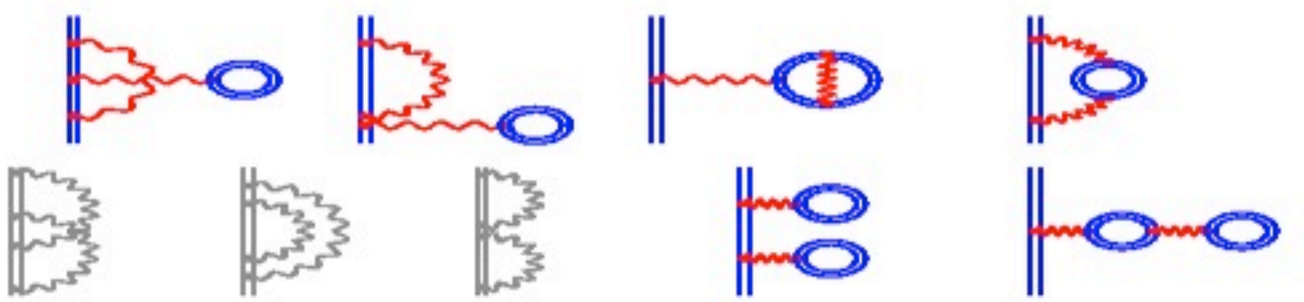

H-like "Two Photon" order $(\alpha/\pi)^2$

QED at order α and α^2

Self Energy

Vacuum Polarization

H-like "One Photon" order (α/π)

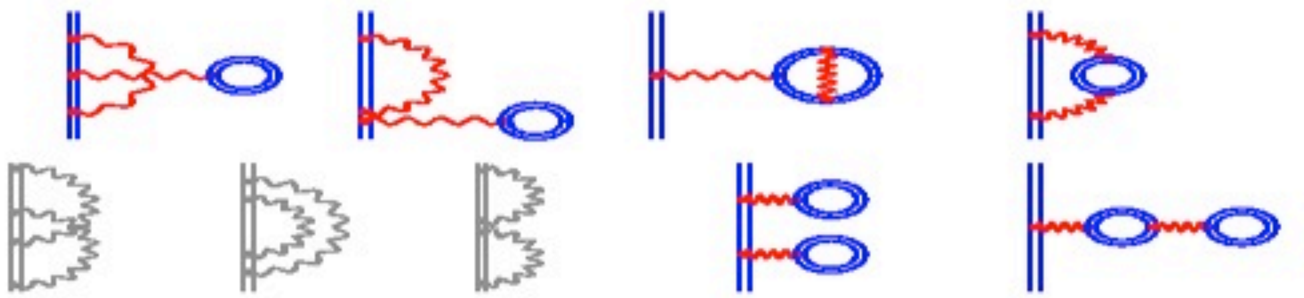

H-like "Two Photon" order $(\alpha/\pi)^2$

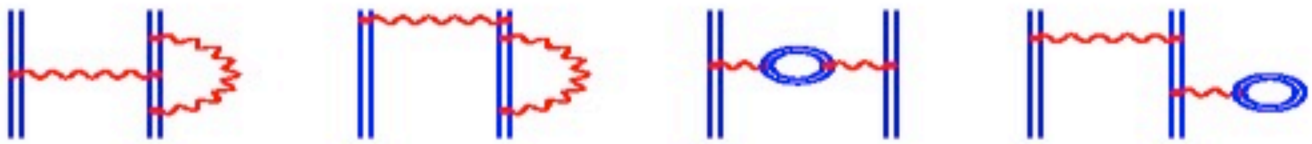

"Screening " order α^2

Alternative methods: two-times Green function

The two-time Green's function method

Almost degenerate states

Almost-degenerate states of "bound-state QED" (e.g., $2s - 2p_{1/2}$ and $2s - 2p_{3/2}$, separated by an energy of order $(Z\alpha)^4$) can be handled by the two-time Green's function method.[1] There is only one other method that works for this case and that we are aware of. [Lindgren]

Effective hamiltonian We construct a finite-sized effective hamiltonian on the set of almost-degenerate states. The effective hamiltonian includes in principle all the QED effects exactly. The effective hamiltonian is built from Green's functions (= propagators = correlation functions):

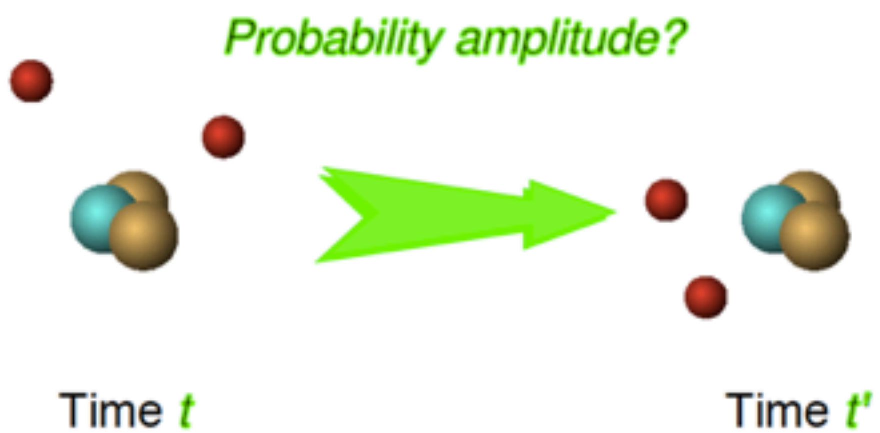

[1] V. M. Shabaev and I. G. Fokeeva, Phys. Rev. A **49**, 4489 (1994).

Alternative methods: two-times Green function

How to find the position of the poles for an isolated level

Useful mathematical identity. . .

If $g(E)$ has a single pole at E_0, then we can recover the position of the pole from g itself:

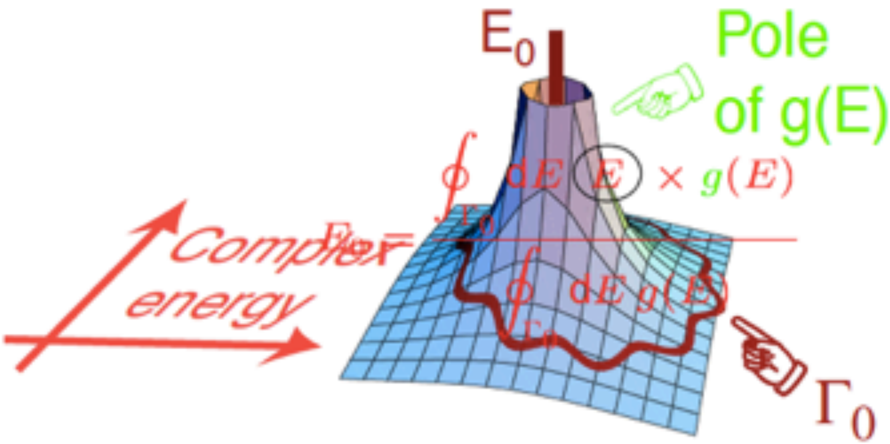

$$E_0 = \frac{\oint_{\Gamma_0} \mathrm{d}E \; E \times g(E)}{\oint_{\Gamma_0} \mathrm{d}E \; g(E)}$$

. . . generalized to almost-degenerate levels

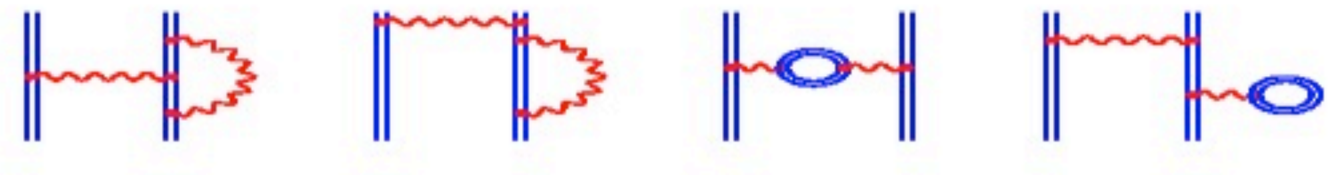

"Screening of S.E. and V. P."

Many body effects in QED

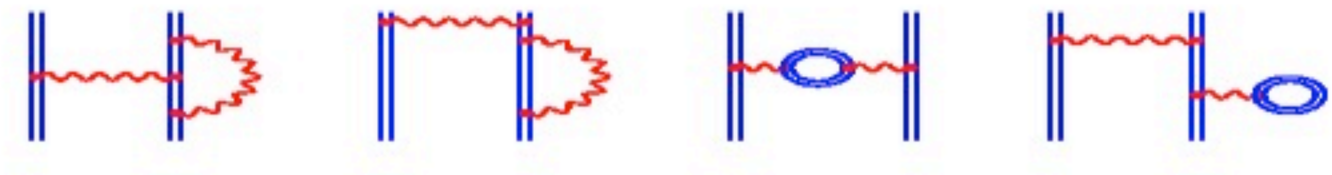

“Screening of S.E. and V. P.”

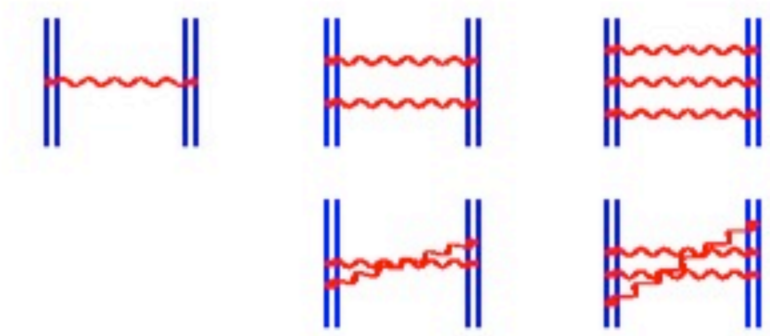

➔RMBPT or MCDF (1/Z expansion!)

➔Non Radiative QED (no Hamiltonian or potential form!)

Non Radiative QED (QED correction to correlation and projection operators…)

Auger shift for auto-ionizing states

Feynman diagrams

- Each contribution to the S-matrix can be decomposed in Feynman diagrams.

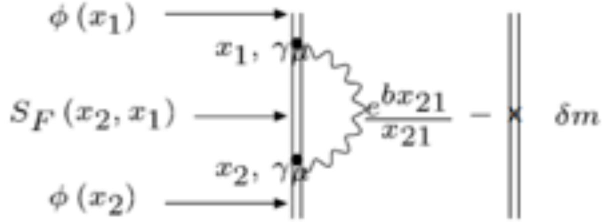

Signification of the Feynman diagrams for self-energy.

The Energy shift is given by

$$\Delta E_n = \frac{\alpha}{2\pi i}\int_C dz \int d\vec{x}_2 \int d\vec{x}_1 \phi_n^\dagger(\vec{x}_2)\alpha_\mu G(\vec{x}_2, \vec{x}_1, z)\alpha^\mu \phi_n(\vec{x}_1)\frac{e^{-bx_{21}}}{x_{21}} - \delta m \int d\vec{x}\, \phi_n^\dagger(\vec{x})\beta\phi_n(\vec{x}),$$

where $b = -i\left[(E_n - z)^2\right]^{1/2}$, $\mathrm{Re}(b) > 0$, and $\vec{x}_{21} = \vec{x}_2 - \vec{x}_1$ The photon propagator $\frac{1}{x_{21}} \times e^{-bx_{21}}$ is just the Coulomb potential with a retardation term (speed of light is finite!)

All orders vs perturbation

- Until 1974, expansion of the propagator was the rule

$$E_{\mathrm{SE}}^{(2)} = \frac{\alpha}{\pi}\frac{(Z\alpha)^4}{n^3}F(Z\alpha)m_{\mathrm{e}}c^2, \tag{19}$$

where

$$\begin{aligned} F(Z\alpha) = {} & A_{41}\ln(Z\alpha)^{-2} + A_{40} + A_{50}(Z\alpha) \\ & + A_{62}(Z\alpha)^2\ln^2(Z\alpha)^{-2} + A_{61}(Z\alpha)^2\ln(Z\alpha)^{-2} \\ & + G_{\mathrm{SE}}(Z\alpha)(Z\alpha)^2. \end{aligned} \tag{20}$$

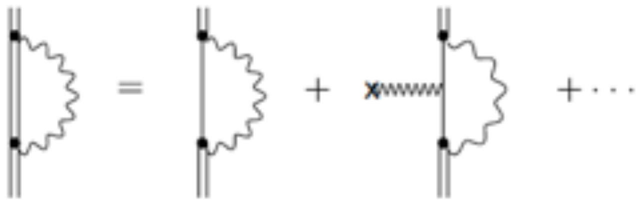

All orders vs perturbation

- Does not work at high-Z

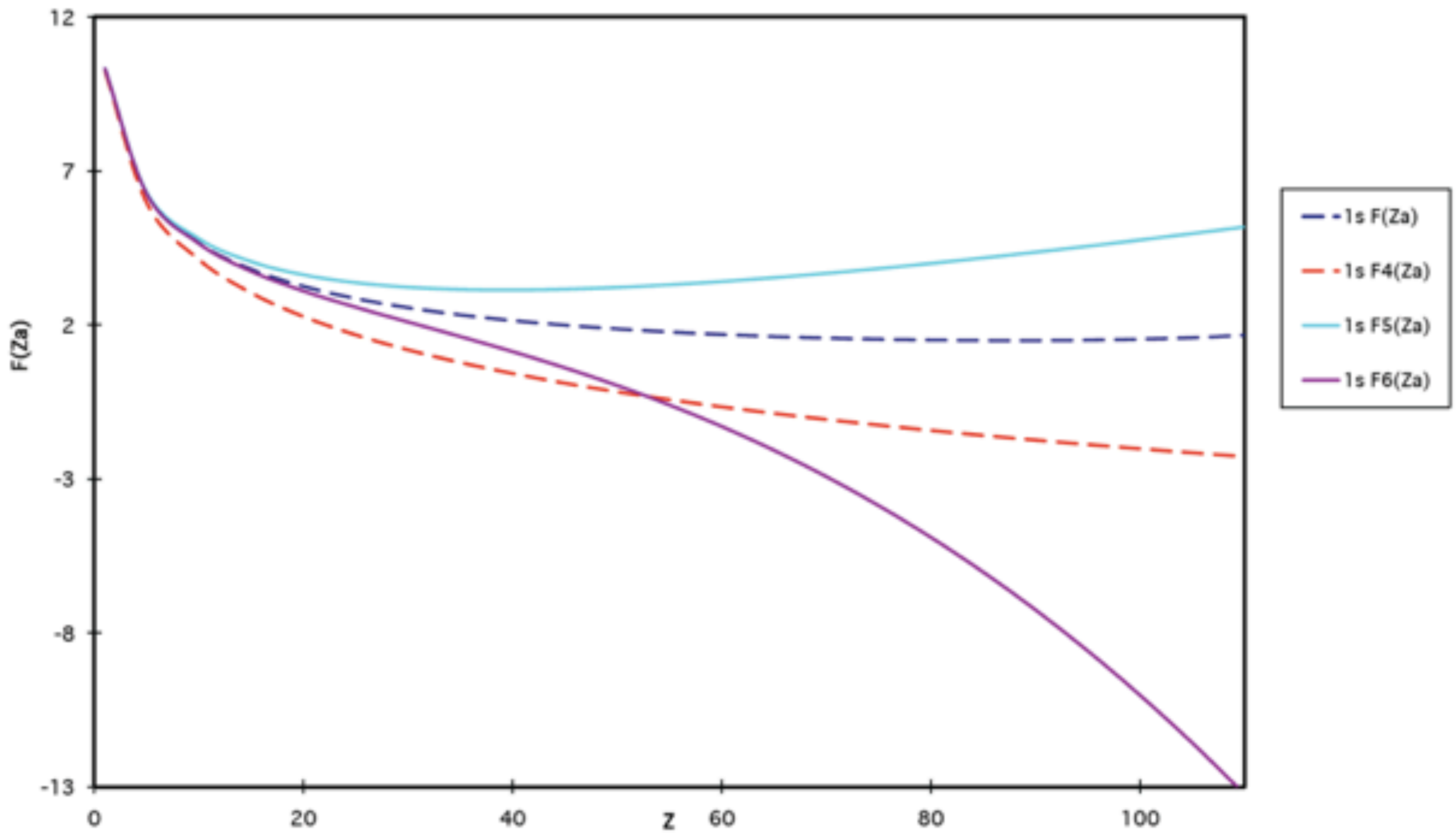

LKB

Non-perturbative bound-states QED

Practical calculations and numerical methods

Singularities

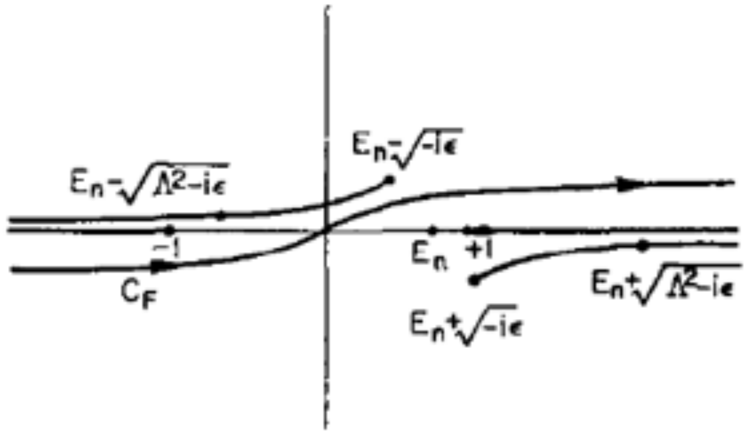

FIG. 3. The contour C_F and the singularities of the integrand in the complex z-plane. The points to the left of $z = +1$ represent the bound-state poles; E_n is the ground-state energy in this diagram.

Singularities

Singularities

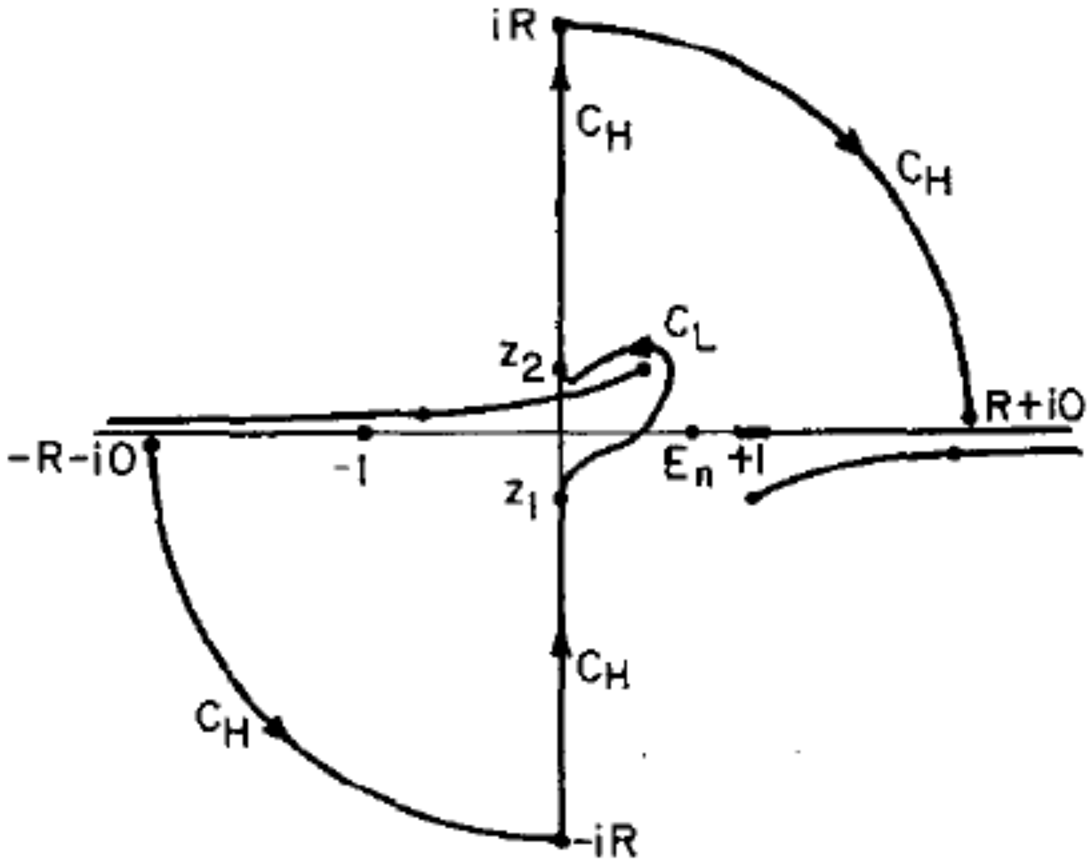

FIG. 4. The new contour in the complex z-plane

Singularities

Singularities

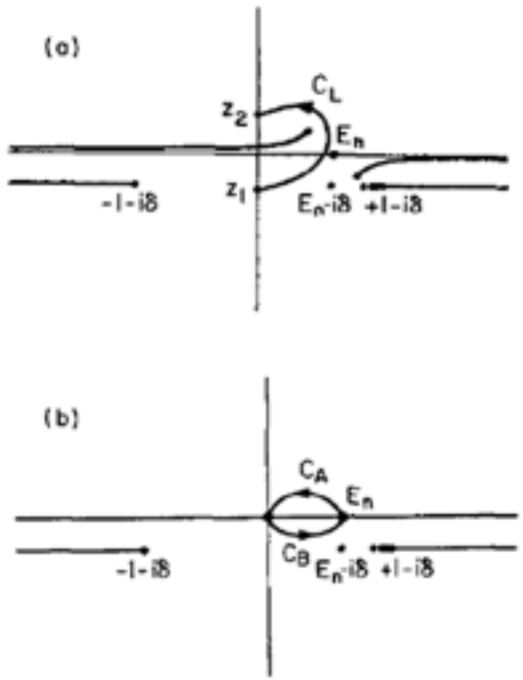

FIG. 5. The complex z-plane with the singularities of the integrand in Eq. (3.2). In the upper diagram, the branch points of b are at $E_n \pm (-i\epsilon)^{1/2}$. As $\epsilon \to 0+$, the branch points meet at E_n. In the lower diagram, the cuts, which are drawn to insure $\mathrm{Re}(b) > 0$, meet at E_n and extend along the real z-axis. In this diagram $z_1 = z_2 = 0$.

Principles of the calculation

ΔE_{SE} is decomposed in a sum $\Delta E_L + \Delta E_H$

$$\Delta E_L = \frac{\alpha}{\pi} E_n - \frac{\alpha}{\pi} P \int_0^{E_n} dz \int d\vec{x}_2 \int d\vec{x}_1 \phi_n^\dagger(\vec{x}_2) \alpha^l G(\vec{x}_2, \vec{x}_1, z) \alpha^m$$

$$\times \phi_n(\vec{x}_1)(\delta_{lm} \vec{\nabla}_2 \cdot \vec{\nabla}_1 - \nabla_2^l \nabla_1^m) \frac{\sin[(E_n - z)x_{21}]}{(E_n - z)^2 x_{21}}$$

and

$$\Delta E_H = \frac{\alpha}{2\pi i} \int_{C_H} dz \int d\vec{x}_2 \int d\vec{x}_1 \phi_n^\dagger(\vec{x}_2) \alpha_\mu G(\vec{x}_2, \vec{x}_1, z) \alpha^\mu \phi_n(\vec{x}_1) \frac{e^{-bx_{21}}}{x_{21}}$$

$$- \delta m \int d\vec{x} \phi_n^\dagger(\vec{x}) \beta \phi_n(\vec{x})$$

Principles of the calculation

ΔE_{SE} is decomposed in a sum $\Delta E_L + \Delta E_H$

$$\Delta E_L = \frac{\alpha}{\pi} E_n - \frac{\alpha}{\pi} P \int_0^{E_n} dz \int d\vec{x}_2 \int d\vec{x}_1 \phi_n^\dagger(\vec{x}_2) \alpha^l G(\vec{x}_2, \vec{x}_1, z) \alpha^m$$

$$\times \phi_n(\vec{x}_1) (\delta_{lm} \vec{\nabla}_2 \cdot \vec{\nabla}_1 - \nabla_2^l \nabla_1^m) \frac{\sin[(E_n - z) x_{21}]}{(E_n - z)^2 x_{21}}$$

and

No IR divergence if in Coulomb gauge

$$\Delta E_H = \frac{\alpha}{2\pi i} \int_{C_H} dz \int d\vec{x}_2 \int d\vec{x}_1 \phi_n^\dagger(\vec{x}_2) \alpha_\mu G(\vec{x}_2, \vec{x}_1, z) \alpha^\mu \phi_n(\vec{x}_1) \frac{e^{-b x_{21}}}{x_{21}}$$

$$- \delta m \int d\vec{x} \phi_n^\dagger(\vec{x}) \beta \phi_n(\vec{x})$$

Spherical symmetry

$$\phi_n(x) = \begin{bmatrix} f_{n,1}(x)\chi_\kappa^\mu(\hat{x}) \\ i f_{n,2}(x)\chi_{-\kappa}^\mu(\hat{x}) \end{bmatrix},$$

Eigenstate of J^2, J_z and parity

$$\chi_\kappa{}^\mu(\hat{x}) = \begin{bmatrix} -\frac{\kappa}{|\kappa|}\left[\frac{\kappa+\frac{1}{2}-\mu}{2\kappa+1}\right]^{1/2} Y^{\mu-(1/2)}_{|\kappa+(1/2)|-(1/2)}(\hat{x}) \\ \left[\frac{\kappa+\frac{1}{2}+\mu}{2\kappa+1}\right]^{1/2} Y^{\mu+(1/2)}_{|\kappa+(1/2)|-(1/2)}(\hat{x}) \end{bmatrix}$$

$$G(\mathbf{x}_2, \mathbf{x}_1, z) = \sum_\kappa \begin{bmatrix} G_\kappa^{11}(x_2, x_1, z)\, \pi_\kappa(\hat{x}_2, \hat{x}_1) & G_\kappa^{12}(x_2, x_1, z)\, i\boldsymbol{\sigma}\cdot\hat{x}_2\pi_{-\kappa}(\hat{x}_2, \hat{x}_1) \\ -G_\kappa^{21}(x_2, x_1, z)\, i\boldsymbol{\sigma}\cdot\hat{x}_2\pi_\kappa(\hat{x}_2, \hat{x}_1) & G_\kappa^{22}(x_2, x_1, z)\, \pi_{-\kappa}(\hat{x}_2, \hat{x}_1) \end{bmatrix}.$$

$$\pi_\kappa(\hat{x}_2, \hat{x}_1) = \sum_\mu \chi_\kappa{}^\mu(\hat{x}_2)\, \chi_\kappa^{\mu\dagger}(\hat{x}_1)$$
$$= (|\kappa|/4\pi)\{I P_{|\kappa+(1/2)|-(1/2)}(\xi) + (1/\kappa)\, i\boldsymbol{\sigma}\cdot(\hat{x}_2\times\hat{x}_1)\, P'_{|\kappa+(1/2)|-(1/2)}(\xi)\}, \tag{A.6}$$

Integrations

Very excited states... Many poles on the real axis...

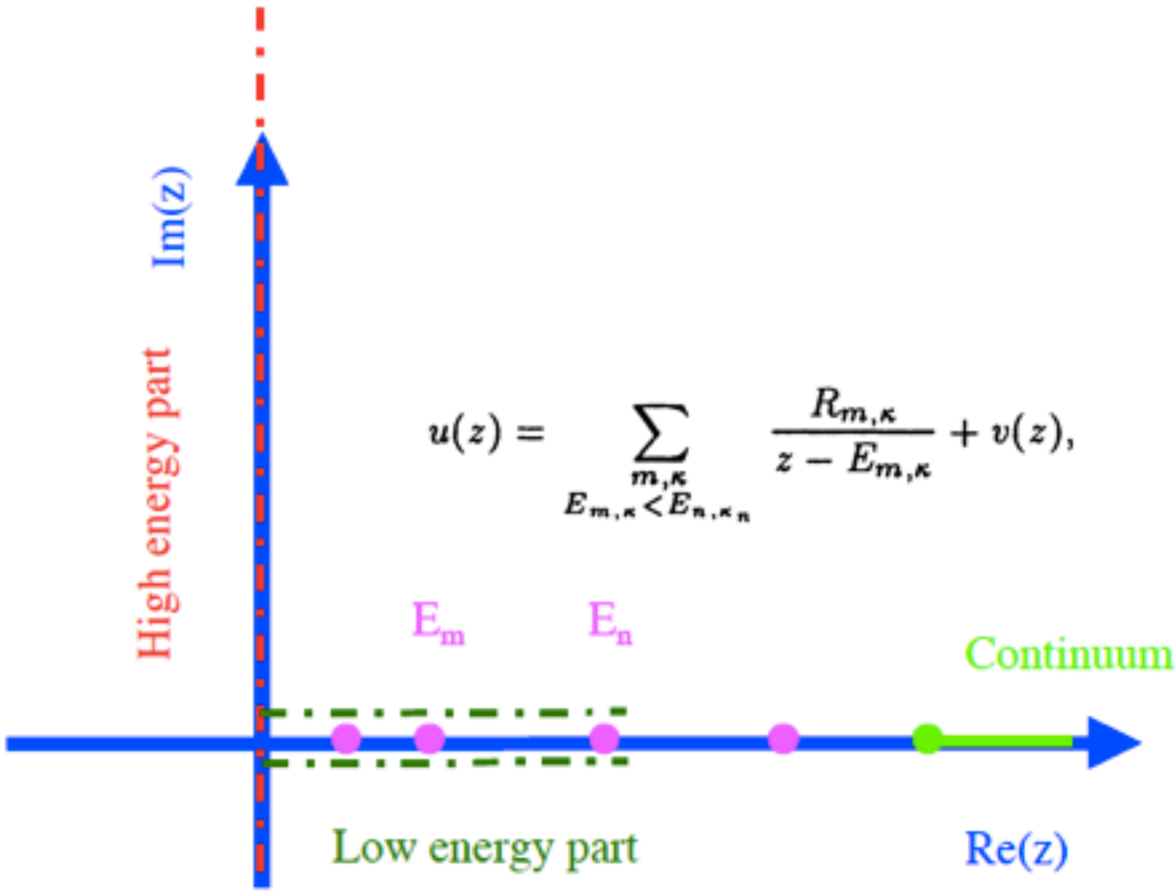

$$u(z)=\sum_{\substack{m,\kappa\\ E_{m,\kappa}<E_{n,\kappa_n}}}\frac{R_{m,\kappa}}{z-E_{m,\kappa}}+v(z),$$

$$\bar{u}(z)=u(z)+\sum_{\substack{m,\kappa\\ E_{m,\kappa}<E_{n,\kappa_n}}}R_{m,\kappa}\left[\frac{1}{E_{n,\kappa_n}}\ln\left(\frac{E_{n,\kappa_n}-E_{m,\kappa}}{E_{m,\kappa}}\right)-\frac{1}{z-E_{m,\kappa}}\right]$$

Ultraviolet divergences

- Although the integration over z in ΔE_H is exponentially damped at large $|z|$ when $x_{21} \neq 0$, the unregulated integral is infinite, because the point $x_{21} = 0$ is included in the range of the coordinate-space integration.
- $x_{21} \to 0$ (short distance) is equivalent to large energy in momentum space. We do an expansion around $x_{21} \to 0$
  - of the Green's function (in term of the free Green's function F)

$$G(\vec{x}_2, \vec{x}_1, z) = F(\vec{x}_2, \vec{x}_1, z) - \int d\vec{x}_3 F(\vec{x}_2, \vec{x}_3, z) V(\vec{x}_3) F(\vec{x}_3, \vec{x}_1, z) + \cdots$$

  - of the potential $V(\vec{x}_3) = V(\vec{x}_2) + \cdots$
  - of the wave function

$$\phi_n(\vec{x}_1) \quad = \quad \phi_n(\vec{x}_2) + (\vec{x}_1 - \vec{x}_2) \cdot \vec{\nabla}_2\, \phi_n(\vec{x}_2) + \cdots$$

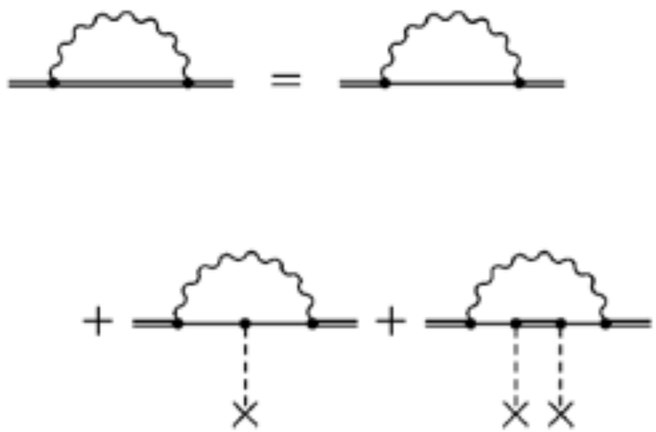

Ultraviolet divergences 2

The free Green's function is itself divergent:

$$F(\vec{x}_2, \vec{x}_1, z) = \left[\left(\frac{c}{x_{21}} + \frac{1}{x_{21}^2}\right) i\vec{\alpha}\cdot\vec{x}_{21} + \beta + z\right] \frac{e^{-cx_{21}}}{4\pi x_{21}}$$

with $c = (1 - z^2)^{1/2}$, $\mathrm{Re}(c) > 0$.

The expansion gives for example $\Delta E_H = \Delta E_H^{(0,0)} + \Delta E_H^{(0,1)} + \Delta E_H^{(1,0)} + \cdots$ with

$$\begin{aligned} \Delta E_H^{(0,0)} &= \frac{\alpha}{2\pi i}\int_{C_H} dz \int d\vec{x}_2 \int d\vec{x}_1\, \phi_n^\dagger(\vec{x}_2)\alpha_\mu F(\vec{x}_2, \vec{x}_1, z)\alpha^\mu \\ &\quad \times \phi_n(\vec{x}_2)\frac{e^{-bx_{21}}}{x_{21}} \\ &= \frac{\alpha}{\pi i}\int_{C_H} dz\ \langle 2\beta - z\rangle \left(\frac{1}{b+c}\right) \end{aligned}$$

$z = iu$. $b \to u$ and $c \to u$ when $u \to \infty$ so integral is logarithmically divergent (first term) or linearly divergent (second term)

Regularization

This integral must then be regularized to have a meaning (i.e., being finite (Pauli-Villars)).

The photon propagator $\frac{e^{-bx_{21}}}{x_{21}}$ is replaced everywhere by

$$\frac{e^{-bx_{21}}}{x_{21}} - \frac{e^{-b'x_{21}}}{x_{21}}$$

with $b = -i\left[(E_n - z)^2 + i\delta\right]^{1/2}$, $\mathrm{Re}(b) > 0$ and
$b' = -i\left[(E_n - z)^2 - \Lambda^2 + i\delta\right]^{1/2}$; $\mathrm{Re}(b') > 0$. $b' \approx \Lambda$ when $\Lambda \to \infty$, and thus we get a Yukawa potential for a particle of mass Λ.

This is can also be understood in momentum space:

$$\frac{1}{q^2 + i\delta} \to \frac{1}{q^2 + i\delta} - \frac{1}{q^2 - \Lambda^2 + i\delta}$$

We add a massive photon, the mass of which $\Lambda \to \infty$ at the end (An infinitely massive photon won't propagate).

Effect of the regularization

The first term gives:

$$\Delta E_H^{(0,0)} = \frac{\alpha}{\pi i}\int_{C_H} dz\ \langle 2\beta - z\rangle \left(\frac{1}{b+c} - \frac{1}{b'+c}\right)$$

$$= \frac{\alpha}{\pi}\Bigg\{ \langle\beta\rangle \left[\ln(\Lambda^2) - 1 + \frac{1-E_n^2}{E_n^2}\ln\left(1+E_n^2\right)\right]$$

$$-E_n\left[\frac{1}{4}\ln(\Lambda^2) + \frac{3E_n^2-2}{8E_n^2} + \frac{1-E_n^4}{4E_n^4}\ln\left(1+E_n^2\right)\right]$$

$$+\mathcal{O}(\frac{1}{\Lambda})\Bigg\}$$

The result is still logarithmically divergent in Λ!

Renormalization

In the perturbation Hamiltonian we had an extra term (called a counter-term) $H_I = j^\mu A_\mu - \delta M(x)$, If we do all calculations for ΔE_H we get

$$\begin{aligned}\Delta E_H &= \frac{\alpha}{\pi}\Big[-\frac{5}{6}E_n - \left(\frac{2}{3}+\frac{3}{8}\right)\langle\beta\rangle - \frac{7}{6}\langle V\rangle + \frac{(Z\alpha)^4}{n^3}f_H(Z\alpha)\\ &+\langle\beta\rangle\ln(\Lambda^2) - E_n\frac{1}{4}\ln(\Lambda^2)\\ &+\langle\vec{\alpha}\cdot\vec{p}\,\rangle\frac{1}{4}\ln(\Lambda^2)\\ &+\langle V\rangle\frac{1}{4}\ln(\Lambda^2) + \mathcal{O}(\frac{1}{\Lambda})\Big] - \langle\delta M\rangle\end{aligned}$$

but remember Dirac equation is $\langle\vec{\alpha}\cdot\vec{p}+\beta+V-E_n\rangle = 0$!!

If we take $\delta M(x) = \frac{\alpha}{\pi}\left(\frac{3}{4}\ln(\Lambda^2)+\frac{3}{8}\right)\phi^\dagger(x)\beta\phi(x)$ the self-energy is finite.

The **miracle** is that all other diagrams containing self-energy loops will be finite to all orders of the theory.

The $\frac{3}{8}$ is included so that the mass of a free electron (when $Z\to 0$) is not changed by self-energy

Orders of magnitude

Self-energy is of order αmc^2

$$\Delta E_{\mathrm{SE}} = \Delta E_L + \Delta E_H .\qquad \Delta E_L = \frac{\alpha}{\pi}\left[\frac{3}{2}E_n + \frac{7}{6}\langle V\rangle + \frac{(Z\alpha)^4}{n^3} f_L(Z\alpha)\right].$$

$$\Delta E_H = \Delta E_{HA} + \Delta E_{HB} \qquad \Delta E_{HA} = \frac{\alpha}{\pi}\left[-\frac{3}{2}E_n - \frac{7}{6}\langle V\rangle + \frac{(Z\alpha)^4}{n^3} f_{HA}(Z\alpha)\right]$$

$$\Delta E_{HB} = \Delta E_H - \Delta E_{HA} = \frac{\alpha}{2\pi i}\int_{C_H} dz \int_0^\infty dx_2\, x_2^2 \int_0^\infty dx_1 x_1^2 \times\left\{\sum_{|\kappa|=1}^{\infty} K_\kappa(x_2,x_1,z) - K_A(x_2,x_1,z)\right\}, \qquad (12)$$

At Z=1 one looses $(\alpha Z)^4 = 2.8\times10^{-9}$ i.e., 9 digits of numerical accuracy

High energy remainder

Very slow convergence for the sum over κ

$$\Delta E_{\mathrm{HB}} = \frac{\alpha}{\pi} \int_0^1 dt \int_0^1 dr \int_0^\infty dy\, S_{\mathrm{HB}}(r,y,t).$$

$$S_{\mathrm{HB}}(r,y,t) = \left(1 + \frac{1}{t^2}\right) \frac{r^2 y^5}{a^6} \sum_{|\kappa|=1}^{\infty} T_{\mathrm{HB},|\kappa|}(r,y,t).$$

$$T_{\mathrm{HB},|\kappa|} = \frac{r^{2|\kappa|}}{|\kappa|}\left[\mathrm{const} + O\left(\frac{1}{|\kappa|}\right)\right], \qquad 0<r\leq 1$$

$t_k = T_{\mathrm{HB},k+1}$ Non-linear Van Wijngaarden condensation transform:

$$\sum_{k=0}^{\infty} t_k = \sum_{j=0}^{\infty} (-1)^j \mathbf{A}_j, \qquad \mathbf{A}_j = \sum_{k=0}^{\infty} 2^k t_{2^k(j+1)-1}.$$

High energy remainder

Very slow convergence for the sum over κ

$$\Delta E_{\mathrm{HB}}=\frac{\alpha}{\pi}\int_0^1 dt\int_0^1 dr\int_0^\infty dy\, S_{\mathrm{HB}}(r,y,t).$$

$$S_{\mathrm{HB}}(r,y,t)\quad=\left(1+\frac{1}{t^2}\right)\frac{r^2y^5}{a^6}\sum_{|\kappa|=1}^{\infty}T_{\mathrm{HB},|\kappa|}(r,y,t).$$

$$T_{\mathrm{HB},|\kappa|}=\frac{r^{2|\kappa|}}{|\kappa|}\left[\mathrm{const}+O\left(\frac{1}{|\kappa|}\right)\right],$$ 0<r≤1

$t_k=T_{\mathrm{HB},k+1}$ Non-linear Van Wijngaarden condensation transform:

$$\sum_{k=0}^{\infty}t_k=\sum_{j=0}^{\infty}(-1)^j\mathbf{A}_j,\qquad \mathbf{A}_j=\sum_{k=0}^{\infty}2^k\,t_{2^k(j+1)-1}.$$

Convergence acceleration

Nonlinear sequence transformations for the acceleration of convergence and the summation of divergent series, E.J. Weniger. Computer Physics Reports **10,** 189-371 (1989).
Convergence acceleration via combined nonlinear-condensation transformations, U.D. Jentschura, P.J. Mohr, G. Soff *et al.* Computer Physics Communications **116,** 28-54 (1999).
Calculation of the Electron Self-Energy for Low Nuclear Charge, U.D. Jentschura, P.J. Mohr et G. Soff. Phys. Rev. Lett. **82,** 53-57 (1999)
Electron self-energy for the K and L shells at low nuclear charge, U.D. Jentschura, P.J. Mohr et G. Soff. Phys. Rev. A **63,** 042512 (2001).

$$\mathbf{S}_n = \sum_{j=0}^{n} (-1)^j \mathbf{A}_j \qquad \mathbf{B}_j = (-1)^j \mathbf{A}_j .$$

$$\delta_n^{(0)}(1, \mathbf{S}_0) = \frac{\displaystyle\sum_{j=0}^{n} (-1)^j \binom{n}{j} \frac{(1+j)_{n-1}}{(1+n)_{n-1}} \frac{\mathbf{S}_j}{\mathbf{B}_{j+1}}}{\displaystyle\sum_{j=0}^{n} (-1)^j \binom{n}{j} \frac{(1+j)_{n-1}}{(1+n)_{n-1}} \frac{1}{\mathbf{B}_{j+1}}},$$

All calculations of S and B must be performed in 128 bits arithmetic for Z=1–5

Two-loop self-energy

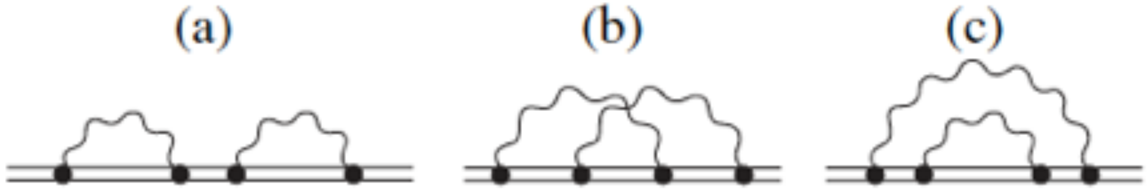

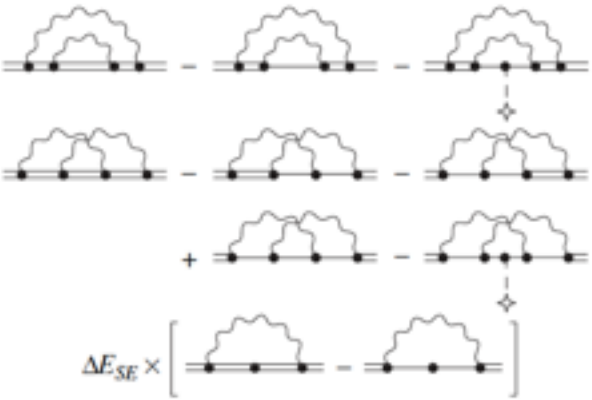

Fig. 2. Schematic view of the UV subtractions for the M term. The identity $(\partial/\partial\varepsilon)(\varepsilon - H)^{-1} = -(\varepsilon - H)^{-2}$ is used for the reducible part.

Fig. 3. Schematic view of the UV subtractions for the P term.

Two-Loop Self-Energy Correction in a Strong Coulomb Nuclear Field, V.A. Yerokhin, P. Indelicato et V.M. Shabaev. JOURNAL OF EXPERIMENTAL AND THEORETICAL PHYSICS **101,** 280–293 (2005).

Difficulties

- Renormalization very hard
- Mixed coordinate-space and momentum space Green function to evaluate numerically some renormalization contributions
- Double sums over angular momenta with slow convergence
- More numerical integrations
- cancellations

Two-loop self-energy (1s)

V. A. Yerokhin, P. Indelicato, and V. M. Shabaev, Phys. rev. A 71, 040101(R) (2005).

$$\Delta E_{\mathrm{SESE}} = m\left(\frac{\alpha}{\pi}\right)^2 (Z\alpha)^4 \{B_{40} + (Z\alpha)B_{50} + (Z\alpha)^2 \times [L^3 B_{63} + L^2 B_{62} + L B_{61} + G^{\mathrm{h.o.}}_{\mathrm{SESE}}(Z)]\},$$

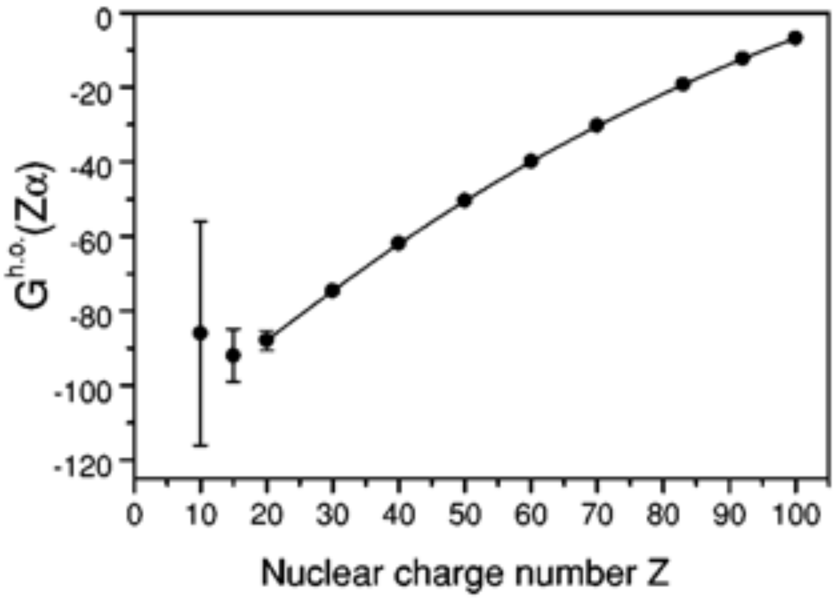

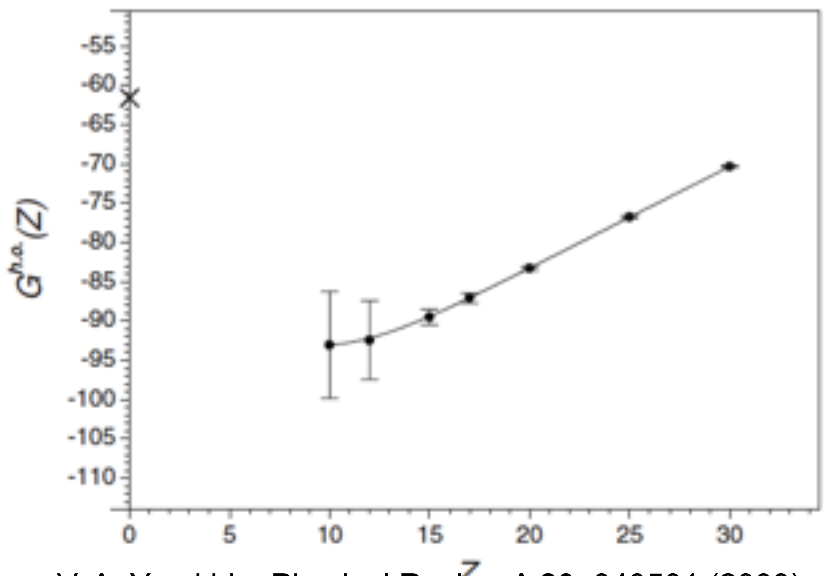

V. A. Yerokhin, Physical Review A **80**, 040501 (2009)

LKB

Evolution at low-Z

All order numerical calculations

V. A. Yerokhin, Phys. Rev. A **80**, 040501 (2009)

$$G^{\mathrm{h.o.}}_{\mathrm{SESE}}(Z=0) \equiv B_{60} = -84(15),$$

V. A. Yerokhin, P. Indelicato, and V. M. Shabaev, Phys. Rev. A 71, 040101(R) (2005).

$$-127(42)$$

Analytic calculations

$$B_{40}=1.409244, \quad B_{50}=-24.2668(31),$$

$$B_{63}=-8/27, \quad B_{62}=16/27-(16/9)\ln 2,$$

K. Pachucki and U. D. Jentschura, Phys. Rev. Lett. **91**, 113005 (4) (2003).

$$B_{60}=-61.6(9.2).$$

U. D. Jentschura, A. Czarnecki, and K. Pachucki, Physical Review A **72**, 062102 (2005).

$$B_{61}=48.388913$$

$$\delta B_{61}=-1.4494\ldots$$

Cancellation at low Z

Z	ΔE_{LAL}	ΔE_F^R	ΔE_P^R	ΔE_M	Sum
10	−0.3577	822.14(2)	−721.34(12)	−100.19(10)	0.25(16)
15	−0.4951	292.902(13)	−235.205(70)	−57.366(48)	−0.164(85)
20	−0.6015	136.911(7)	−102.026(55)	−34.764(16)	−0.481(58)
30	−0.7565	44.729(3)	−29.410(25)	−15.465(5)	−0.903(26)
40	−0.8711	19.505(3)	−11.575(30)	−8.253(5)	−1.194(31)
			−11.41(15)[a]	−8.27(18)[a]	−1.05(23)[a]
50	−0.9734	10.025(2)	−5.488(26)	−5.001(3)	−1.437(26)
			−5.41(8)[a]	−4.99(6)[a]	−1.34(10)[a]
60	−1.082	5.723(1)	−2.970(18)	−3.341(2)	−1.670(18)
			−2.93(4)[a]	−3.342(21)[a]	−1.63(4)[a]
70	−1.216	3.497(1)	−1.757(25)	−2.412(11)	−1.888(27)
83	−1.466	1.938	−1.057(13)	−1.764(4)	−2.349(14)
92	−1.734	1.276	−0.812(10)	−1.513(3)	−2.783(10)
100	−2.099	0.825	−0.723(7)	−1.384(3)	−3.381(8)

Note: All of the data are given in units of $F(Z\alpha)$. [a] The data from [13].

Laboratoire Kastler Brossel
Physique quantique et applications

Exemple of experimental results

Pushing QED to the limit

The anomalous magnetic moment of **free** leptons

Third order

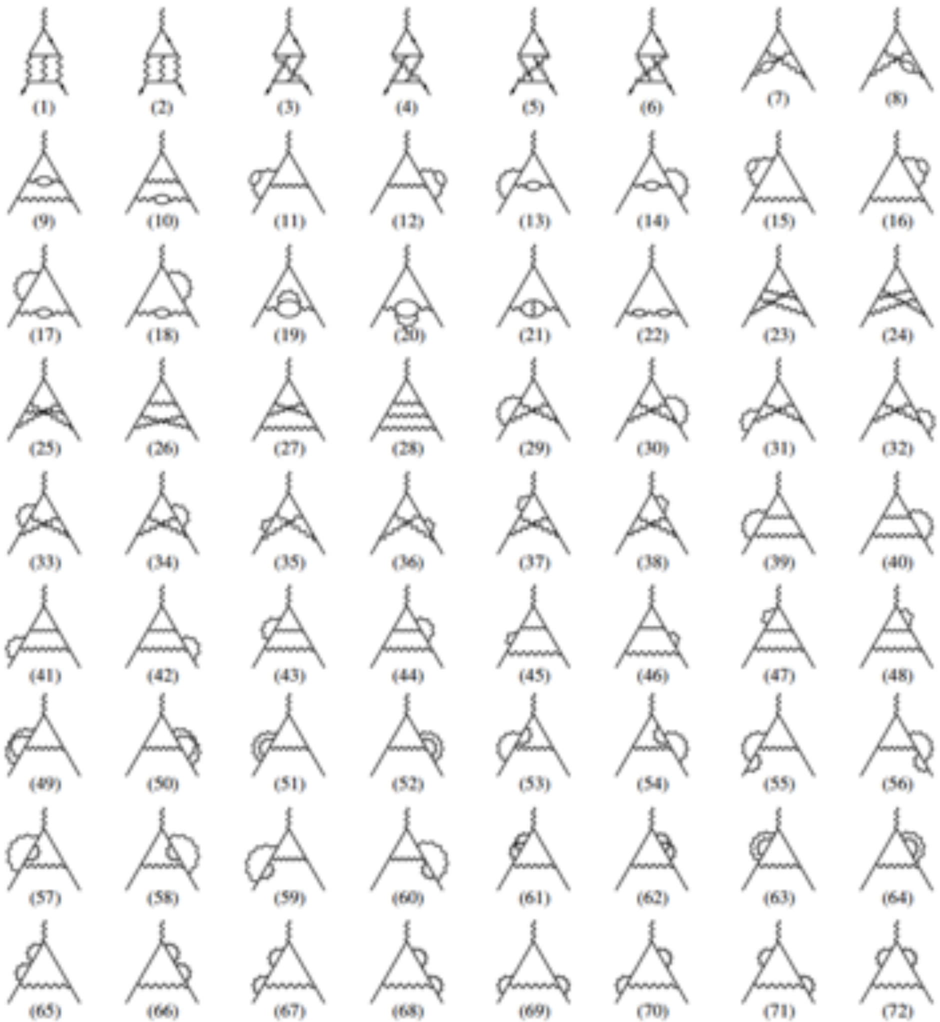

Fig. 10. The universal third order contribution to a_μ. All fermion loops here are muon-loops. Graphs (1) to (6) are the light-by-light scattering diagrams. Graphs (7) to (22) include photon vacuum polarization insertions. All non-universal contributions follow by replacing at least one muon in a closed loop by some other fermion.

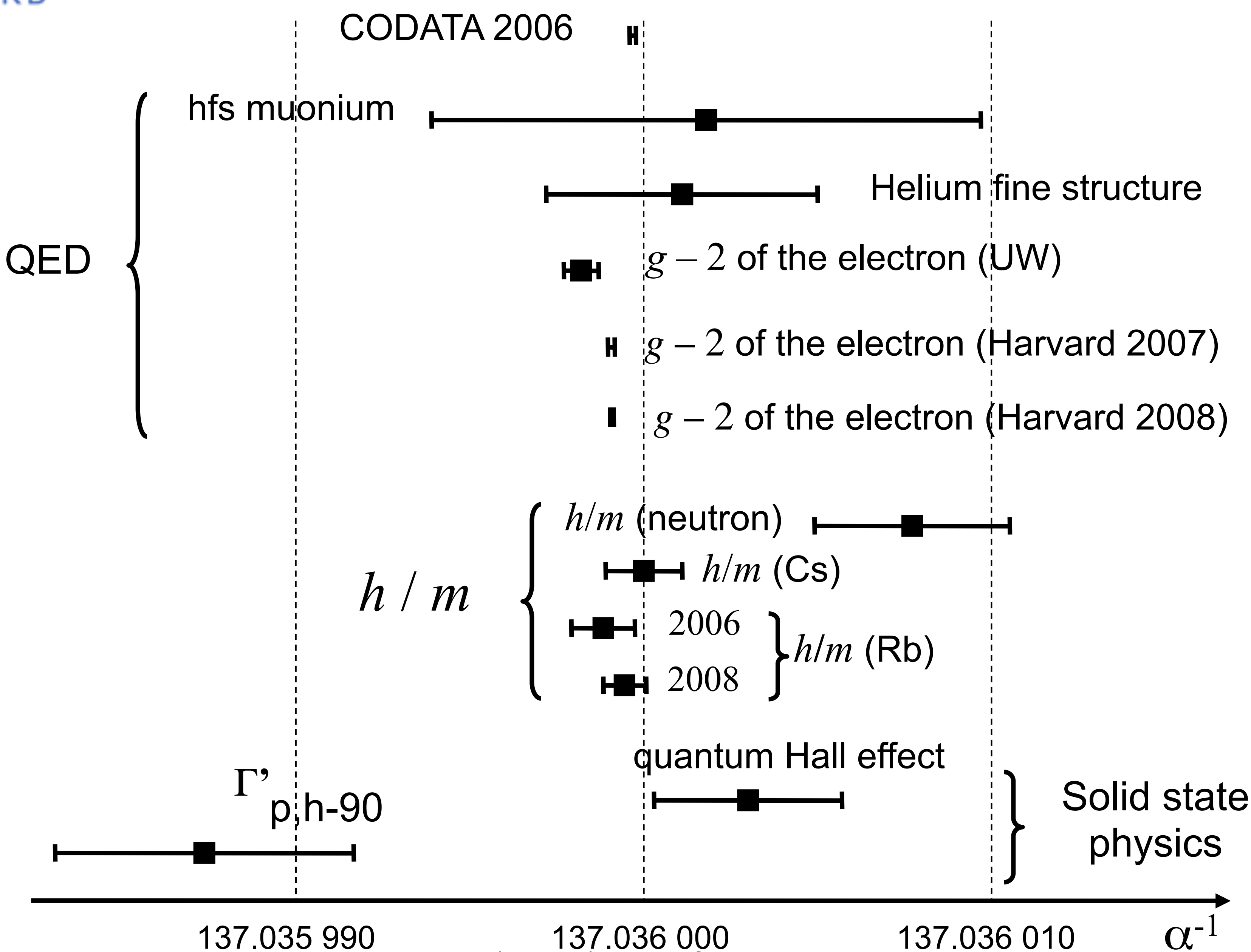
CODATA 2006
QED
hfs muonium
Helium fine structure
$g-2$ of the electron (UW)
$g-2$ of the electron (Harvard 2007)
$g-2$ of the electron (Harvard 2008)
h/m
h/m (neutron)
h/m (Cs)
2006
2008
h/m (Rb)
quantum Hall effect
$\Gamma'_{p,h-90}$
Solid state physics
137.035 990
137.036 000
137.036 010
α^{-1}

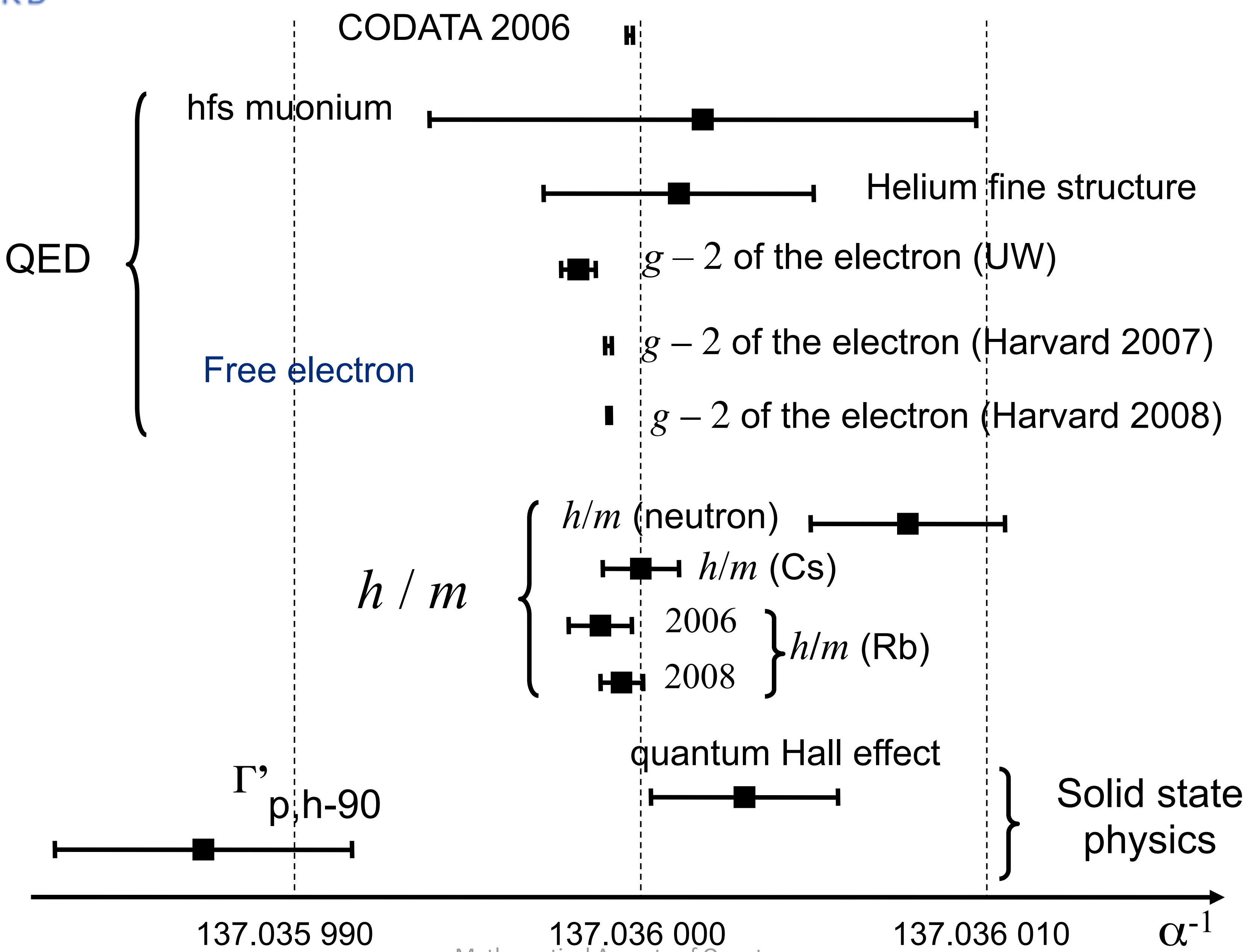

samedi 11 décembre 2010

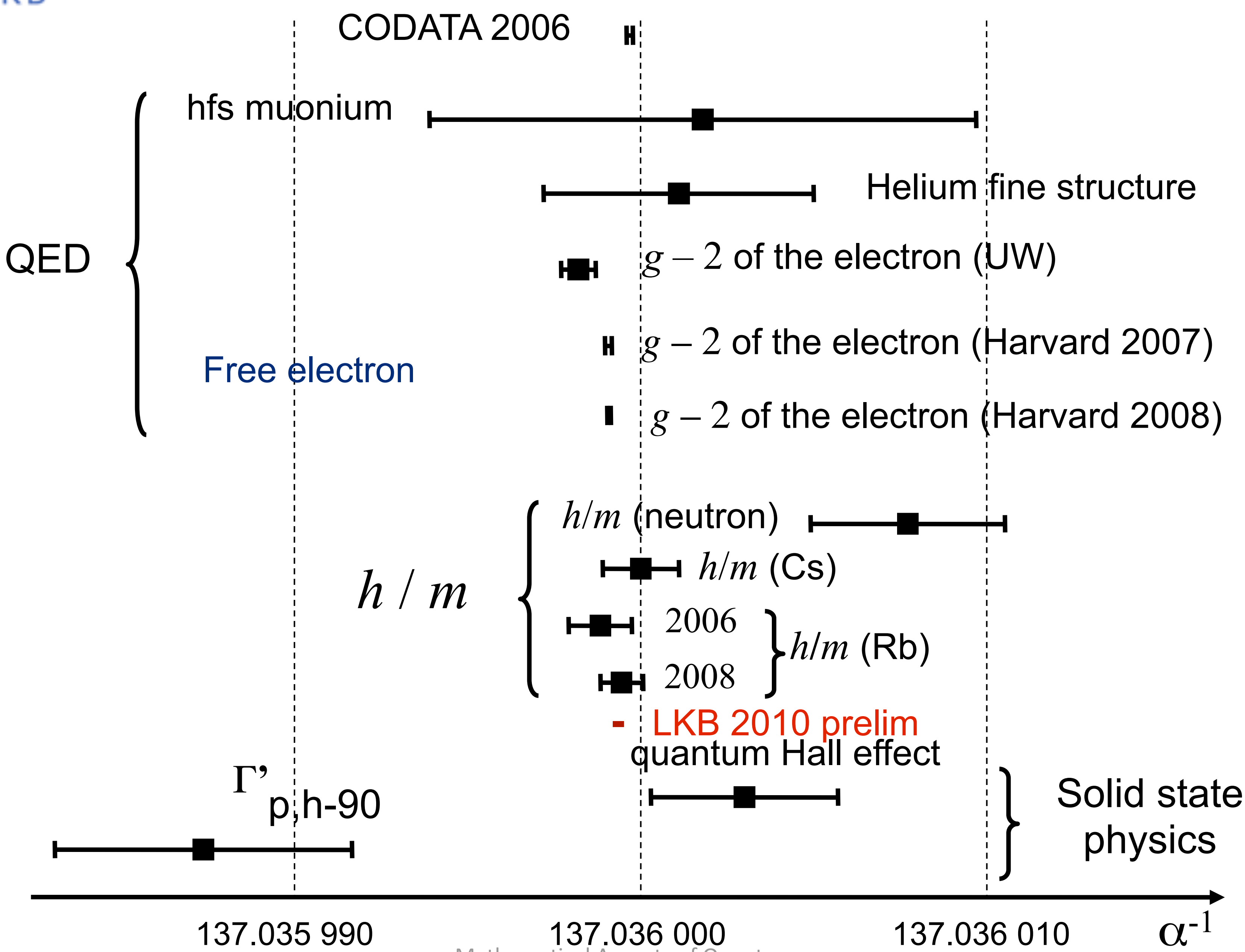
CODATA 2006
hfs muonium
Helium fine structure
QED
g – 2 of the electron (UW)
g – 2 of the electron (Harvard 2007)
Free electron
g – 2 of the electron (Harvard 2008)
h/m (neutron)
h/m (Cs)
h / m
2006
2008
h/m (Rb)
LKB 2010 prelim
quantum Hall effect
Γ'p,h-90
Solid state physics
137.035 990
137.036 000
137.036 010
α-1

La constante de Rydberg

Elle défini les énergies des niveaux des atomes

Précision de la mesure de R_H

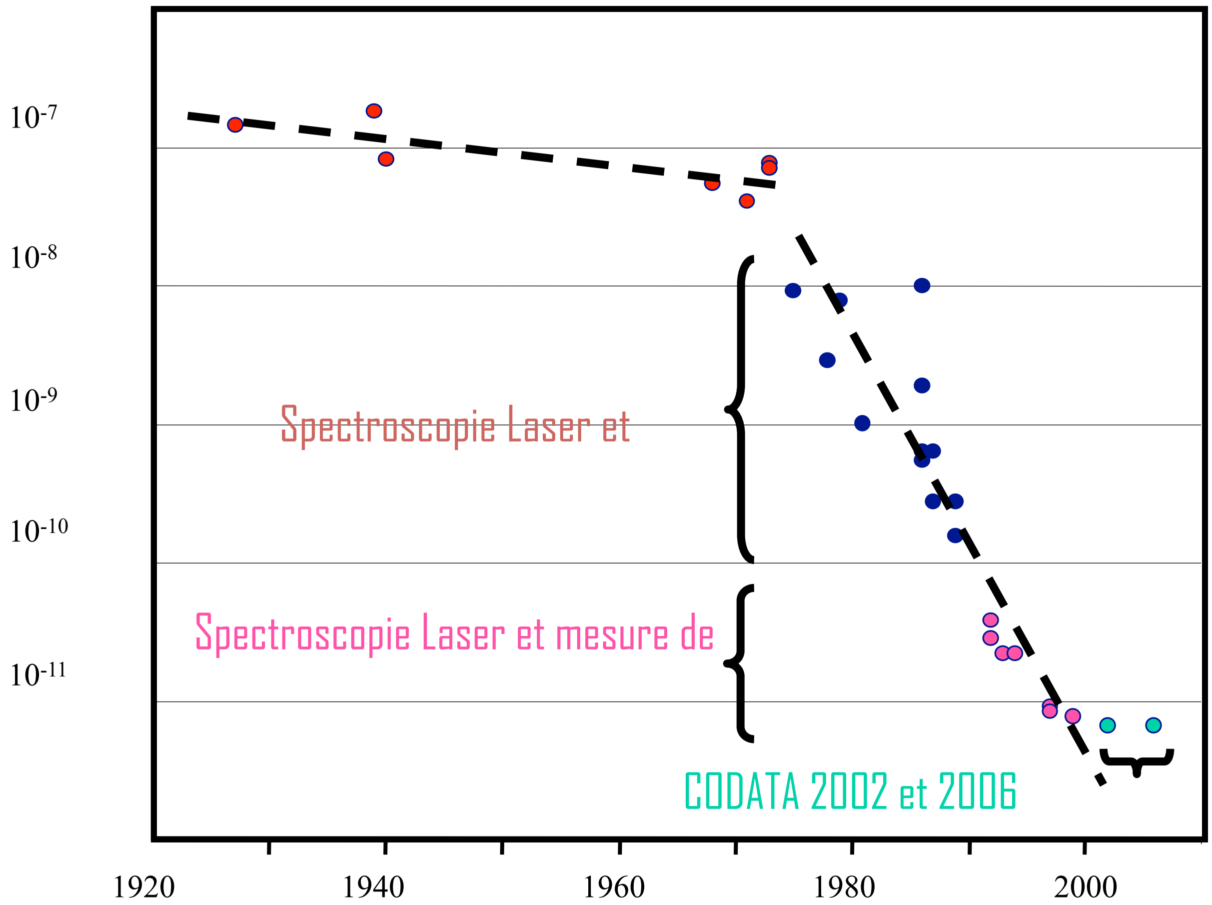

LKB

La constante de Rydberg

Elle défini les énergies des niveaux des atomes

Progrès scientifique

Progrès technique

Précision de la mesure de R_H

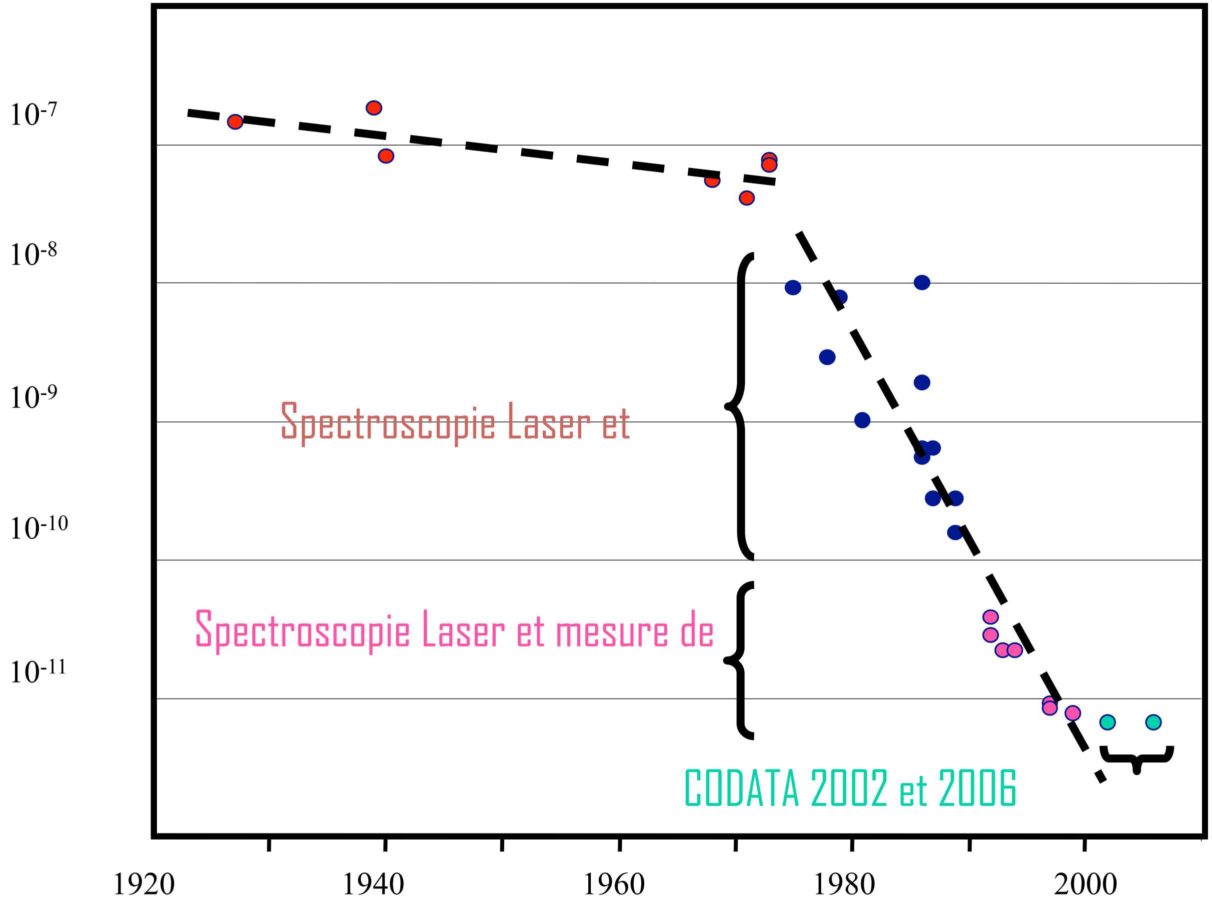

samedi 11 décembre 2010

Pourquoi remesurer le rayon du proton?

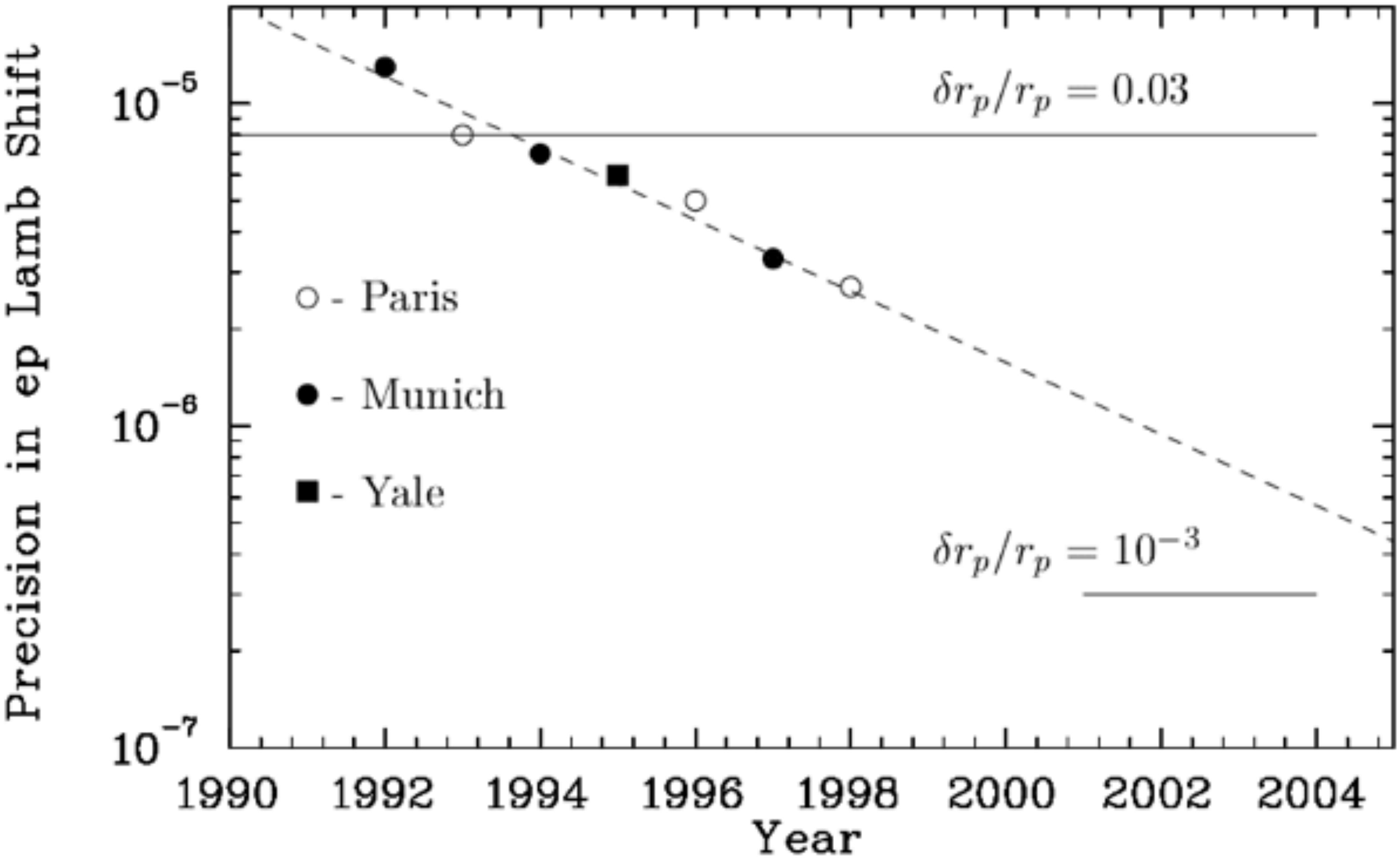

L'hydrogène

L'hydrogène

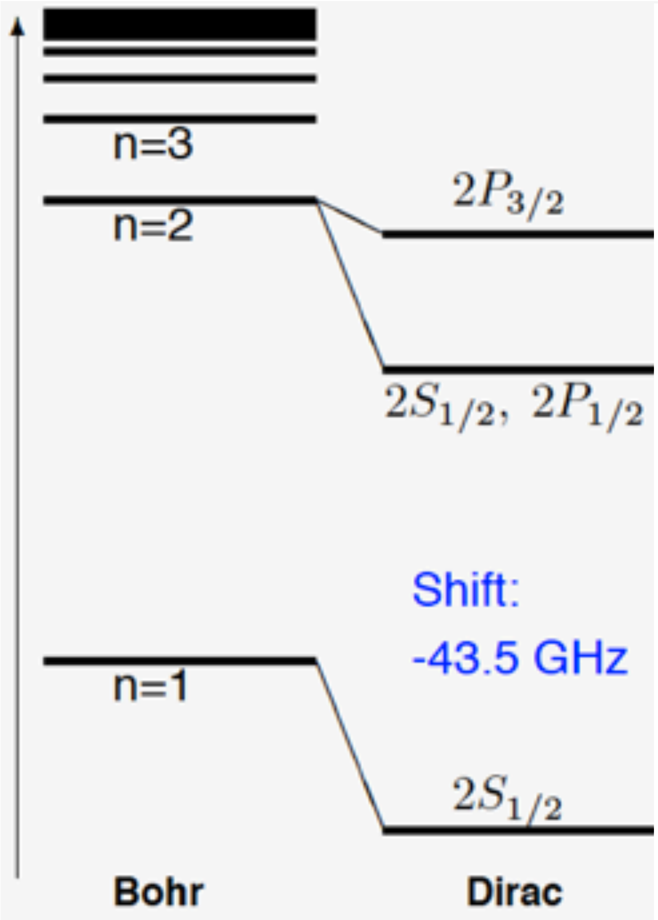

L'hydrogène

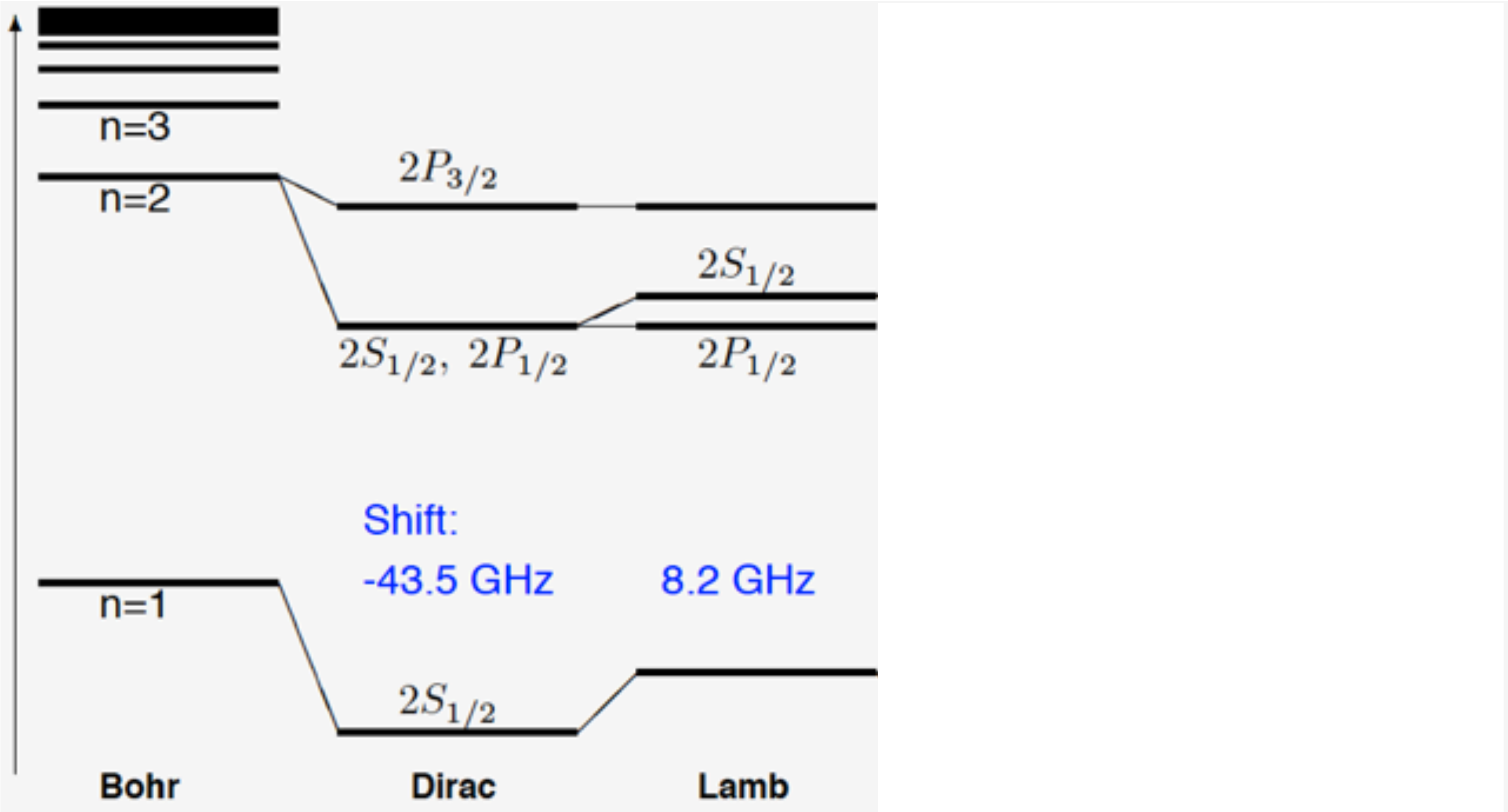
n=3
n=2
$2P_{3/2}$
$2S_{1/2}$
$2S_{1/2},\ 2P_{1/2}$
$2P_{1/2}$
Shift:
-43.5 GHz
8.2 GHz
n=1
$2S_{1/2}$
Bohr
Dirac
Lamb

L'hydrogène

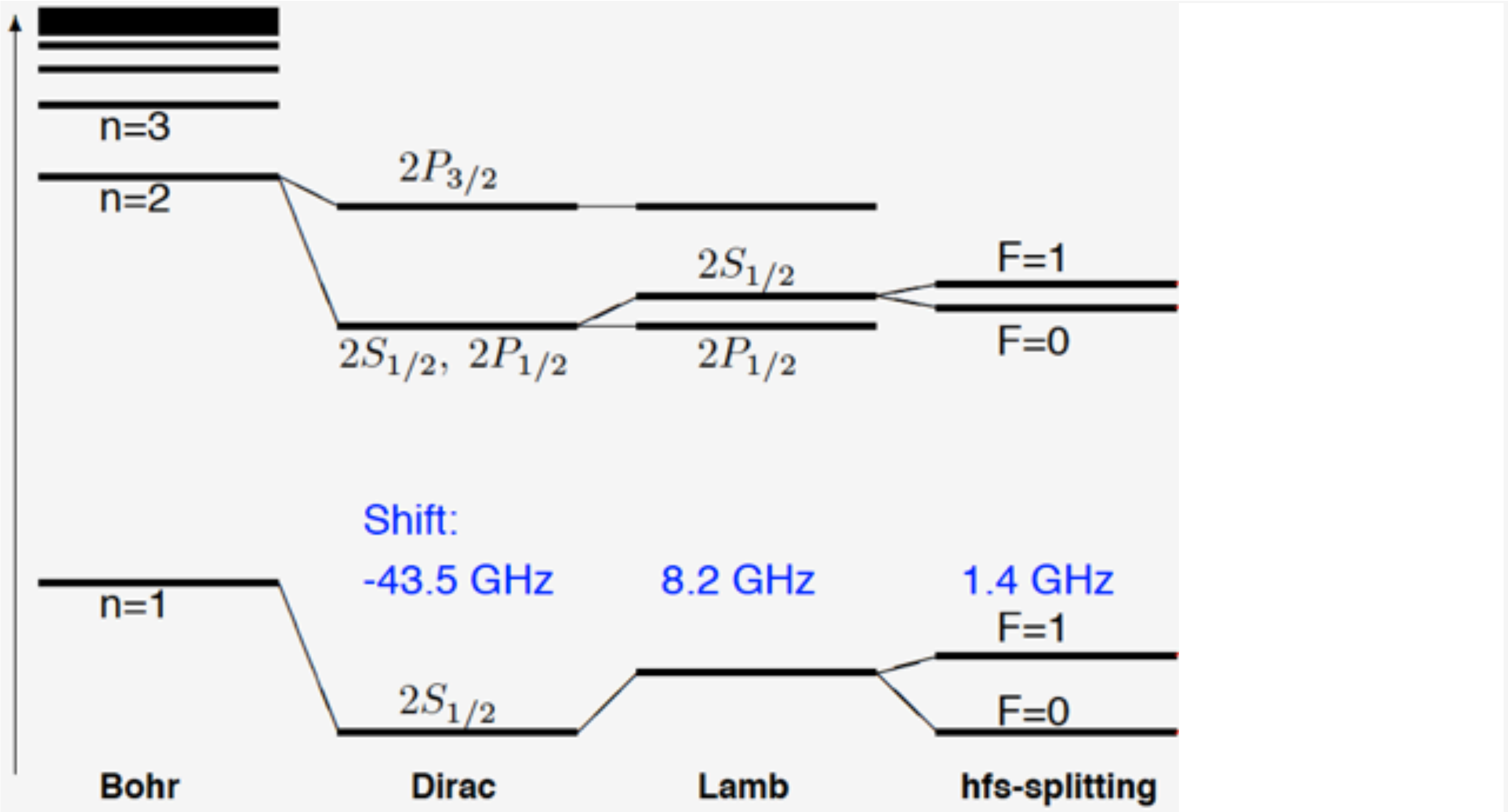

n=3
n=2
$2P_{3/2}$
$2S_{1/2}$
F=1
F=0
$2S_{1/2},\ 2P_{1/2}$
$2P_{1/2}$
Shift:
-43.5 GHz
8.2 GHz
1.4 GHz
n=1
F=1
$2S_{1/2}$
F=0
Bohr
Dirac
Lamb
hfs-splitting

L'hydrogène

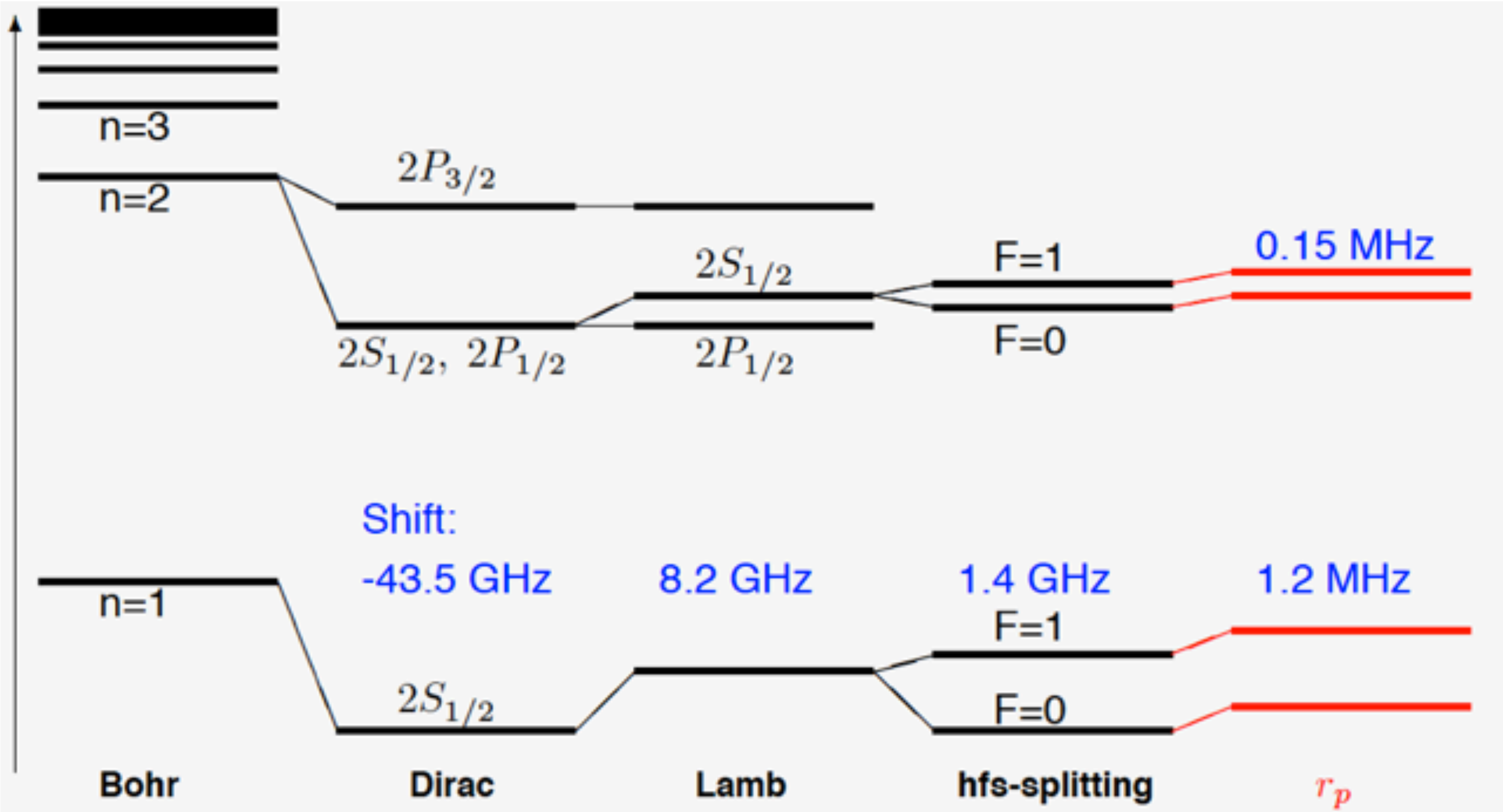
n=3
n=2
$2P_{3/2}$
$2S_{1/2}$
F=1
0.15 MHz
$2S_{1/2}, 2P_{1/2}$
$2P_{1/2}$
F=0
Shift:
-43.5 GHz
8.2 GHz
1.4 GHz
1.2 MHz
n=1
F=1
$2S_{1/2}$
F=0
Bohr
Dirac
Lamb
hfs-splitting
r_p

L'hydrogène

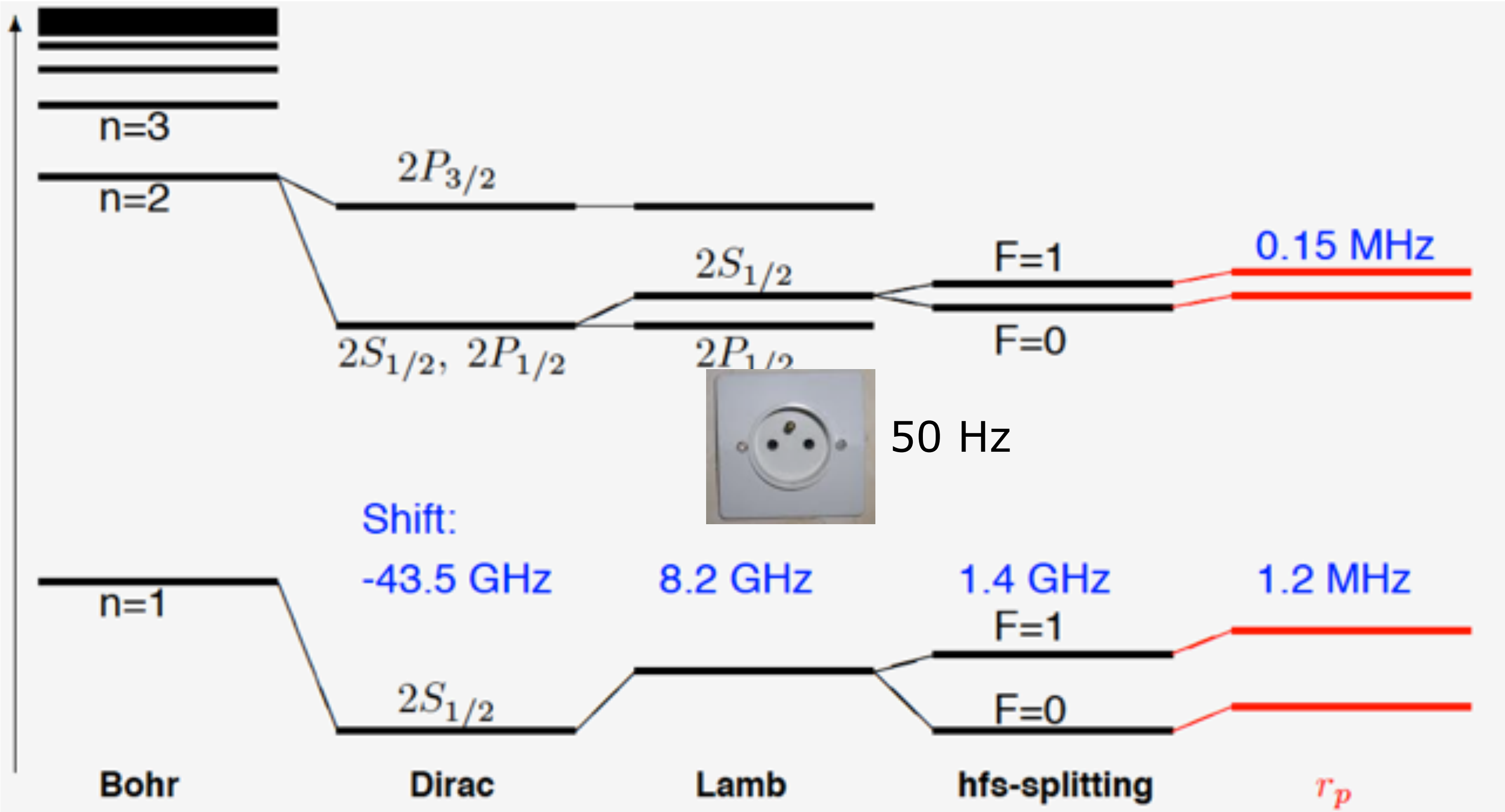

samedi 11 décembre 2010

L'hydrogène

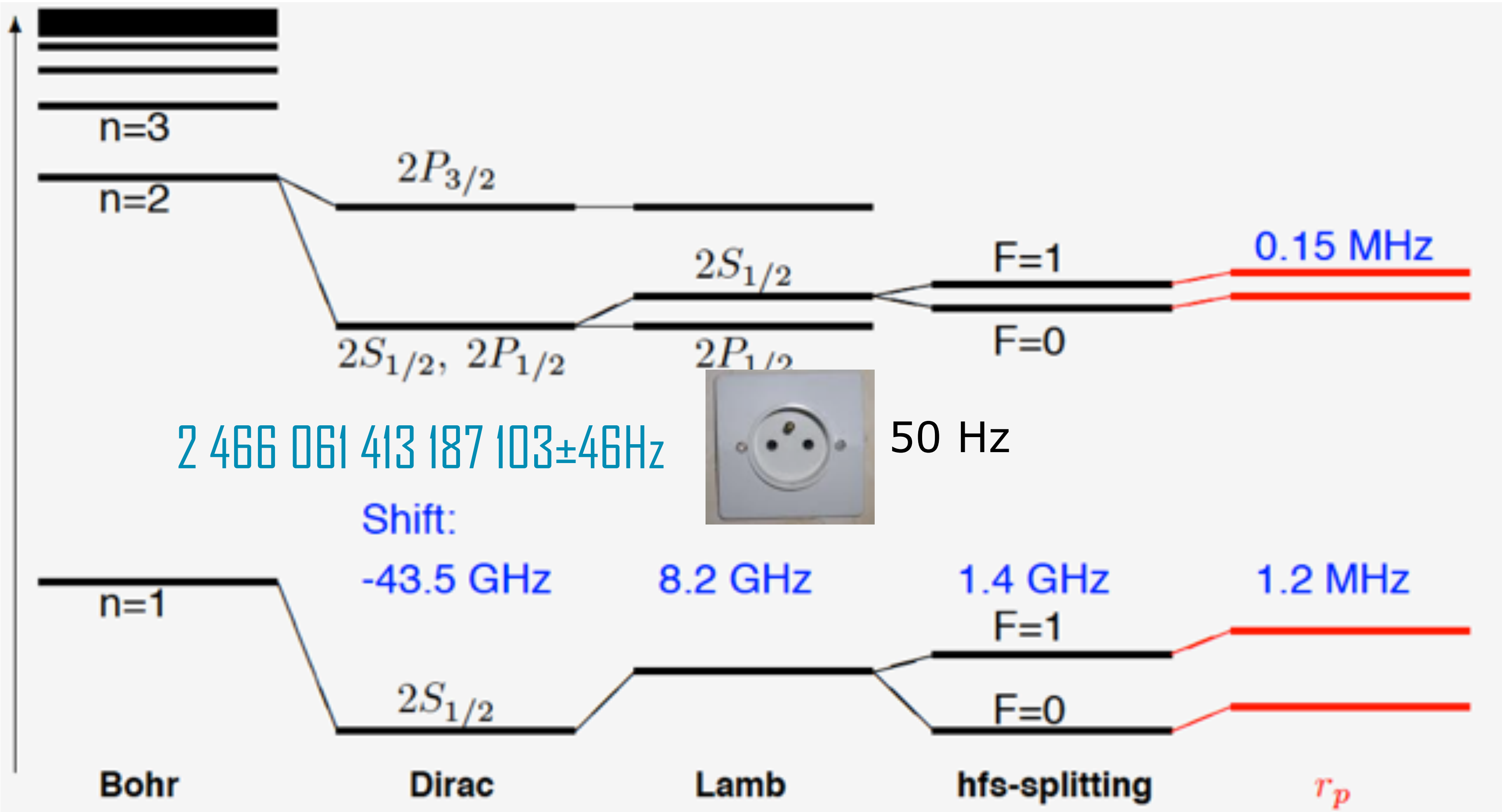
n=3
n=2
$2P_{3/2}$
$2S_{1/2}$
$2S_{1/2},\ 2P_{1/2}$
$2P_{1/2}$
F=1
F=0
0.15 MHz
2 466 061 413 187 103±46Hz
50 Hz
Shift:
-43.5 GHz
8.2 GHz
1.4 GHz
1.2 MHz
n=1
$2S_{1/2}$
F=1
F=0
Bohr
Dirac
Lamb
hfs-splitting
r_p

Déplacement de Lamb

Plus la particule est lourde plus c'est petit!

Polarisation du vide
Plus on est près plus c'est fort!

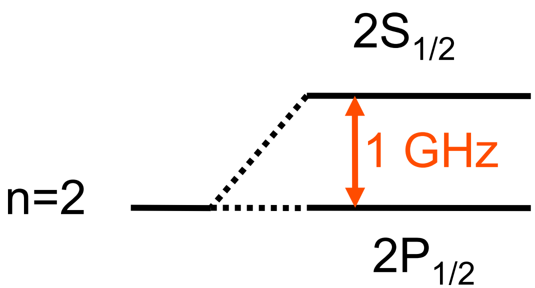

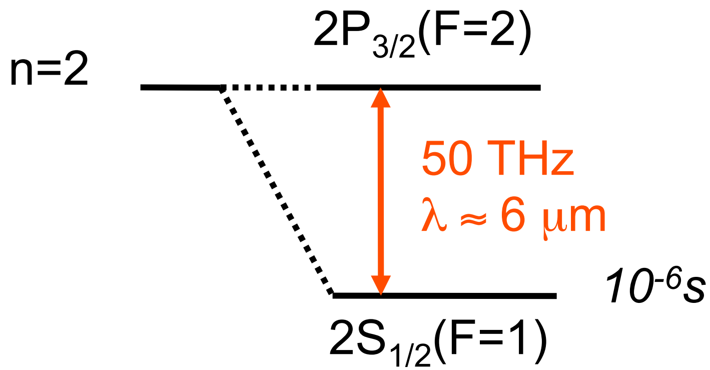

Hydrogène (électron)

Hydrogène muonique (muon 207 fois plus lourd que l'électron)

muonic hydrogen : $2S_{1/2}(F=1)$ - $2P_{3/2}(F=2)$

LKB

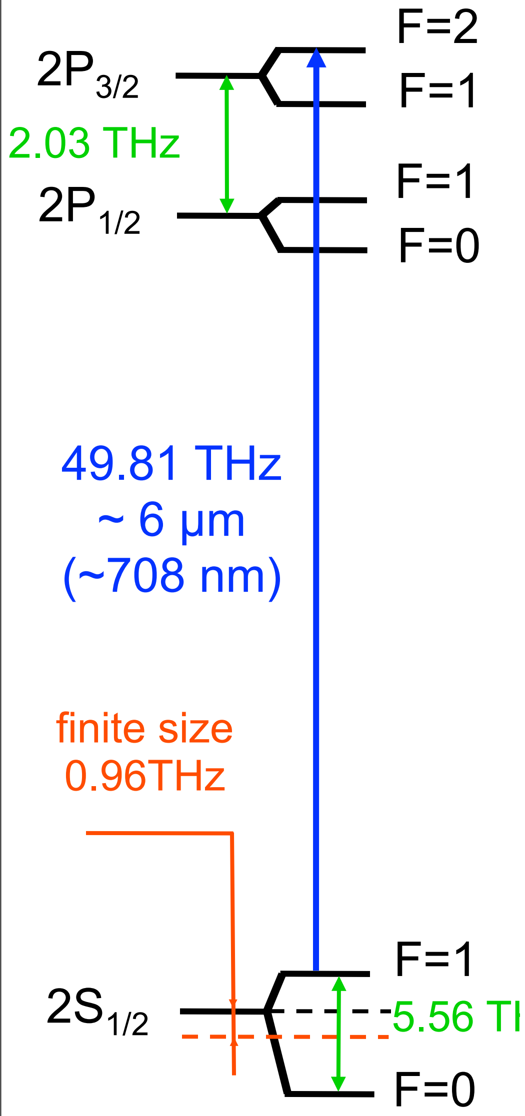

- 550 events measured
- 155 backgrounds
- 31 FP fringes
- 250 hours

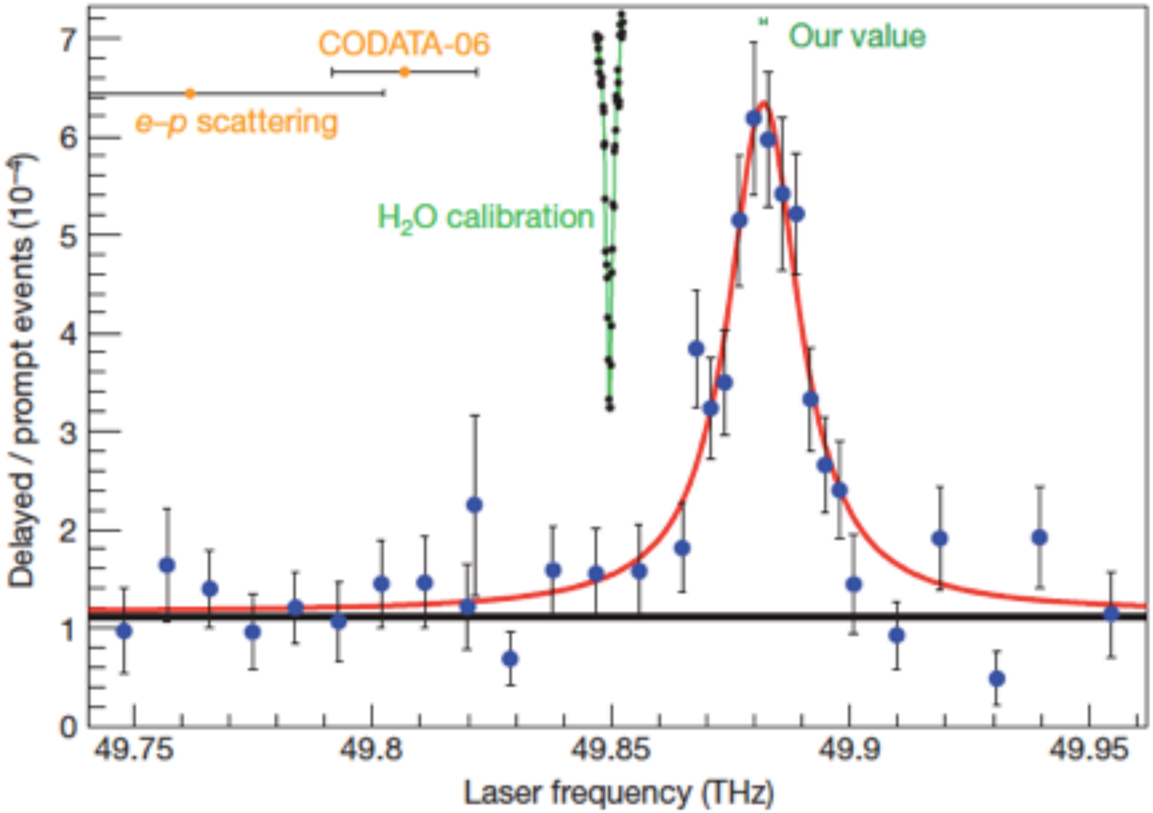

R. Pohl, A. Antognini, F. Nez, et al., Nature 466, 213 (2010).

→ proton charge radius (~0.1%)

muonic hydrogen: $2S_{1/2}(F=0)$- $2P_{3/2}(F=1)$

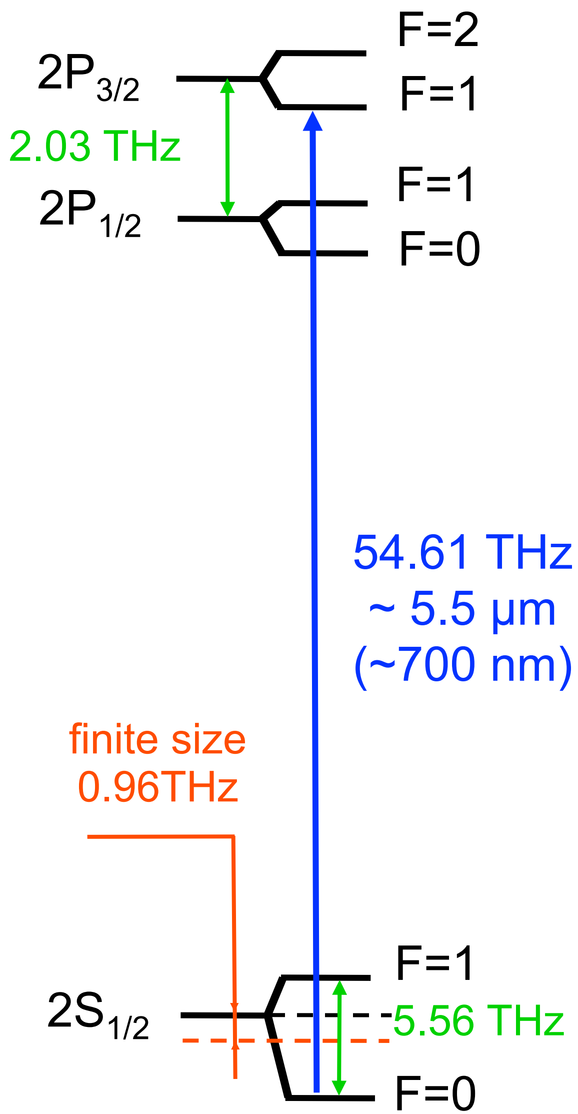

- measured position fits with our proton radius (preliminary)
- laser worked even better at 5.5 µm

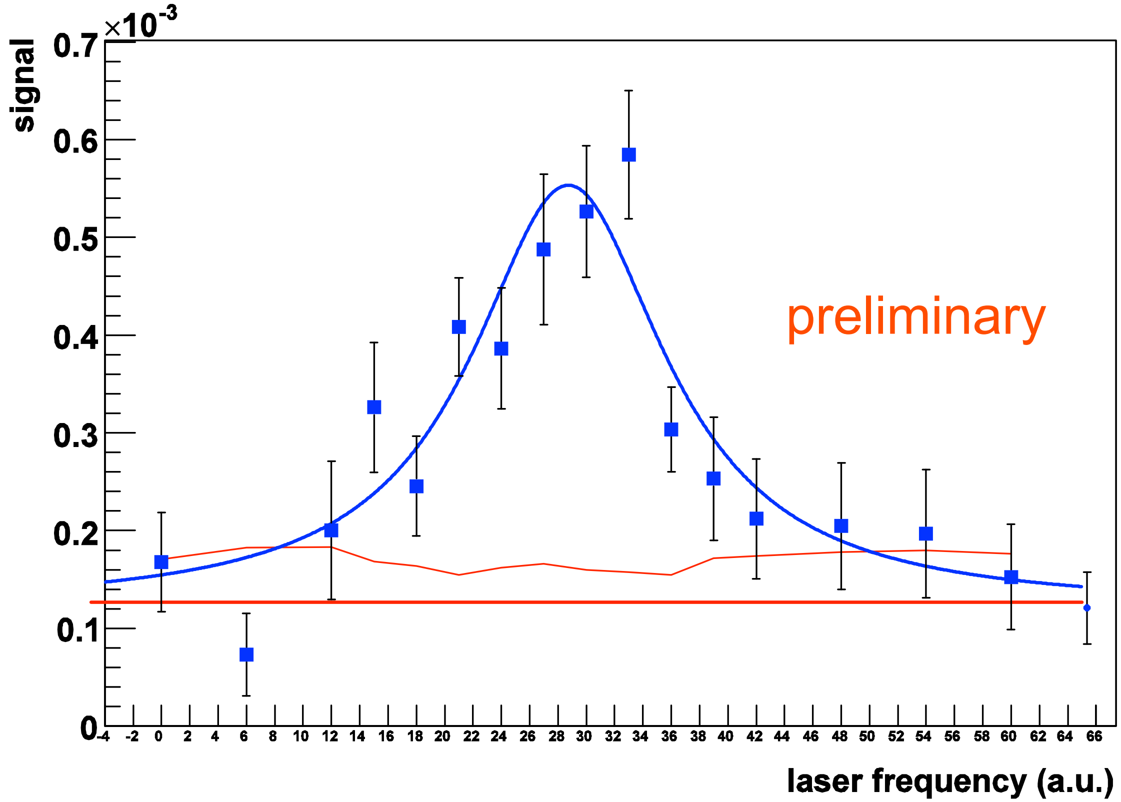

~ at the position deduced with new r_p → hfs : Zeemach radius (few %)

History of the proton radius

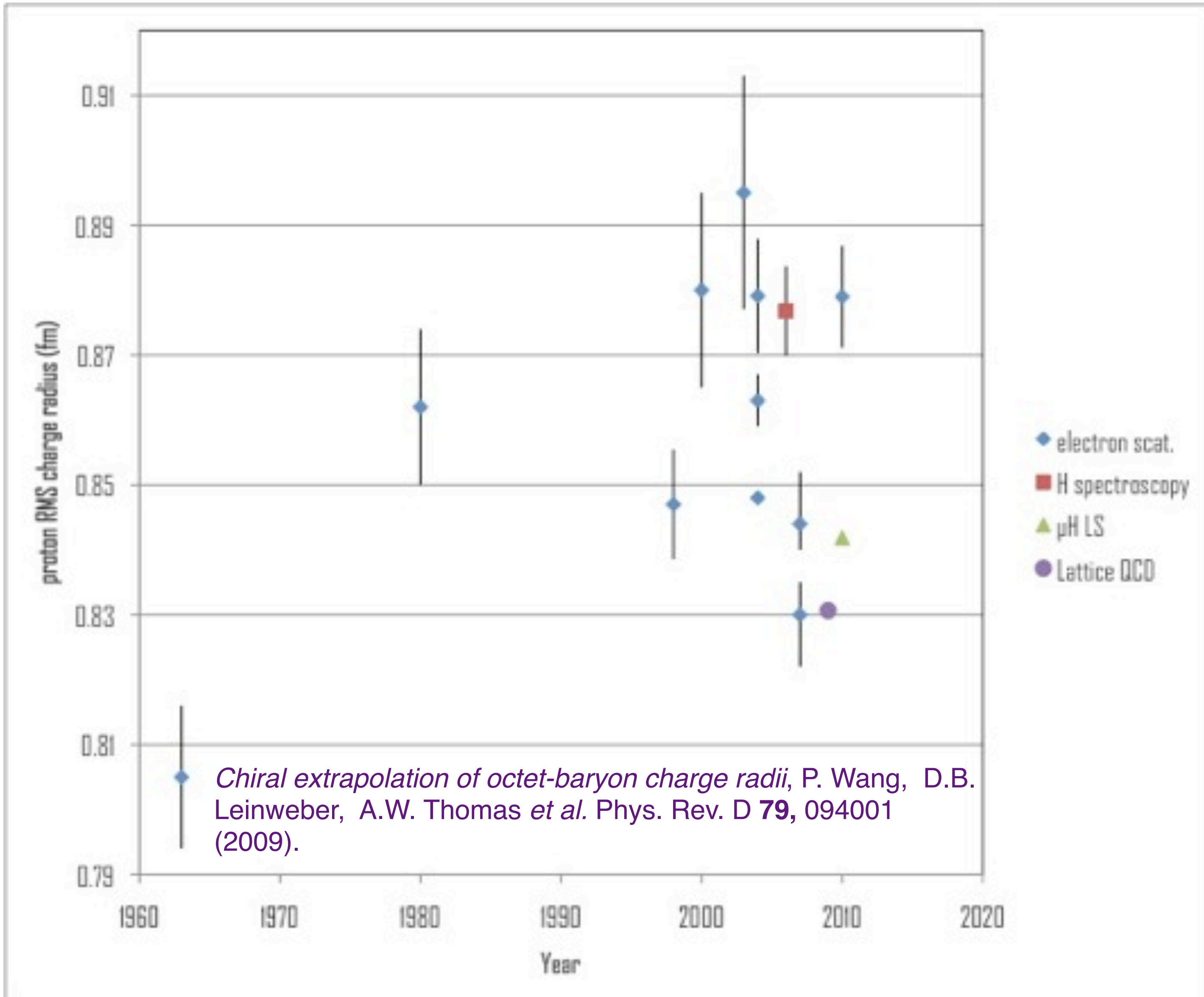

Chiral extrapolation of octet-baryon charge radii, P. Wang, D.B. Leinweber, A.W. Thomas *et al.* Phys. Rev. D **79,** 094001 (2009).

History of the proton radius

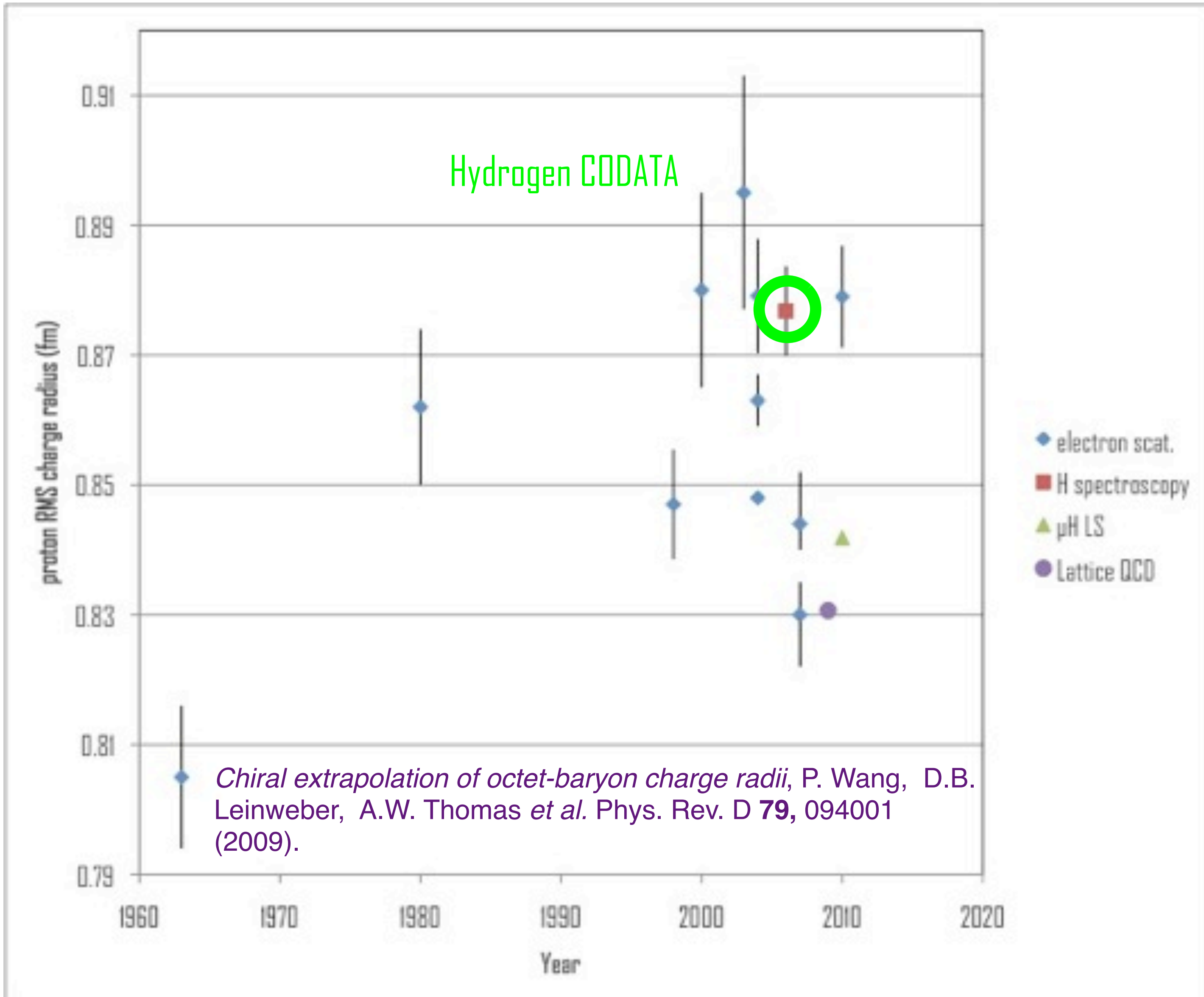

Chiral extrapolation of octet-baryon charge radii, P. Wang, D.B. Leinweber, A.W. Thomas *et al.* Phys. Rev. D **79,** 094001 (2009).

History of the proton radius

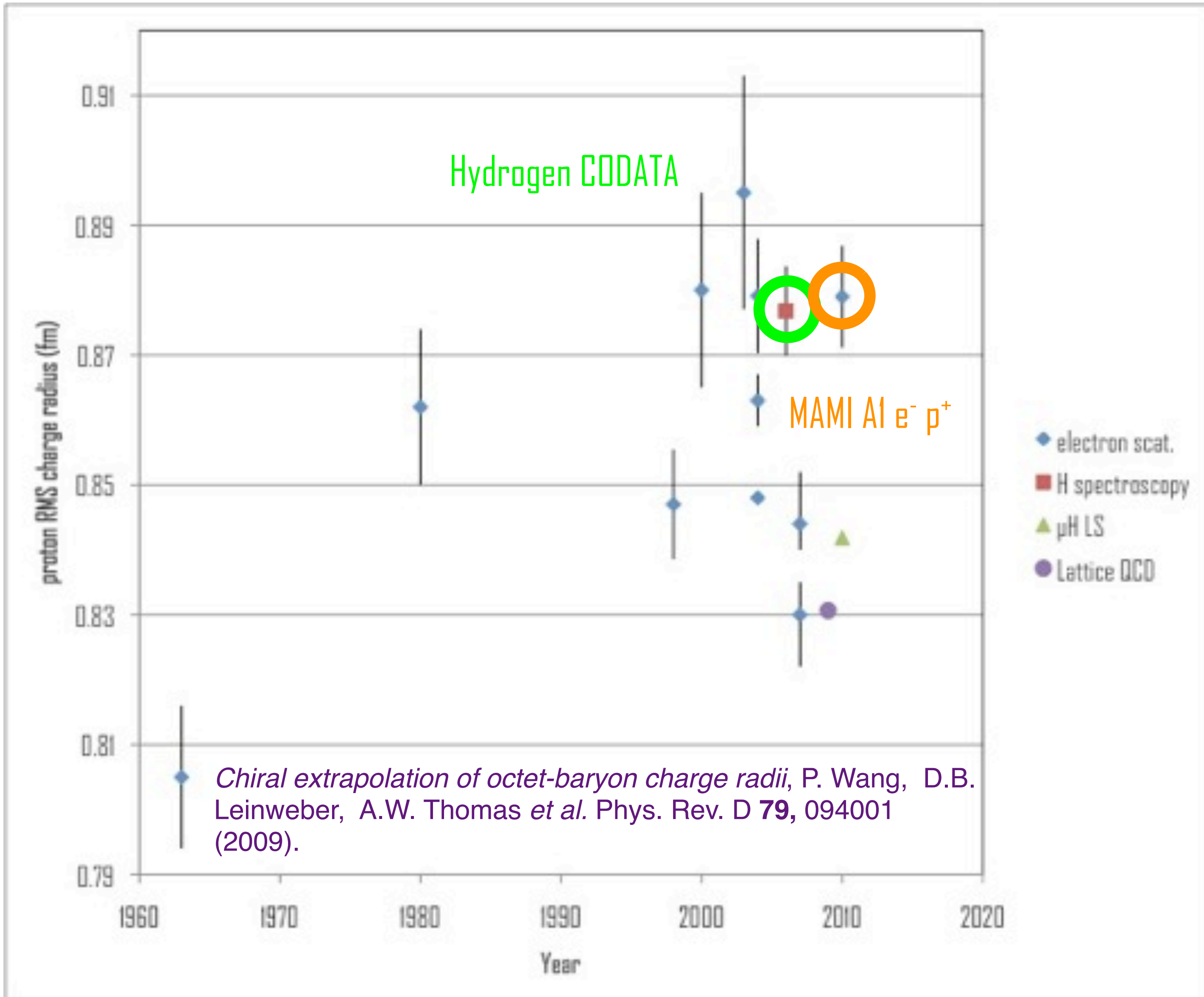

Chiral extrapolation of octet-baryon charge radii, P. Wang, D.B. Leinweber, A.W. Thomas *et al.* Phys. Rev. D **79,** 094001 (2009).

History of the proton radius

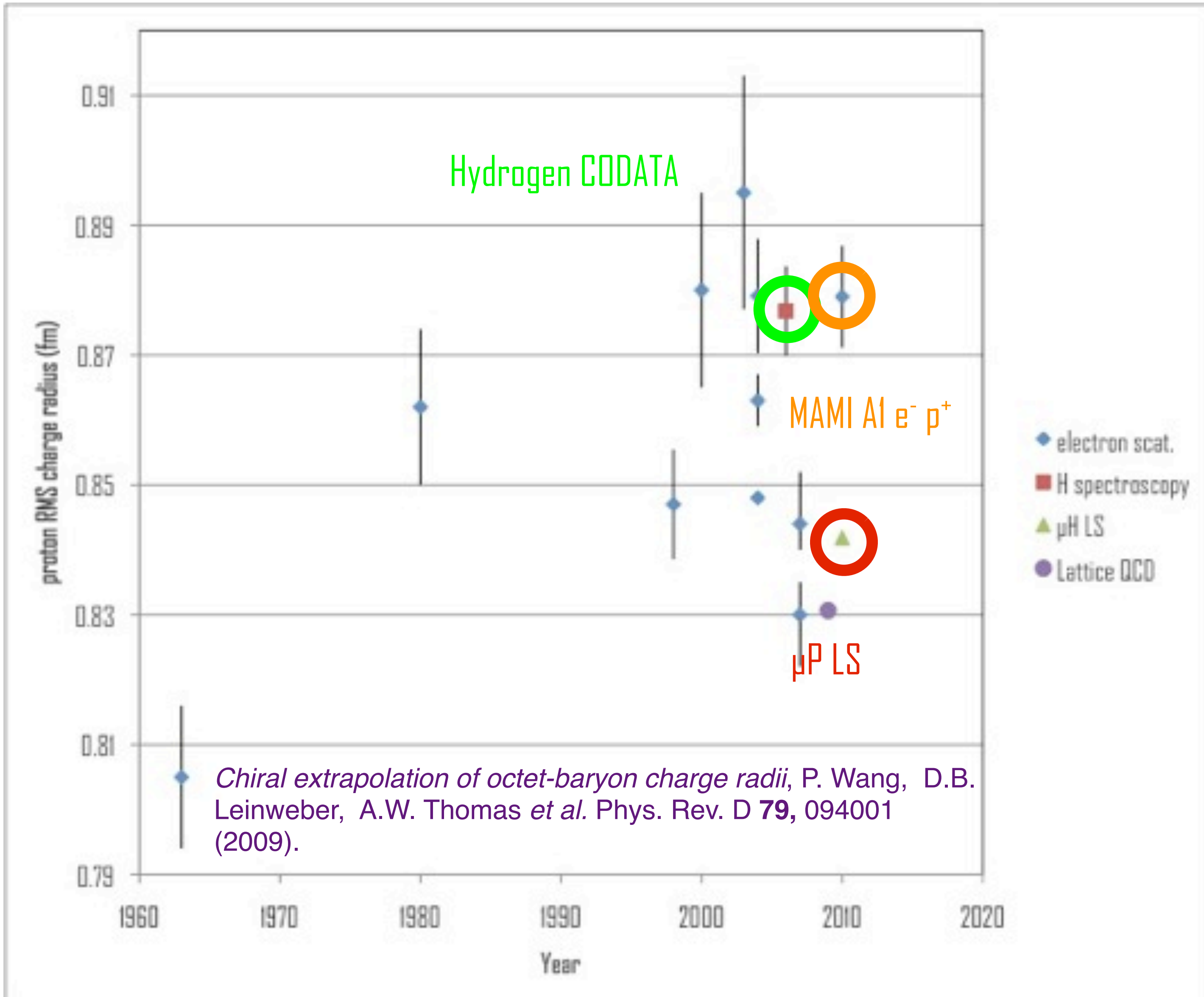

Chiral extrapolation of octet-baryon charge radii, P. Wang, D.B. Leinweber, A.W. Thomas *et al.* Phys. Rev. D **79,** 094001 (2009).


8 July 2010 | www.nature.com/nature | $10
THE INTERNATIONAL WEEKLY JOURNAL OF SCIENCE
nature
OIL SPILLS
There's more to come
PLAGIARISM
It's worse than you think
CHIMPANZEES
The battle for survival
0.84184 fm
SHRINKING THE PROTON
New value from exotic atom trims radius by four per cent
NATUREJOBS
Reseachers for hire

Highly charged ions

Recent progress

Atomic Physics in Strong Coulomb Fields

Atomic Physics in Strong Coulomb Fields

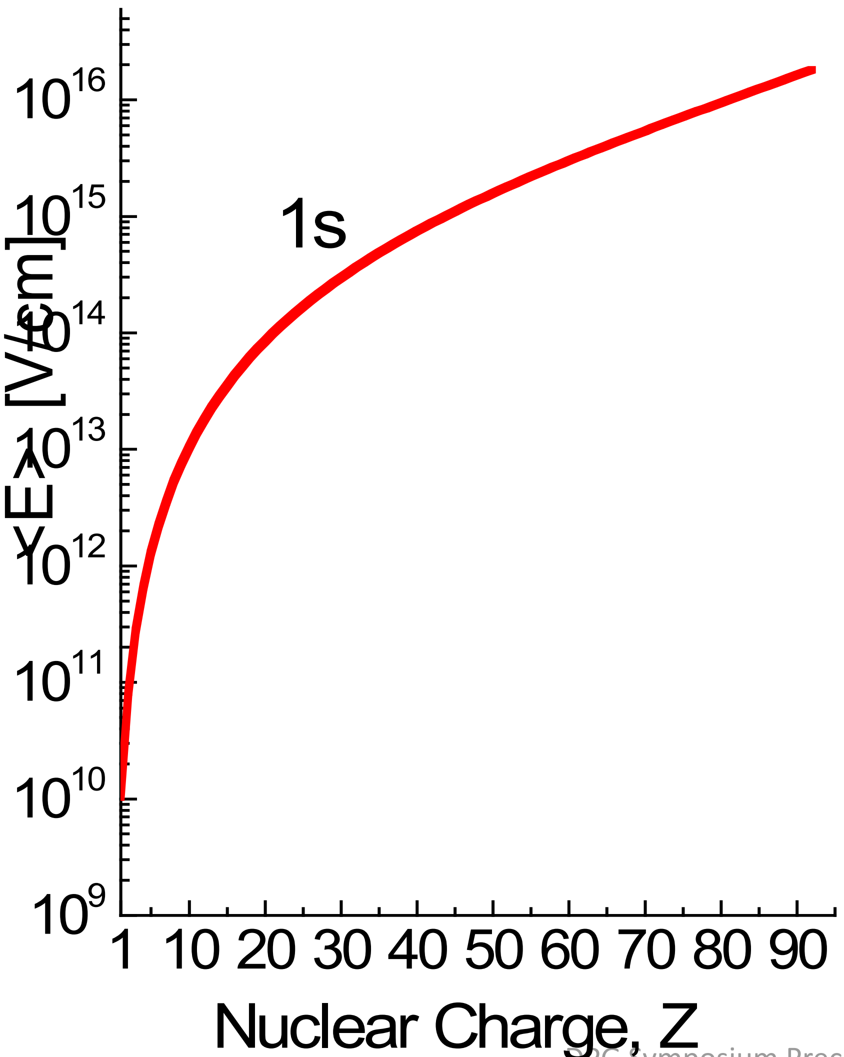

Atomic Physics in Strong Coulomb Fields

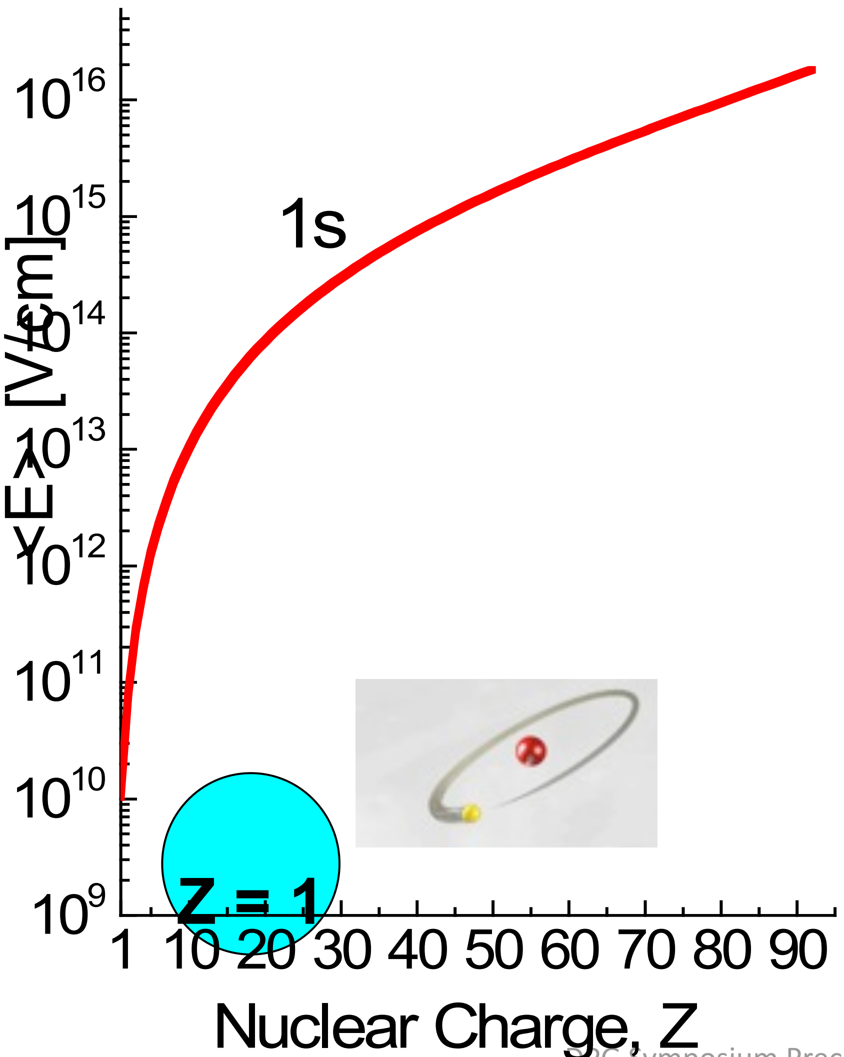

Hydrogen
E_K = -13.6 eV
<E>= 1 • 10^{10} V/cm

Atomic Physics in Strong Coulomb Fields

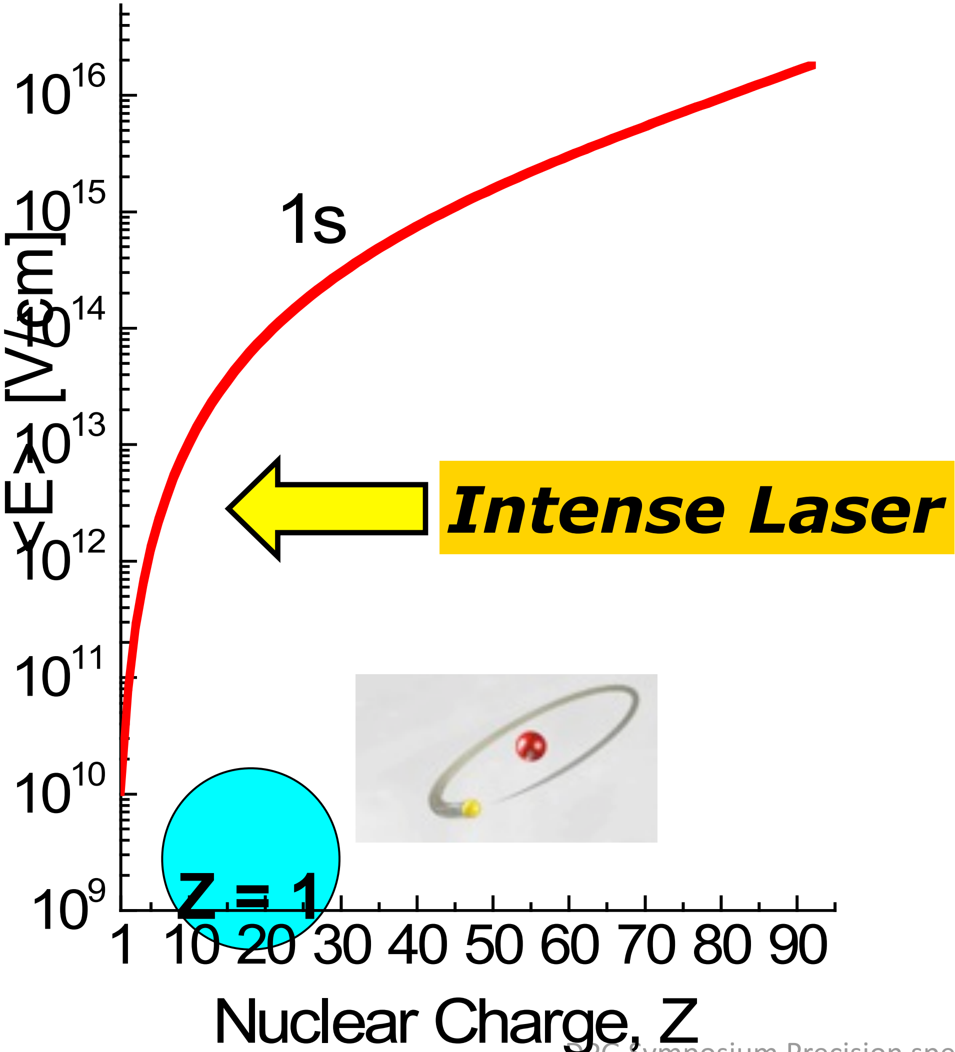

Hydrogen
E_K = -13.6 eV
<E>= 1 • 10^{10} V/cm

samedi 11 décembre 2010

Atomic Physics in Strong Coulomb Fields

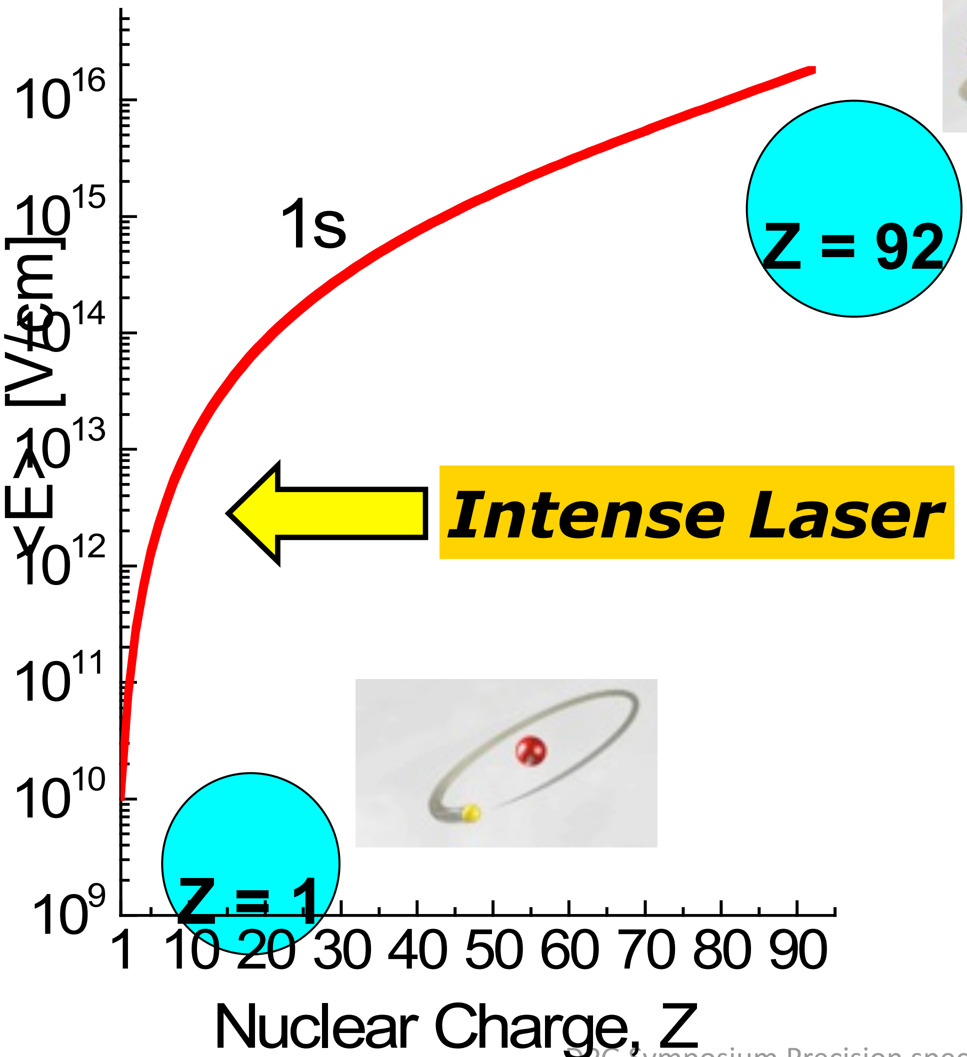

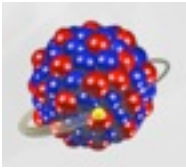

H-like Uranium
E_K = -132 • 10^3 eV
$<E>$= 1.8 • 10^{16} V/cm

Hydrogen
E_K = -13.6 eV
$<E>$= 1 • 10^{10} V/cm

Atomic Physics in Strong Coulomb Fields

Atomic Structure at High-Z

- bound state quantum electrodynamics (QED)
- effects of relativity on the atomic structure
- electron correlation in the presence of strong fields

How to make HCI ?

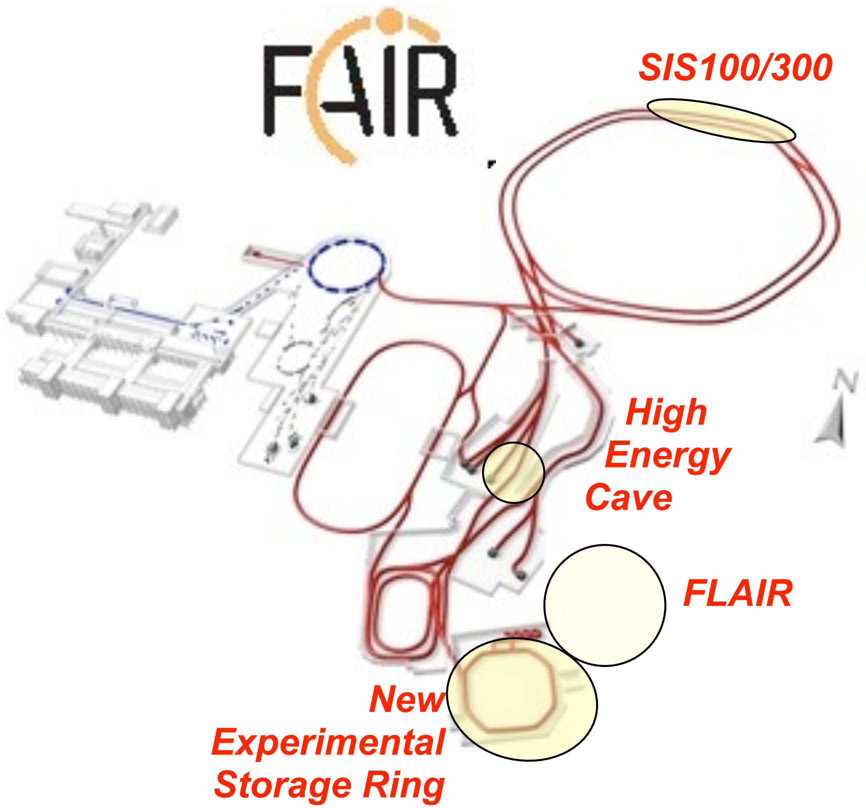

The large factory vs the mechanics around the corner

How to make HCI ?

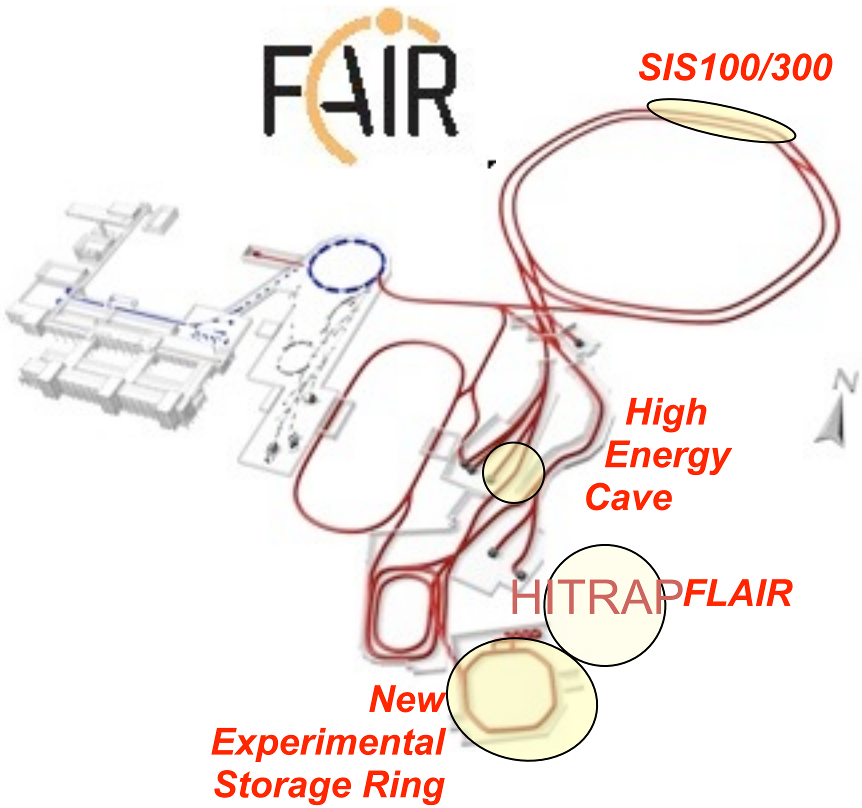

The large factory vs the mechanics around the corner

How to make HCI ?

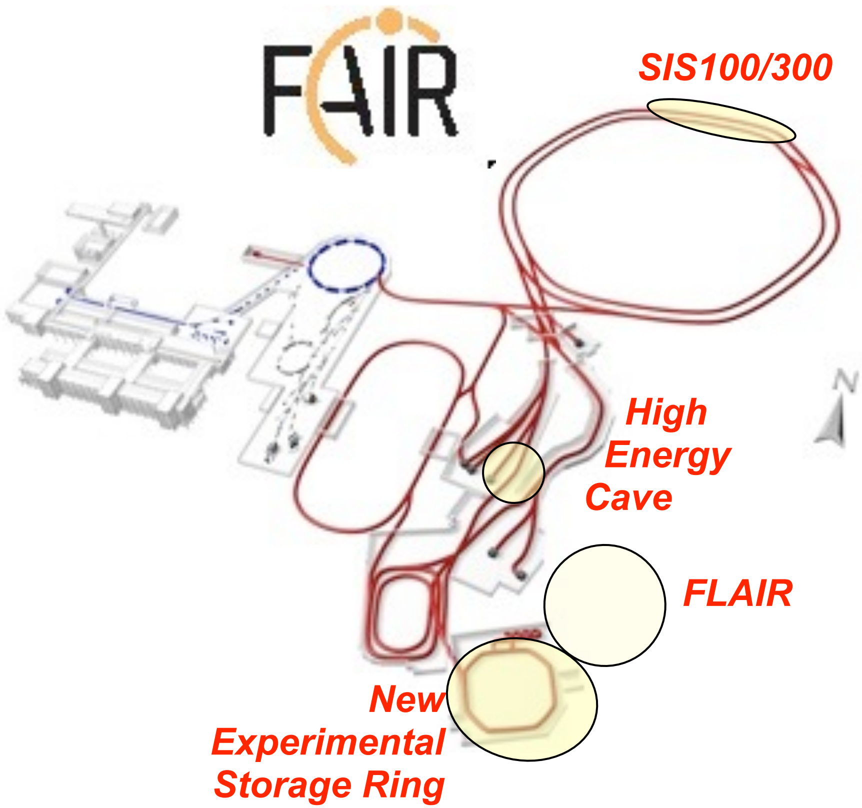

The large factory vs the mechanics around the corner

How to make HCI ?

The large factory vs the mechanics around the corner

How to make HCI ?

ECRIS

The large factory vs the mechanics around the corner

How to make HCI ?

The large factory vs the mechanics around the corner

How to make HCI ?

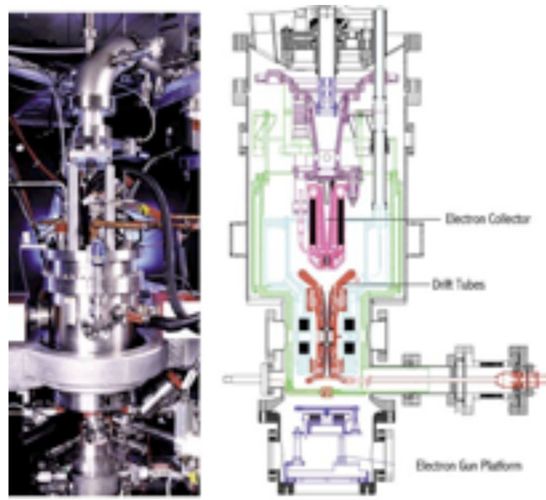

EBIT

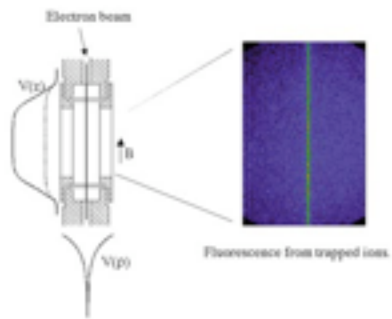

The large factory vs the mechanics around the corner

samedi 11 décembre 2010

He-like U: 1s2p $^3P_2$-1s2s $^3S_1$

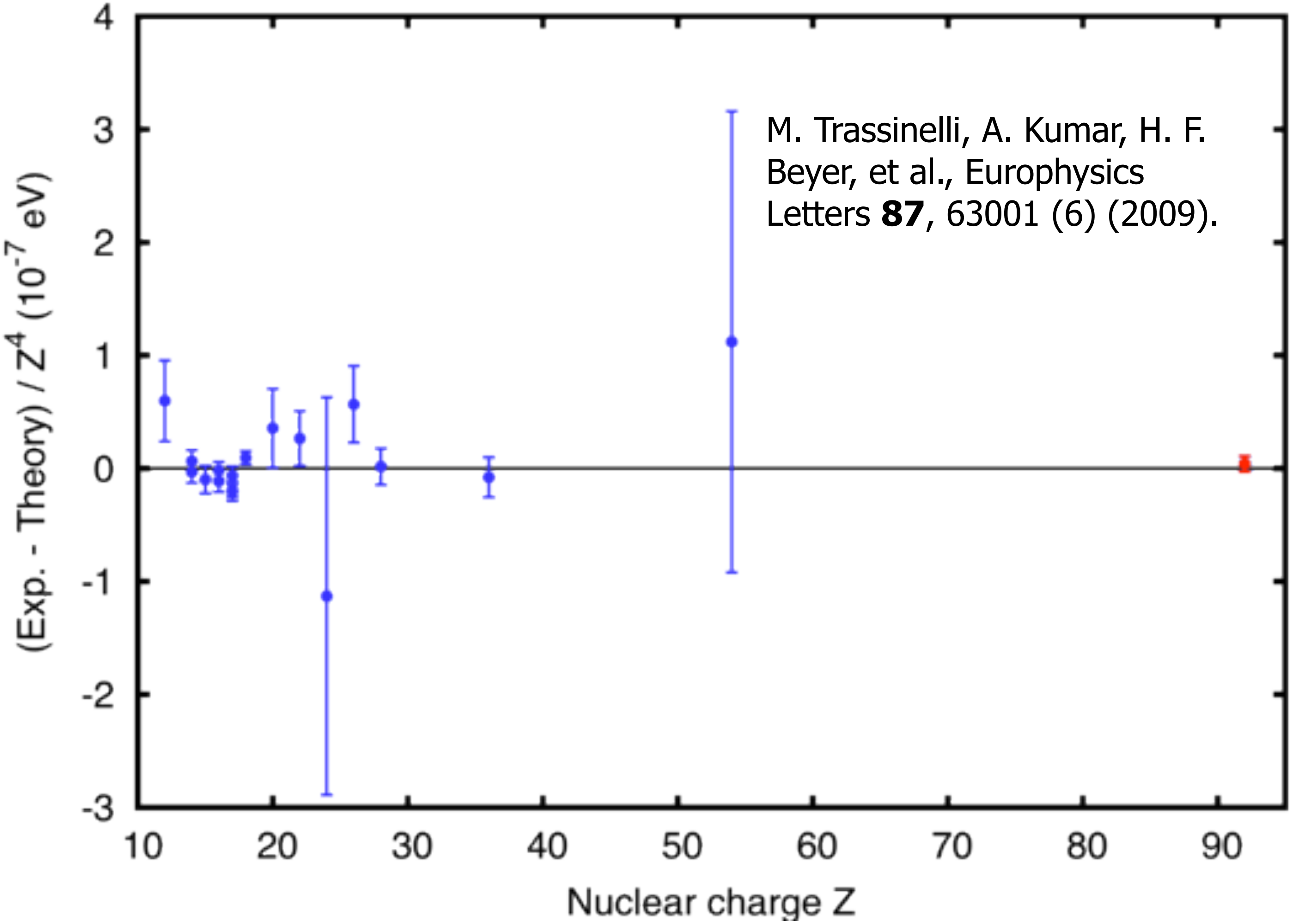

E_{He} = 4510.32 ± $(0.45)_{stat}$ ± $(0.22)_{syst}$ eV

EBIT: Heidelberg

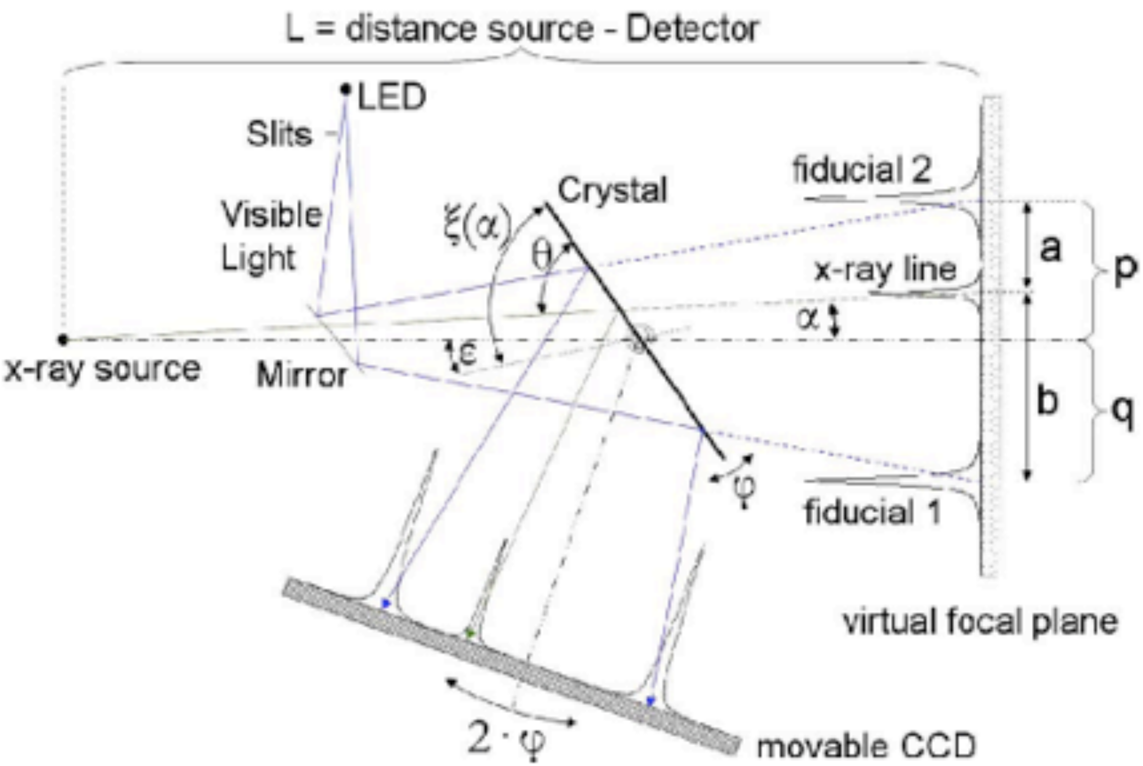

FIG. 1. Principle of the method. For simplicity, possible eccentricities of crystal and camera are not shown. The horizontal dashed-dotted line represents the main instrumentation axis. X rays are reflected under the Bragg angle θ, and α is the angle between the main axis and the x ray. The reflection position on the crystal depends on the crystal angle $\xi(\alpha)$ which, due to alignment of the spectrometer, includes an arbitrary offset angle ϵ (which is constant for all measurements).

EBIT: Heidelberg

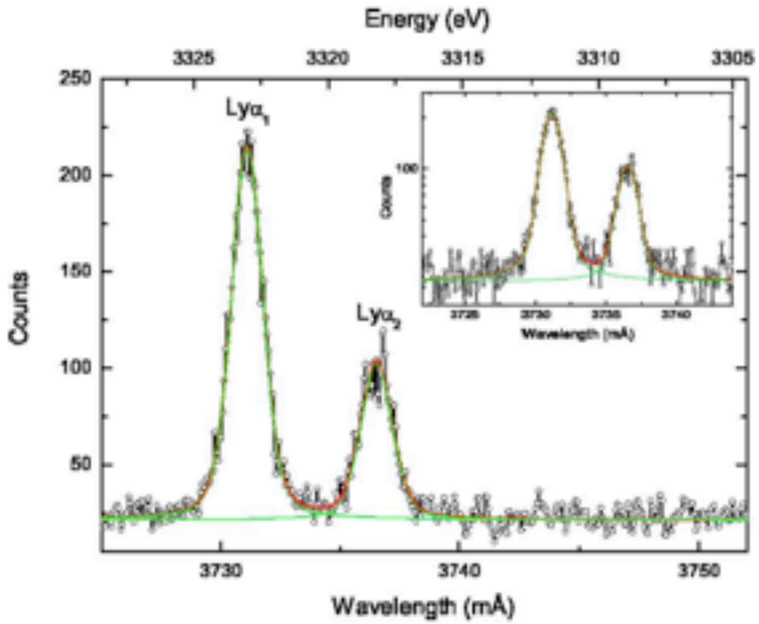

FIG. 4. Sum of all 24 Lyman-α spectra after relative calibration (24 h total measuring time). The line describes a Voigt fit to the spectrum, the inset shows the spectrum with a logarithmic scale. There is no indication for shifts of the Lyman-α lines due to close-lying satellites.

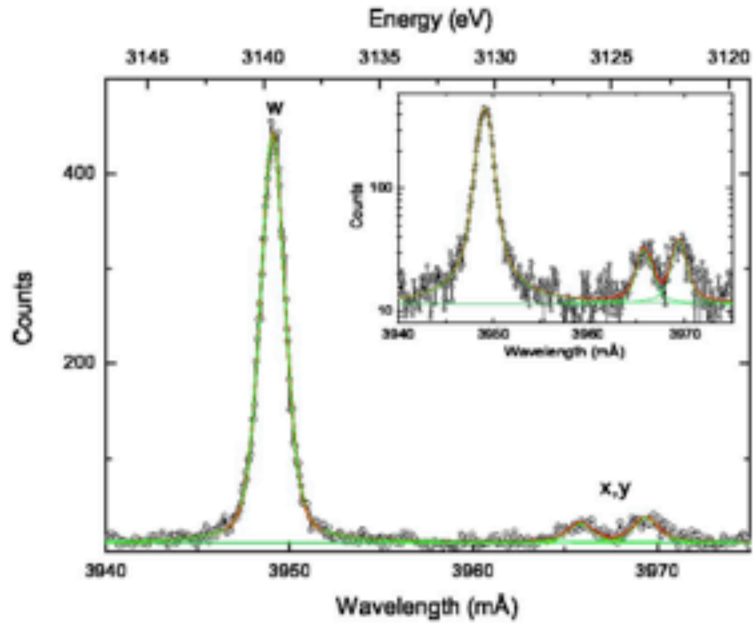

FIG. 5. Sum of all 23 w spectra after relative calibration (11.5 h total measuring time). The line describes a Voigt fit to the spectrum and the insert shows the spectrum with a logarithmic scale. There is no indication for shifts of the w-line due to close-lying satellites.

EBIT: Heidelberg

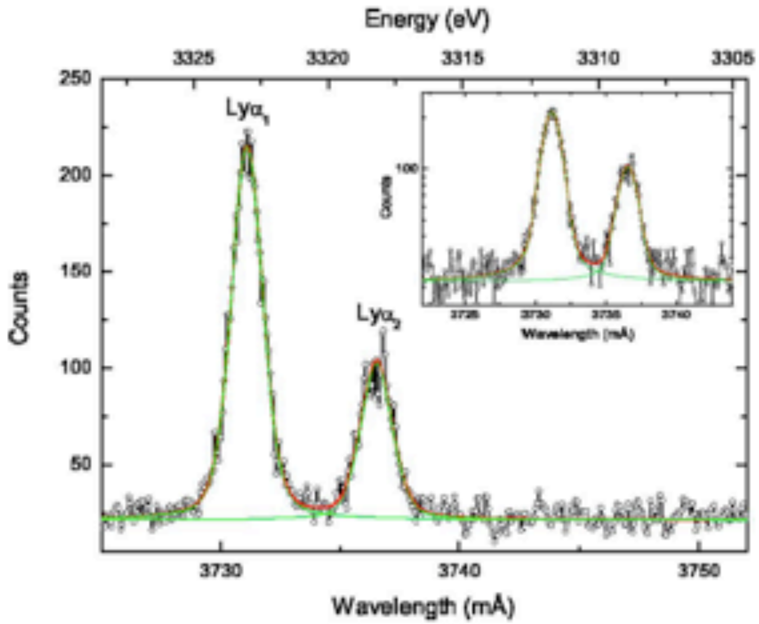

FIG. 4. Sum of all 24 Lyman-α spectra after relative calibration (24 h total measuring time). The line describes a Voigt fit to the spectrum, the inset shows the spectrum with a logarithmic scale. There is no indication for shifts of the Lyman-α lines due to close-lying satellites.

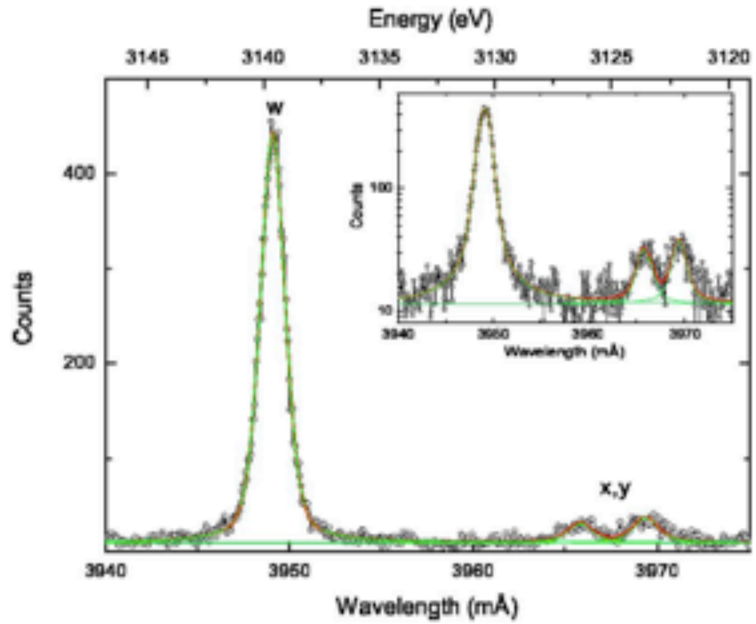

FIG. 5. Sum of all 23 w spectra after relative calibration (11.5 h total measuring time). The line describes a Voigt fit to the spectrum and the insert shows the spectrum with a logarithmic scale. There is no indication for shifts of the w-line due to close-lying satellites.

Heidelberg EBIT (2)

Table 1. Present experimental results and theoretical values.

Transition	E_{theo} (eV)	E_{exp} (eV)	Error (ppm)
Cl^{16+} Ly-α_1	2962.352 [22]	**2962.344(30)** [28]	**10.0**
S^{14+} w	2460.629 [5]	**2460.641(32)**	**13.0**
Ar^{16+} w	3139.582 [5]	**3139.583(6)** [28]	**1.9**

Novel technique for high-precision Bragg-angle determination in crystal x-ray spectroscopy, J. Braun, H. Bruhns, M. Trinczek *et al.* Rev. Sci. instrum. **76,** 073105-6 (2005).
Testing QED Screening and Two-Loop Contributions with He-Like Ions, H. Bruhns, J. Braun, K. Kubiček *et al.* Phys. Rev. Let. **99,** 113001-4 (2007).
Two-loop QED contributions tests with mid-Z He-like ions, K. Kubiček, H. Bruhns, J. Braun *et al.* J. Phys.: Conf. Ser. 012007 (2009)

Spectra: Relativistic M1 in He-like Argon

First absolute measurement of highly-charged ions transition energies and width

$1s\,2s\ {}^3S_1 - 1s^2\ {}^1S_0$ in He-like Argon ($Z\alpha \sim 0.13$)

Typical parallel spectrum

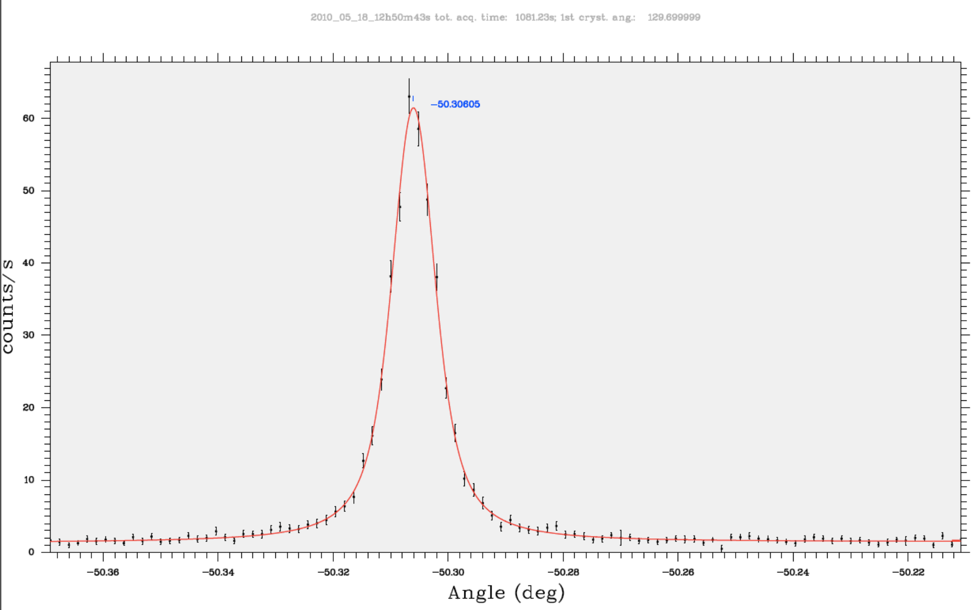

M1 $1s\,2s\ {}^3S_1 \rightarrow 1s^2\ {}^1S_0$

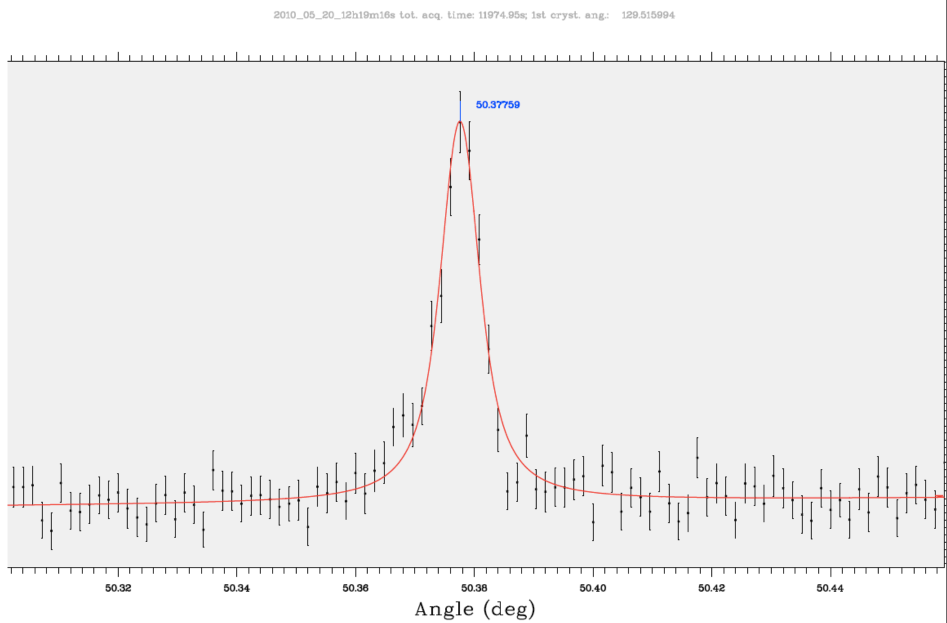

Typical acquisition time 40 mn parallel side and ~3:30h antiparallel

Other production methods (accelerators, Electron-Beam Ion Traps) provide diagram lines like the $1s\,2p\ {}^1P_1 - 1s^2\ {}^1S_0$ line

1s lamb-shift in H-like ions

No experiment to date, except on Hydrogen, tests the two-loop contributions

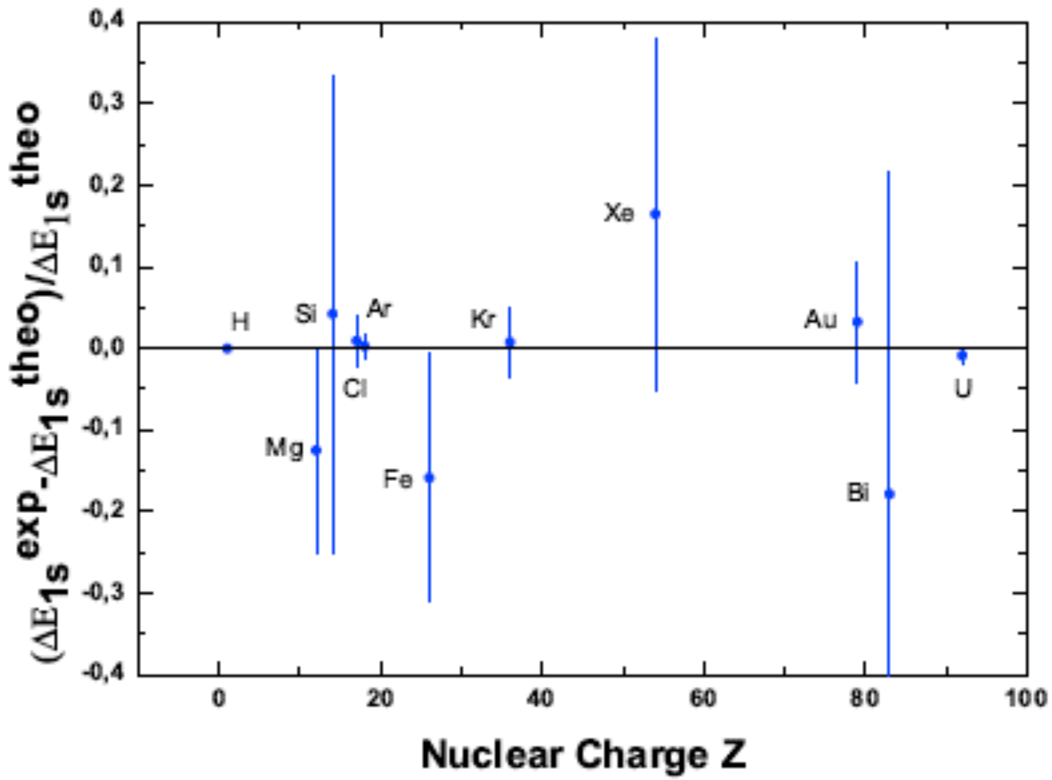

From K. Kubiček, H. Bruhns, J. Braun, J.R.C. Lopez-Urrutia et J. Ullrich. J. Phys.: Conf. Series. 012007, (2009).

1s lamb-shift in H-like ions

No experiment to date, except on Hydrogen, tests the two-loop contributions

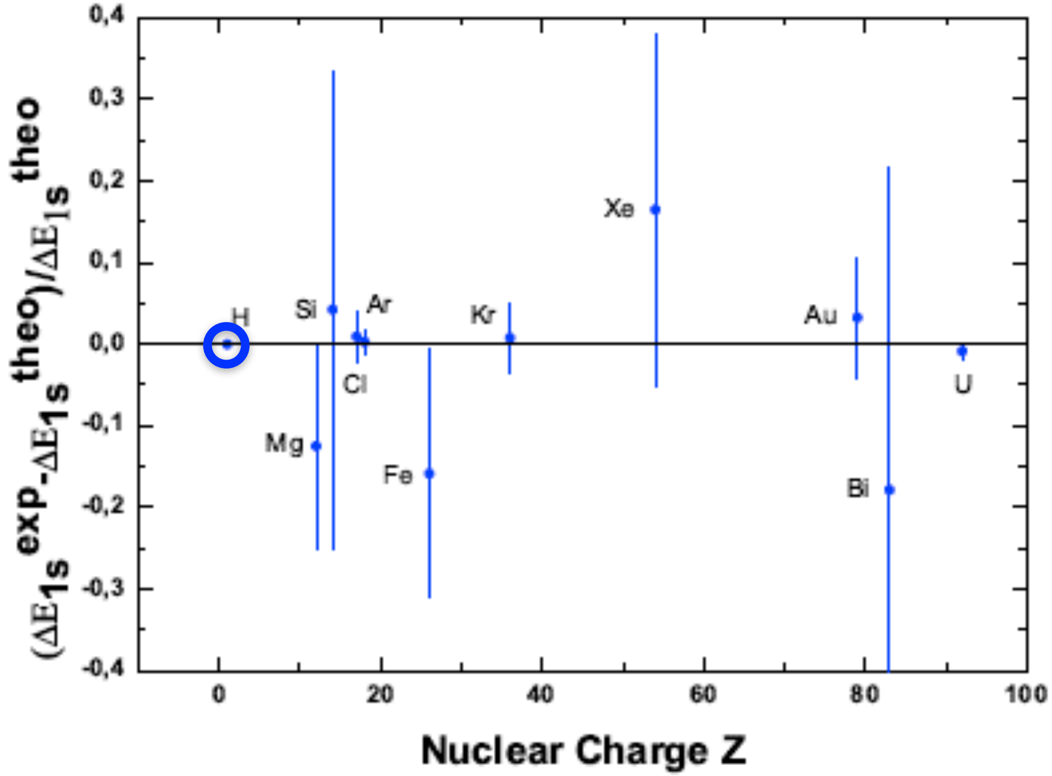

From K. Kubiček, H. Bruhns, J. Braun, J.R.C. Lopez-Urrutia et J. Ullrich. J. Phys.: Conf. Series. 012007, (2009).

1s lamb-shift in H-like ions

No experiment to date, except on Hydrogen, tests the two-loop contributions

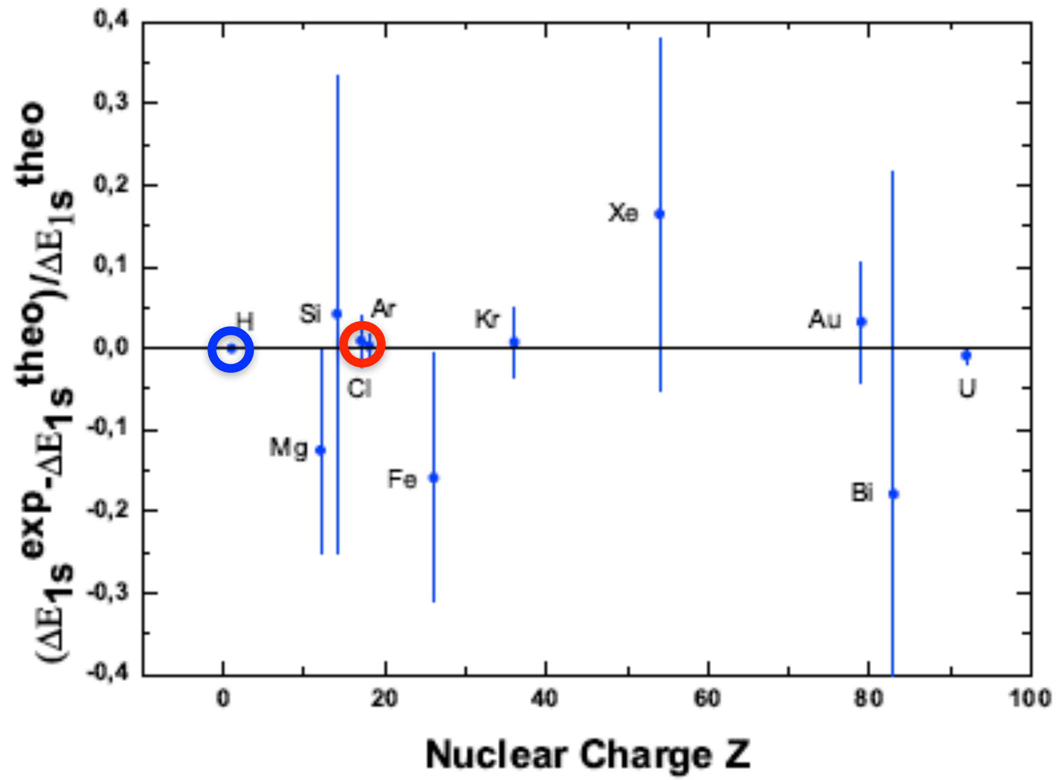

From K. Kubiček, H. Bruhns, J. Braun, J.R.C. Lopez-Urrutia et J. Ullrich. J. Phys.: Conf. Series. 012007, (2009).

1s lamb-shift in H-like ions

No experiment to date, except on Hydrogen, tests the two-loop contributions

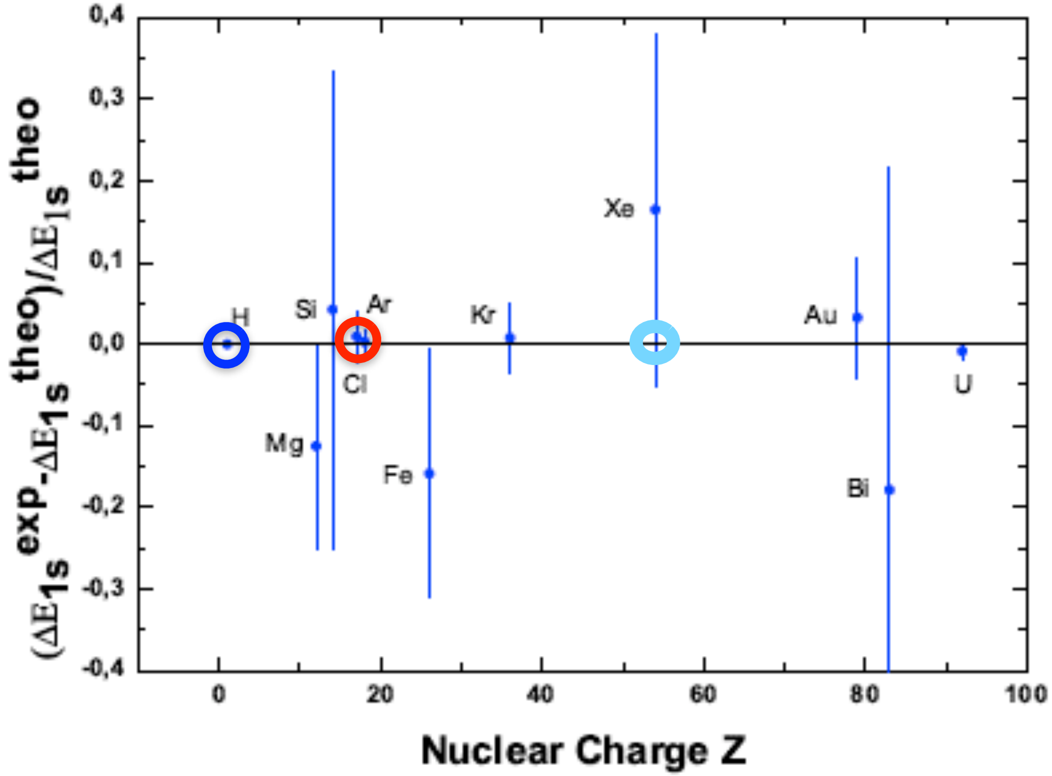

From K. Kubiček, H. Bruhns, J. Braun, J.R.C. Lopez-Urrutia et J. Ullrich. J. Phys.: Conf. Series. 012007, (2009).

1s lamb-shift in H-like ions

No experiment to date, except on Hydrogen, tests the two-loop contributions

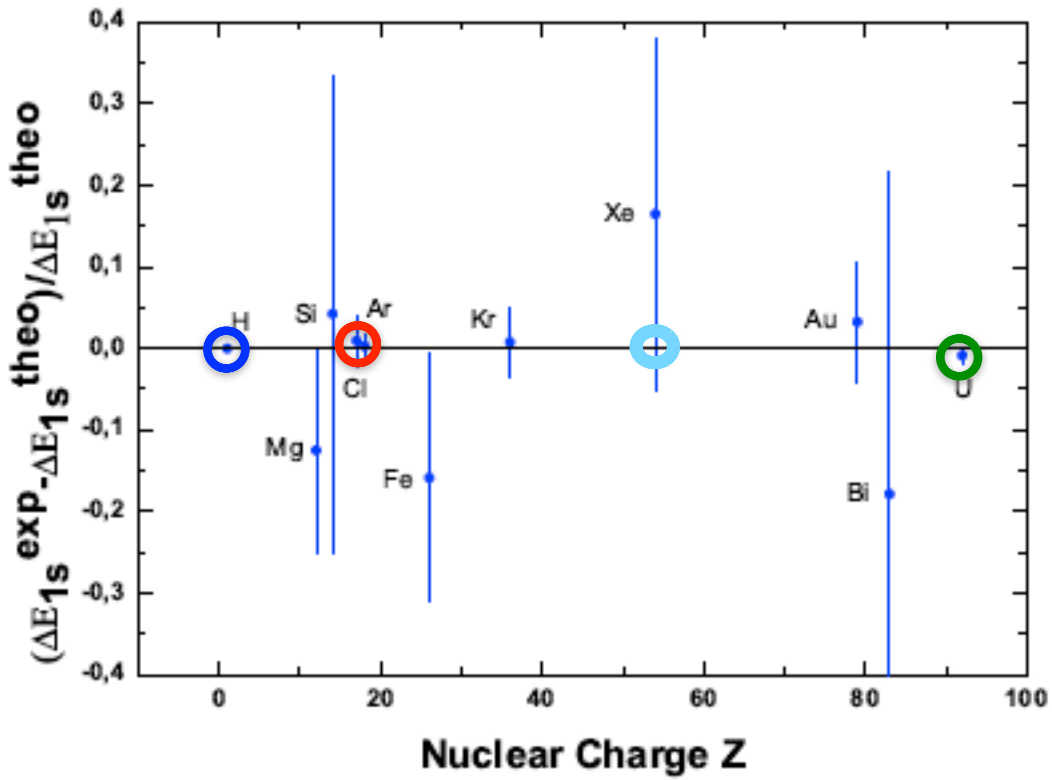

From K. Kubiček, H. Bruhns, J. Braun, J.R.C. Lopez-Urrutia et J. Ullrich. J. Phys.: Conf. Series. 012007, (2009).

Helium-like ions 1s2p $^1P_1 \rightarrow 1s^2$

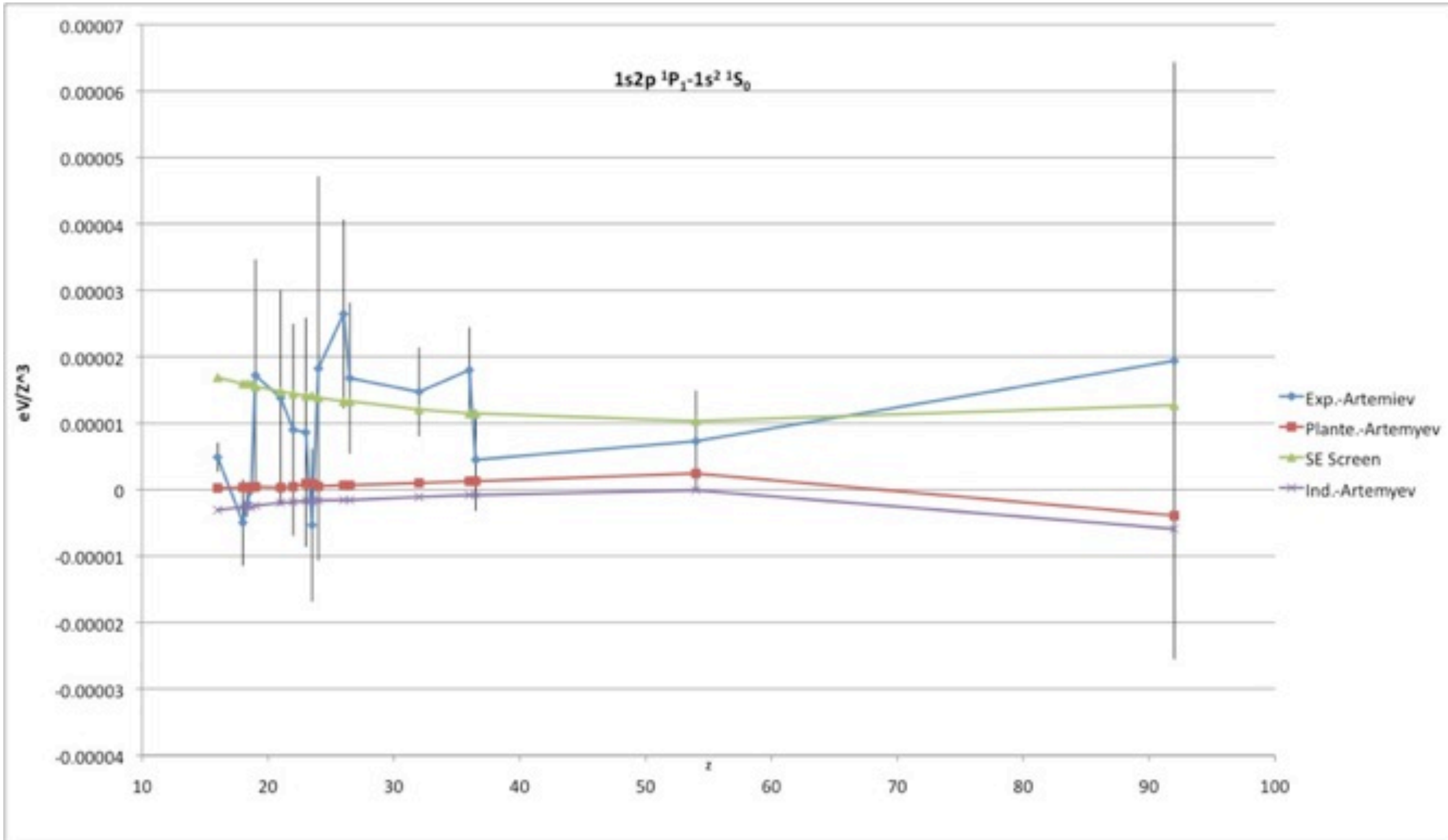

Helium-like ions M1: 1s2s $^3S_1 \rightarrow 1s^2$

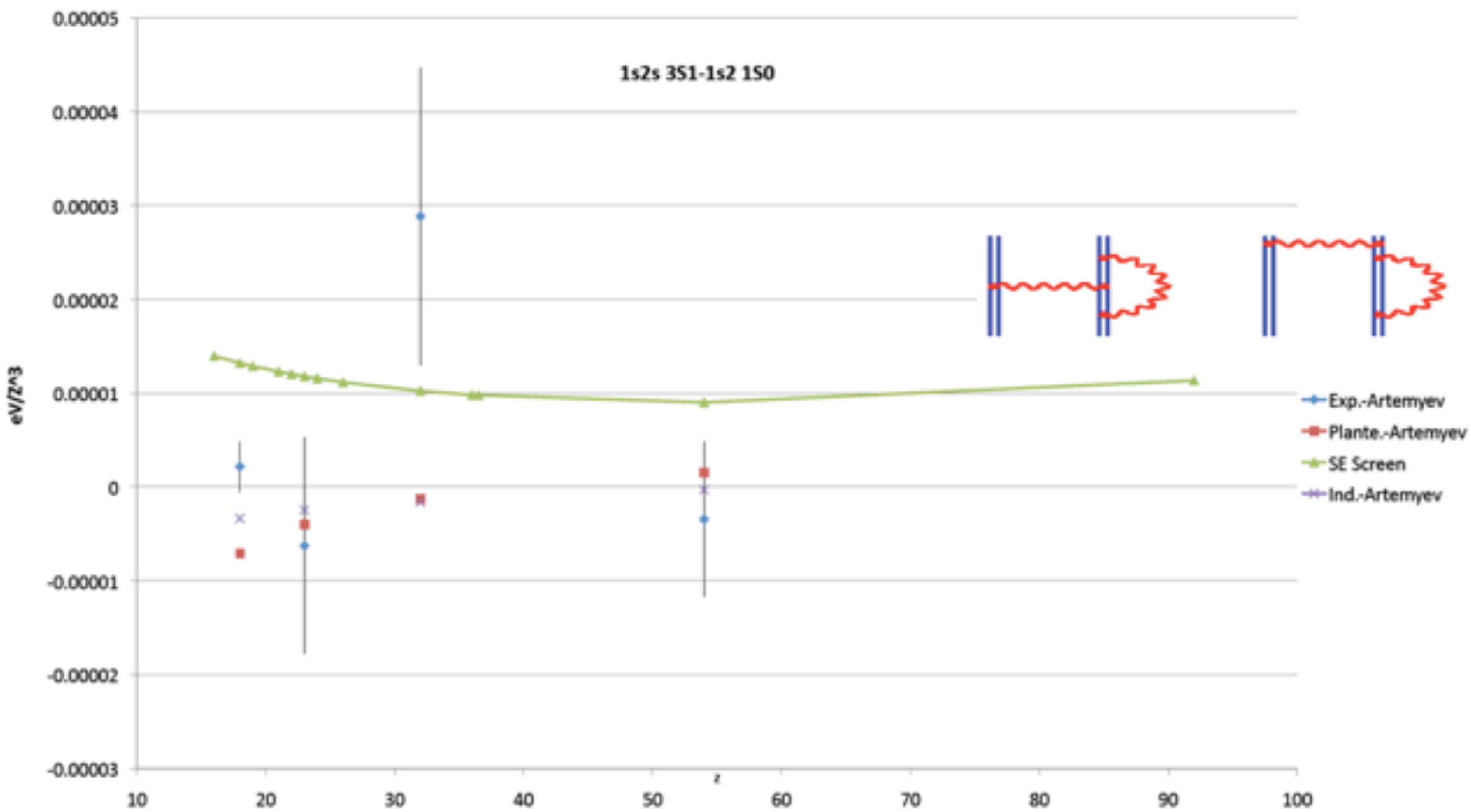

NRQED

The hydrogen/muonic hydrogen puzzle

μP theory

Discrepancy=0.31 meV
Th. uncertainty=0.005 meV
$\Longrightarrow 60\delta(\text{theory})$ deviation

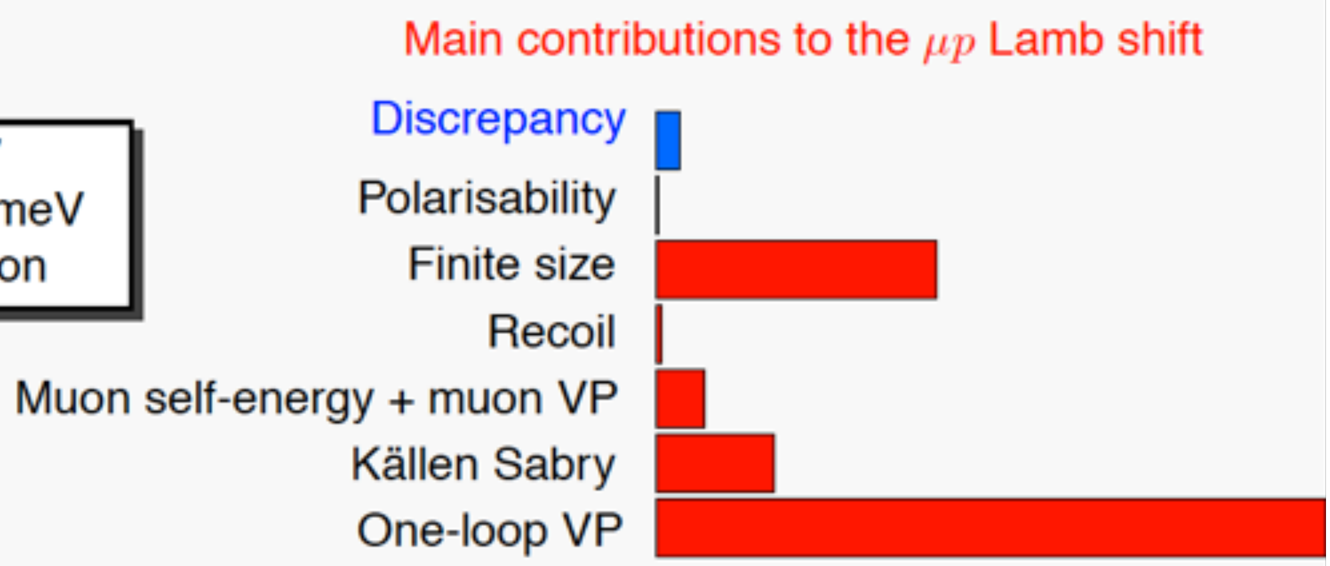

Most important contributions 1

Diagram	Value (in meV)	Name & order	References
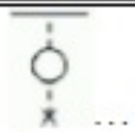	205.0074(1)	leading order VP $[\alpha(Z\alpha)^2]$	Galanin and Pomeranchuk [1952], Pachucki [1999, Table I], Eides et al. [2001, Eq. (208)]
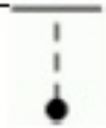	−3.862(108)	leading nuclear size contribution $[(Z\alpha)^4 m_r^3 \langle r^2 \rangle]$	Eides et al. [2001, § 9.6], Pachucki [1999, Table I]
	1.5079(1)	two-loop EVP $[\alpha^2(Z\alpha)^2 m]$	Di Giacomo [1969], Pachucki [1999, Table I], Eides et al. [2001, Eq. (213)]
	−0.6677(1)	muon self-energy + muon VP	Pachucki [1999, Table I], Eides et al. [2001, § 9.5]
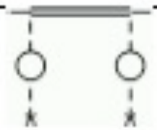	0.1509(1)	double EVP $[\alpha^2(Z\alpha)^2]$	Pachucki [1999, Table I], -0.3268 Eides et al. [2001, Eq. (215)], Pachucki [1996, Eq. (31)]
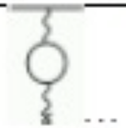	0.0594(1)	rel. corr. to EVP $[\alpha(Z\alpha)^4]$	Pachucki [1996], Pachucki [1999, Table I], Eides et al. [2001, Eq. (223)]
	0.0575(1)	recoil of order α^4 $[\alpha^4]$	Barker and Glover [1955], Pachucki [1999, Table I], Eides et al. [2001, Table 11]
	−0.0440(1)	recoil corrections of order $(Z\alpha)^n \frac{m}{M} m$	Eides et al. [2001, § 9.5], Pachucki [1999, Table I]

- Shift to recover the CODATA radius:
  ➡-0.327 meV
- Strategy: check all large contributions

Most important contributions 1

Diagram	Value (in meV)	Name & order	References
	205.0074(1)	leading order VP $[\alpha(Z\alpha)^2]$	Galanin and Pomeranchuk [1952], Pachucki [1999, Table I], Eides et al. [2001, Eq. (208)]
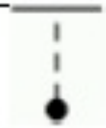	−3.862(108)	leading nuclear size contribution $[(Z\alpha)^4 m_r^3 \langle r^2 \rangle]$	Eides et al. [2001, § 9.6], Pachucki [1999, Table I]
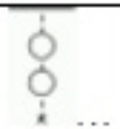	1.5079(1)	two-loop EVP $[\alpha^2(Z\alpha)^2 m]$	Di Giacomo [1969], Pachucki [1999, Table I], Eides et al. [2001, Eq. (213)]
	−0.6677(1)	muon self-energy + muon VP	Pachucki [1999, Table I], Eides et al. [2001, § 9.5]
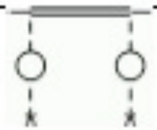	0.1509(1)	double EVP $[\alpha^2(Z\alpha)^2]$	Pachucki [1999, Table I], Eides et al. [2001, Eq. (215)], Pachucki [1996, Eq. (31)] -0.3268
	0.0594(1)	rel. corr. to EVP $[\alpha(Z\alpha)^4]$	Pachucki [1996], Pachucki [1999, Table I], Eides et al. [2001, Eq. (223)]
	0.0575(1)	recoil of order α^4 $[\alpha^4]$	Barker and Glover [1955], Pachucki [1999, Table I], Eides et al. [2001, Table 11]
	−0.0440(1)	recoil corrections of order $(Z\alpha)^n \frac{m}{M} m$	Eides et al. [2001, § 9.5], Pachucki [1999, Table I]

- Shift to recover the CODATA radius:
  ➡-0.327 meV
- Strategy: check all large contributions

samedi 11 décembre 2010

Most important contributions 2

	0.03(3)	light by light electron-loop contribution of order $\alpha^2(Z\alpha)^3 m$ $[\alpha^2(Z\alpha)^3 m]$	Pachucki [1996, p. 2095], Eides et al. [2001, § 9.3.2]
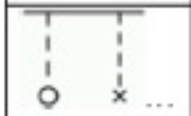	0.0232(15)	nuclear size correction of order $(Z\alpha)^5$ $[(Z\alpha)^5 m_r^3 \langle r^3\rangle_{(2)} m]$	Pachucki [1996], Faustov and Martynenko [2000], Eides et al. [2001, Eq. (256)], Pachucki [1999]
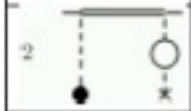	−0.0126(1)	(part of the) EVP with finite size $[\alpha(Z\alpha)^4 m_r^3 \langle r^2\rangle]$	Pachucki [1996], Pachucki [1999, Table I], Eides et al. [2001, Eq. (268)]
	0.012(2)	proton polarizability $[(Z\alpha)^5 m]$	Startsev et al. [1976], Rosenfelder [2000], Faustov and Martynenko [2000], Pachucki [1999, Table I], Eides et al. [2001, Eq. (261)]
	0.0108(4)	hadronic polarization, order $\alpha(Z\alpha)^4 m$ $[\alpha(Z\alpha)^4 m]$	Folomeshkin [1974], Friar et al. [1999], Faustov and Martynenko [1999], Eides et al. [2001, Eq. (252)], Pachucki [1999, Table I]
	−0.0099(1)	proton self-energy	Pachucki [1999, Table I]
	−0.0095(1)	radiative-recoil corrections of order $\alpha(Z\alpha)^n \frac{m}{M} m$	Eides et al. [2001, § 9.5]
	−0.0083(1)	(part of the) EVP with finite size $[\alpha(Z\alpha)^4 m_r^3 \langle r^2\rangle]$	Friar [1979a], Friar [1981], Pachucki [1996], Pachucki [1999, Table I], Eides et al. [2001, Eq. (266)]
	−0.006(1)	muon self-energy with electron VP $[\alpha^2(Z\alpha)^4]$	Pachucki [1996, Eqs. (40) and (45)], Pachucki [1999, Table I], Eides et al. [2001, Eq. (237)]
	0.0053(1)	three-loop electron polarization contribution, order $\alpha^3(Z\alpha)^2$ $[\alpha^3(Z\alpha)^2 m]$	Kinoshita and Nio [1999], Eides et al. [2001, Eq. (214)], Pachucki [1999, Table I]

268

- No term looks large enough to be able to explain the difference in size

ober 14,

Most important contributions 2

	0.03(3)	light by light electron-loop contribution of order $\alpha^2(Z\alpha)^3m$ $[\alpha^2(Z\alpha)^3m]$	Pachucki [1996, p. 2095], Eides et al. [2001, § 9.3.2]
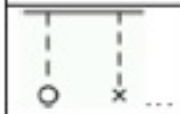	0.0232(15)	nuclear size correction of order $(Z\alpha)^5$ $[(Z\alpha)^5m_r^2\langle r^3\rangle_{(2)}m]$	Pachucki [1996], Faustov and Martynenko [2000], Eides et al. [2001, Eq. (256)], Pachucki [1999]
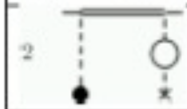	−0.0126(1)	(part of the) EVP with finite size $[\alpha(Z\alpha)^4m_r^3\langle r^2\rangle]$	Pachucki [1996], Pachucki [1999, Table I], Eides et al. [2001, Eq. (268)]
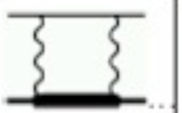	0.012(2)	proton polarizability $[(Z\alpha)^5m]$	Startsev et al. [1976], Rosenfelder [2000], Faustov and Martynenko [2000], Pachucki [1999, Table I], Eides et al. [2001, Eq. (261)]
	0.0108(4)	hadronic polarization, order $\alpha(Z\alpha)^4m$ $[\alpha(Z\alpha)^4m]$	Folomeshkin [1974], Friar et al. [1999], Faustov and Martynenko [1999], Eides et al. [2001, Eq. (252)], Pachucki [1999, Table I]
	−0.0099(1)	proton self-energy	Pachucki [1999, Table I]
	−0.0095(1)	radiative-recoil corrections of order $\alpha(Z\alpha)^n\frac{m}{M}m$	Eides et al. [2001, § 9.5]
	−0.0083(1)	(part of the) EVP with finite size $[\alpha(Z\alpha)^4m_r^3\langle r^2\rangle]$	Friar [1979a], Friar [1981], Pachucki [1996], Pachucki [1999, Table I], Eides et al. [2001, Eq. (266)]
	−0.006(1)	muon self-energy with electron VP $[\alpha^2(Z\alpha)^4]$	Pachucki [1996, Eqs. (40) and (45)], Pachucki [1999, Table I], Eides et al. [2001, Eq. (237)]
	0.0053(1)	three-loop electron polarization contribution, order $\alpha^3(Z\alpha)^2$ $[\alpha^3(Z\alpha)^2m]$	Kinoshita and Nio [1999], Eides et al. [2001, Eq. (214)], Pachucki [1999, Table I]

268

ober 14,

Most important contributions 2

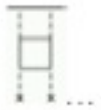	0.03(3)	light by light electron-loop contribution of order $\alpha^2(Z\alpha)^3m$ $[\alpha^2(Z\alpha)^3m]$	Pachucki [1996, p. 2095], Eides et al. [2001, § 9.3.2]
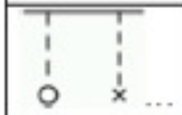	0.0232(15)	nuclear size correction of order $(Z\alpha)^5$ $[(Z\alpha)^5m_r^2\langle r^3\rangle_{(2)}m]$	Pachucki [1996], Faustov and Martynenko [2000], Eides et al. [2001, Eq. (256)], Pachucki [1999]
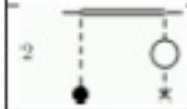	−0.0126(1)	(part of the) EVP with finite size $[\alpha(Z\alpha)^4m_r^3\langle r^2\rangle]$	Pachucki [1996], Pachucki [1999, Table I], Eides et al. [2001, Eq. (268)]
	0.012(2)	proton polarizability $[(Z\alpha)^5m]$	Startsev et al. [1976], Rosenfelder [2000], Faustov and Martynenko [2000], Pachucki [1999, Table I], Eides et al. [2001, Eq. (261)]
	0.0108(4)	hadronic polarization, order $\alpha(Z\alpha)^4m$ $[\alpha(Z\alpha)^4m]$	Folomeshkin [1974], Friar et al. [1999], Faustov and Martynenko [1999], Eides et al. [2001, Eq. (252)], Pachucki [1999, Table I]
	−0.0099(1)	proton self-energy	Pachucki [1999, Table I]
	−0.0095(1)	radiative-recoil corrections of order $\alpha(Z\alpha)^n\frac{m}{M}m$	Eides et al. [2001, § 9.5]
	−0.0083(1)	(part of the) EVP with finite size $[\alpha(Z\alpha)^4m_r^3\langle r^2\rangle]$	Friar [1979a], Friar [1981], Pachucki [1996], Pachucki [1999, Table I], Eides et al. [2001, Eq. (266)]
	−0.006(1)	muon self-energy with electron VP $[\alpha^2(Z\alpha)^4]$	Pachucki [1996, Eqs. (40) and (45)], Pachucki [1999, Table I], Eides et al. [2001, Eq. (237)]
	0.0053(1)	three-loop electron polarization contribution, order $\alpha^3(Z\alpha)^2$ $[\alpha^3(Z\alpha)^2m]$	Kinoshita and Nio [1999], Eides et al. [2001, Eq. (214)], Pachucki [1999, Table I]

268

New calculation: S. G. Karshenboim, V. G. Ivanov, E. Y. Korzinin, et al., Phys. Rev. A 81, 060501 (2010) and 1 S. Karshenboim, E. Korzinin, V. Ivanov, et al., JETP Letters 92, 8 (2010).
0.00115(1) meV

ober 14,

LKB

Check point nucleus

Non relativistic

Pachucki 1996 calculation	205.006
Pachucki 1999 calculation	205.007 4
Numerical calc with Pachucki data	205.007 385
Numerical calc with CODATA 2006 data	205.007 359

Relativistic

Borie calc with ? data	205.028 2
PI calc with CODATA 2006 data	205.028 20
PM calc with CODATA 2006 data	205.028 201

Energies in meV

Comparison of charge densities

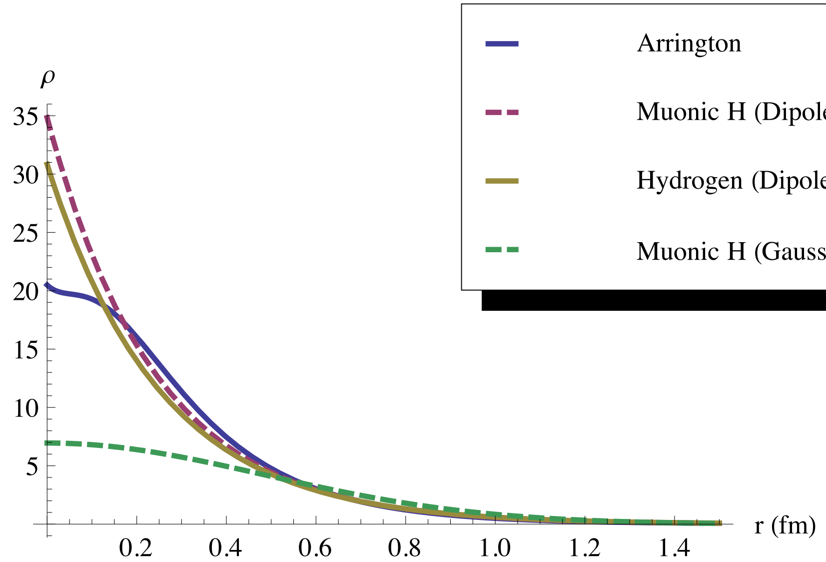

[1] QED is not endangered by the proton's size, A. De Rújula. Physics Letters B 693, 555-558 (2010).

Comparison of charge densities

[1] QED is not endangered by the proton's size, A. De Rújula. Physics Letters B 693, 555-558 (2010).

Comparison of charge densities

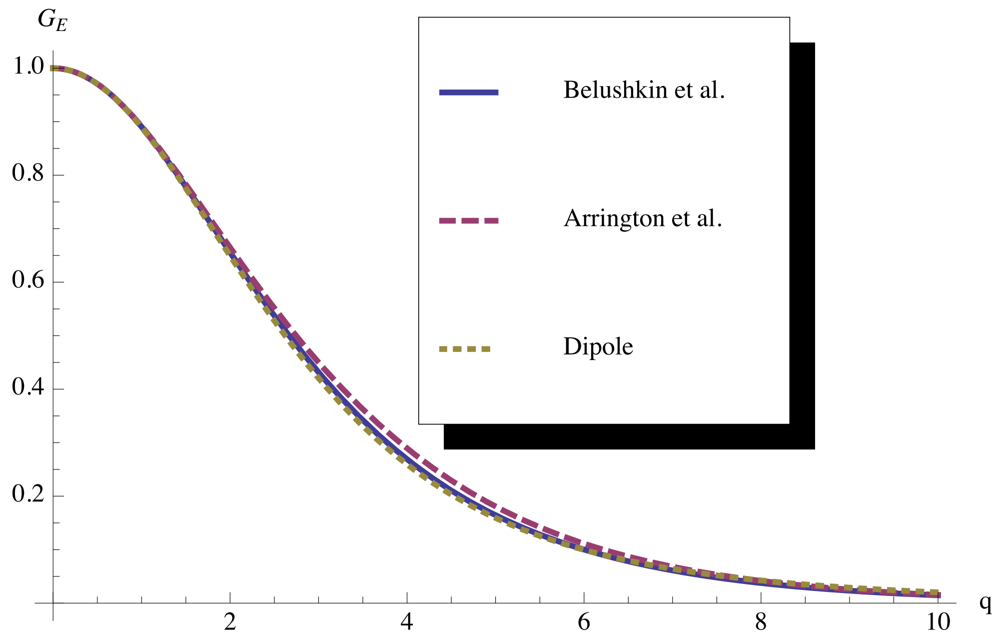

[1] QED is not endangered by the proton's size, A. De Rújula. Physics Letters B 693, 555-558 (2010).

Comparison of charge densities

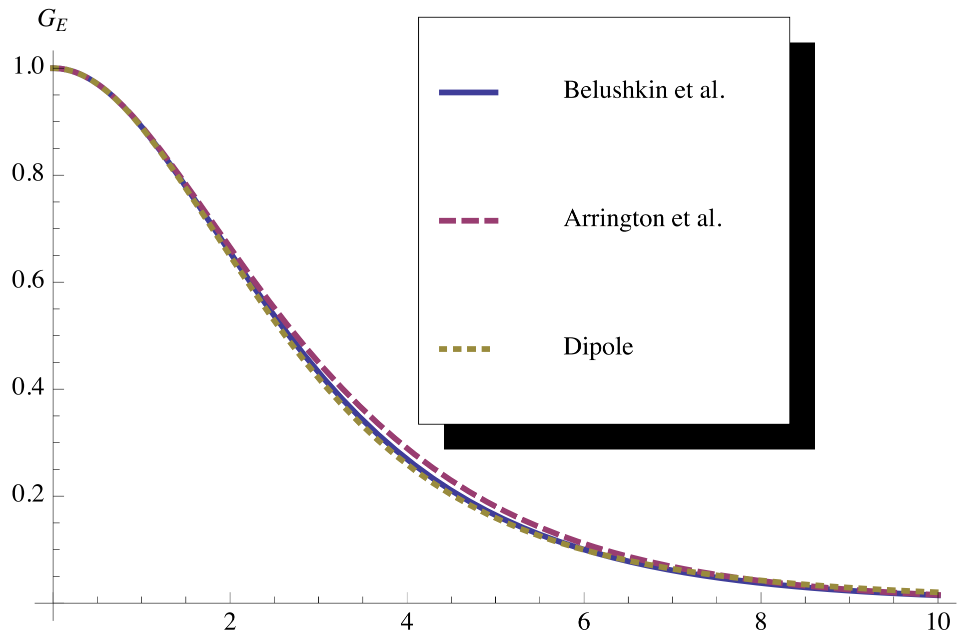

- $\langle r^3\rangle_{(2)}=3.789\ \langle r^2\rangle^{3/2}$ Dipole
- $\langle r^3\rangle_{(2)}=1.960\ \langle r^2\rangle^{3/2}$ Gauss
- $\langle r^3\rangle_{(2)}=3.983\ \langle r^2\rangle^{3/2}$ Arrington et al.

- $\langle r^3\rangle_{(2)}=36.6\pm7.3=43\ \langle r^2\rangle^{3/2}$ De Rùjula ?!

[1] QED is not endangered by the proton's size, A. De Rújula. Physics Letters B 693, 555-558 (2010).

Charge radius dependence Coul.+VP

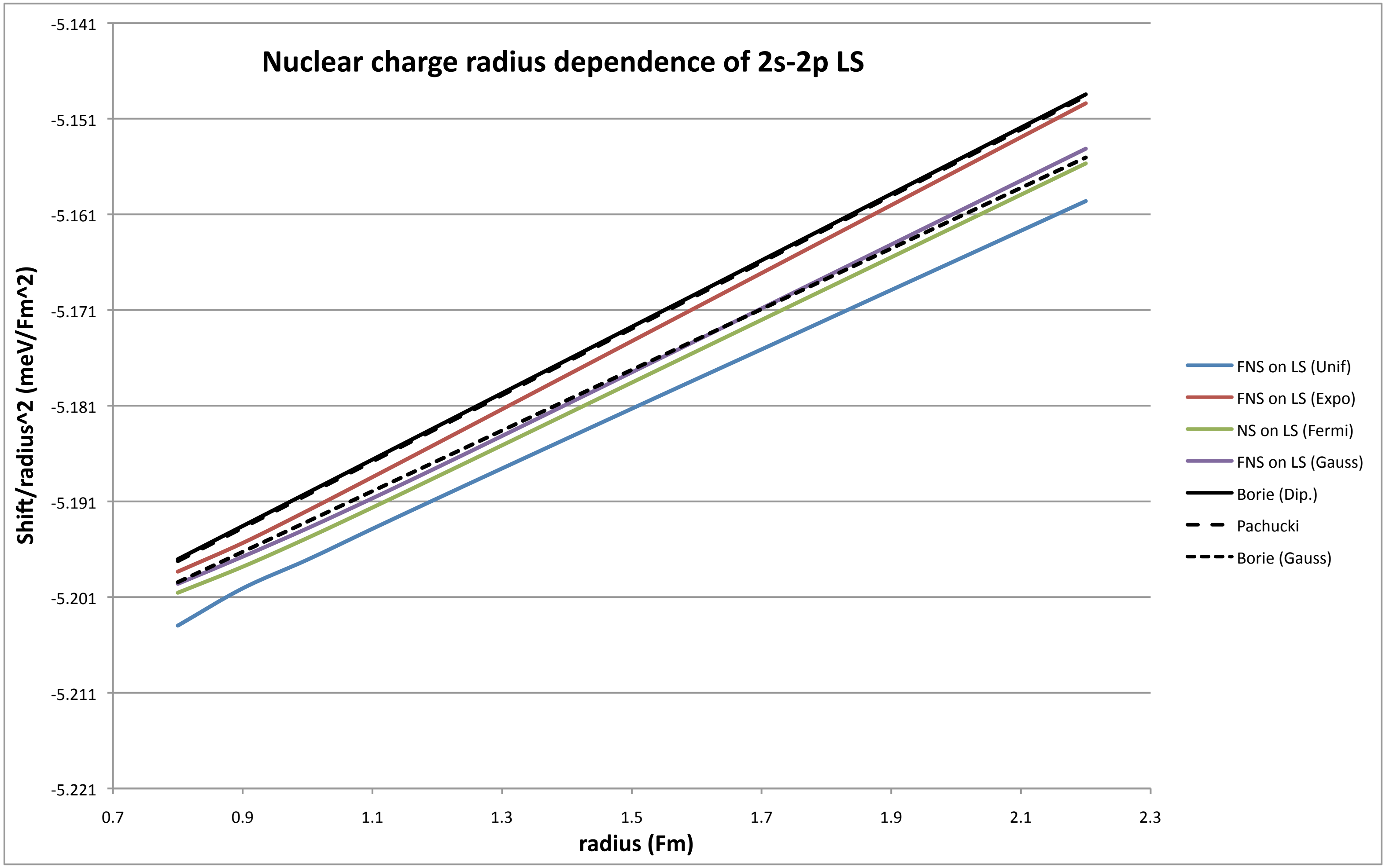

Fig. 3. Dependence of $\frac{\Delta E_{\mathrm{V11FN}}}{R^2}$ as a function of R in meV/fm^2 for different charge distribution models.

LKB

Charge radius dependence Coul.+VP

Model	a (meV/fm^2)	b (meV/fm^3)
Uniform	−5.2284	0.0313
Dipole	−5.2271	0.0353
Fermi	−5.2271	0.0324
Gauss	−5.2265	0.0328
Ref.[34], Dip.	−5.2248	0.0347
Ref.[32]	−5.225	0.0347
Ref.[34], Gauss	−5.2248	0.0317

Källen and Sabry

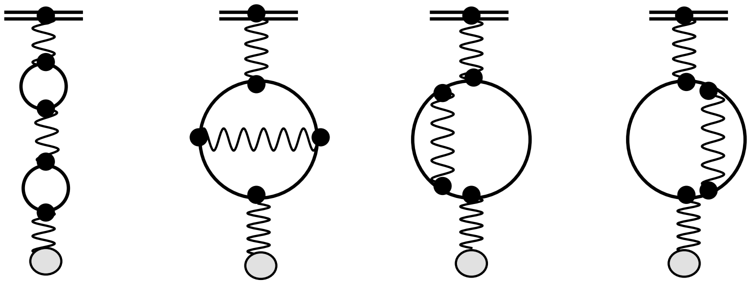

$$\Delta E = aR^2 + bR^3 + cR^4$$

Model	Uniform	Exponential	Fermi	Gaussian
a	-0.0002145	-0.0002145	-0.0002146	-0.0002145
b	0.0000078	0.0000086	0.0000082	0.0000083
c	-0.0000008	-0.0000009	-0.0000008	-0.0000009

LKB

Finite size correction on muon self-energy

All-orders calculations

$$E_{SE-NS}=\left(4\ln 2-\frac{23}{4}\right)\alpha(Z\alpha)\mathcal{E}_{NS}$$

$$\mathcal{E}_{NS}=\frac{2}{3}\left(\frac{\mu_r}{m_\mu}\right)^3\frac{(Z\alpha)^2}{n^3}m_\mu\left(\frac{Z\alpha<r>}{\lambda\!\!\!^{-}_C}\right)^2$$

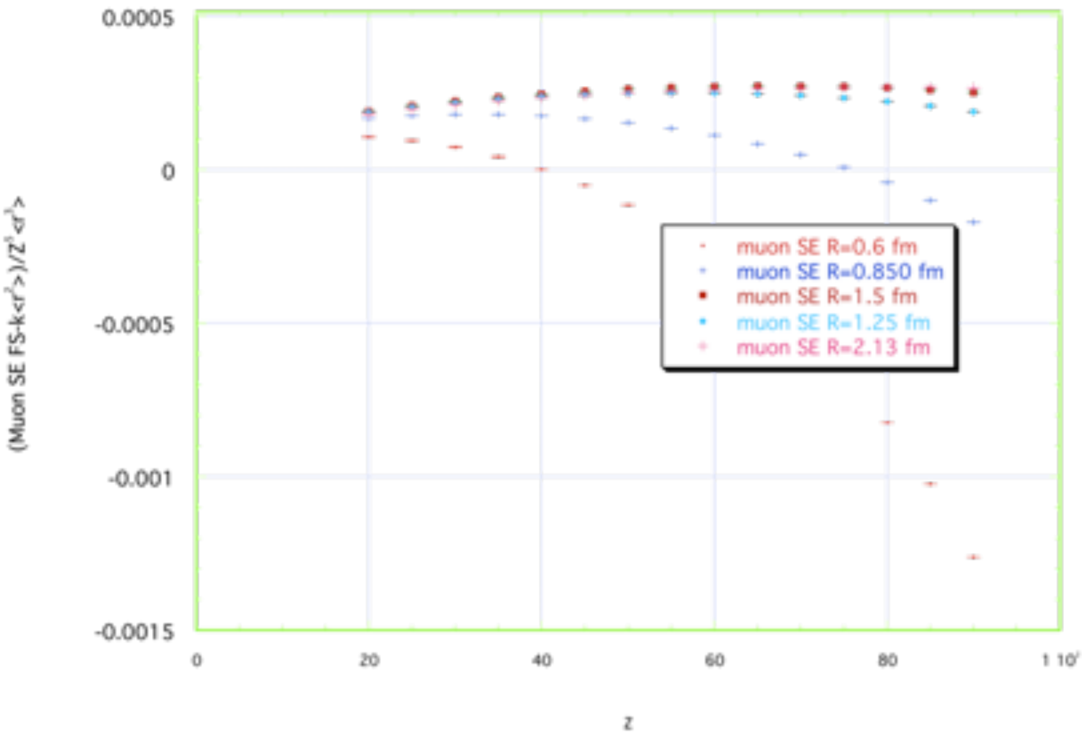

$$E_{SE-NS}=-0.000824<r^2>$$

(All-orders calculations-E_{SE-NS}<r^2>)/Z^5 <r^3>

$1.8\pm1\times10^{-5}$

samedi 11 décembre 2010

Example of unsolved problems

Dyson: the expansion in α of QED has zero convergence radius... e→-e, plus d'état lié!

Divergence of Perturbation Theory in Quantum Electrodynamics, F.J. Dyson. Physical Review 85, 631–632 (1952).

Example of unsolved problems

Example of unsolved problems

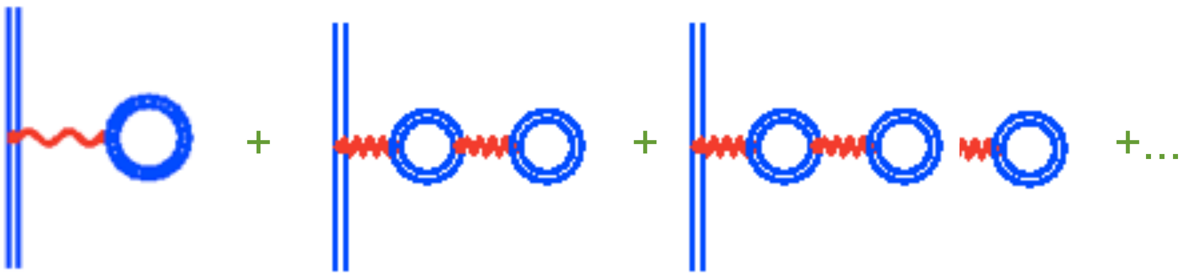

Vacuum Polarization re-summation

$$V_{\mathrm{VP}\infty}\left(k^2\right) = \frac{1}{k^2}\left[1+\Pi\left(k^2\right)+\Pi\left(k^2\right)\frac{1}{k^2}\Pi\left(k^2\right)+\Pi\left(k^2\right)\frac{1}{k^2}\Pi\left(k^2\right)\frac{1}{k^2}\Pi\left(k^2\right)+\cdots\right]$$

$$= \frac{\Pi\left(k^2\right)}{1-\Pi\left(k^2\right)}$$

$$\Pi\left(k^2\right) = \frac{2\alpha k^2}{3\pi}\int_1^\infty dz\frac{1}{z}\left(\frac{1}{z}+\frac{1}{2z^3}\right)\frac{\sqrt{z^2-1}}{4m_e^2z^2+k^2}.$$

Singularity at $k_0 = e^{\frac{3\pi}{2\alpha}+\frac{5}{6}} \approx 6.53\times 10^{280}$ **huge momenta = very short distances**

S. Brodsky, P. J. Mohr, P. Indelicato

LKB

Results

Nonrelativistic contributions of order to the Lamb shift in muonic hydrogen and deuterium, and in the muonic helium ion,
S.G. Karshenboim, V.G. Ivanov, E.Y. Korzinin *et al.* Phys. Rev. A **81,** 060501 (2010).

Light by light diagrams

$$206.05329710 - 5.227310 \langle r^2\rangle + 0.03489 \langle r^3\rangle + 0.000043 \langle r^4\rangle$$

R = 0.84130 fm in place of 0.84184(67) fm

From hydrogen (CODATA) : 0.8768(69) fm

Où on retrouve le vide

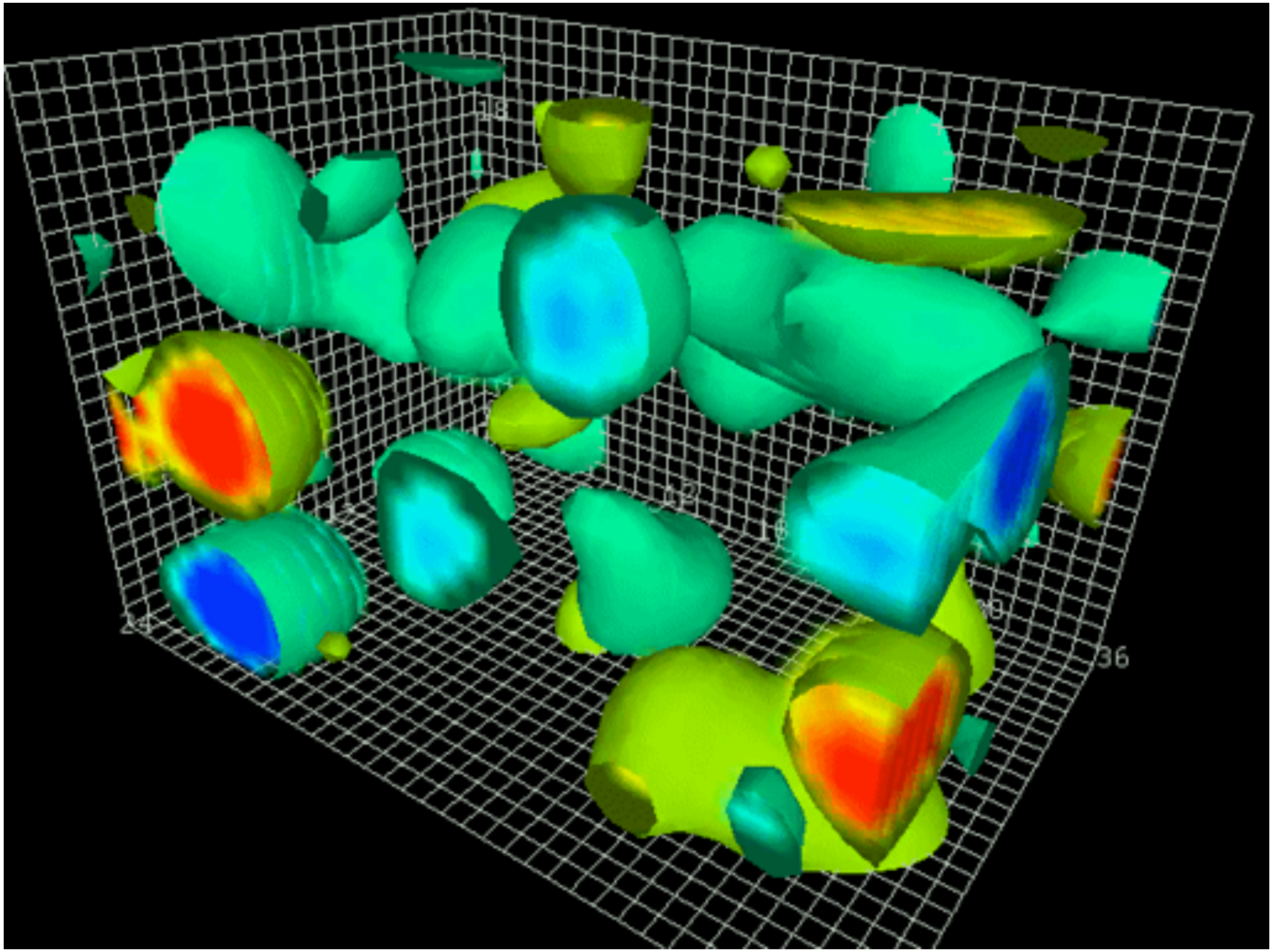

http://www.physics.adelaide.edu.au/~dleinweb/VisualQCD/QCDvacuum/welcome.html

Interaction avec un proton

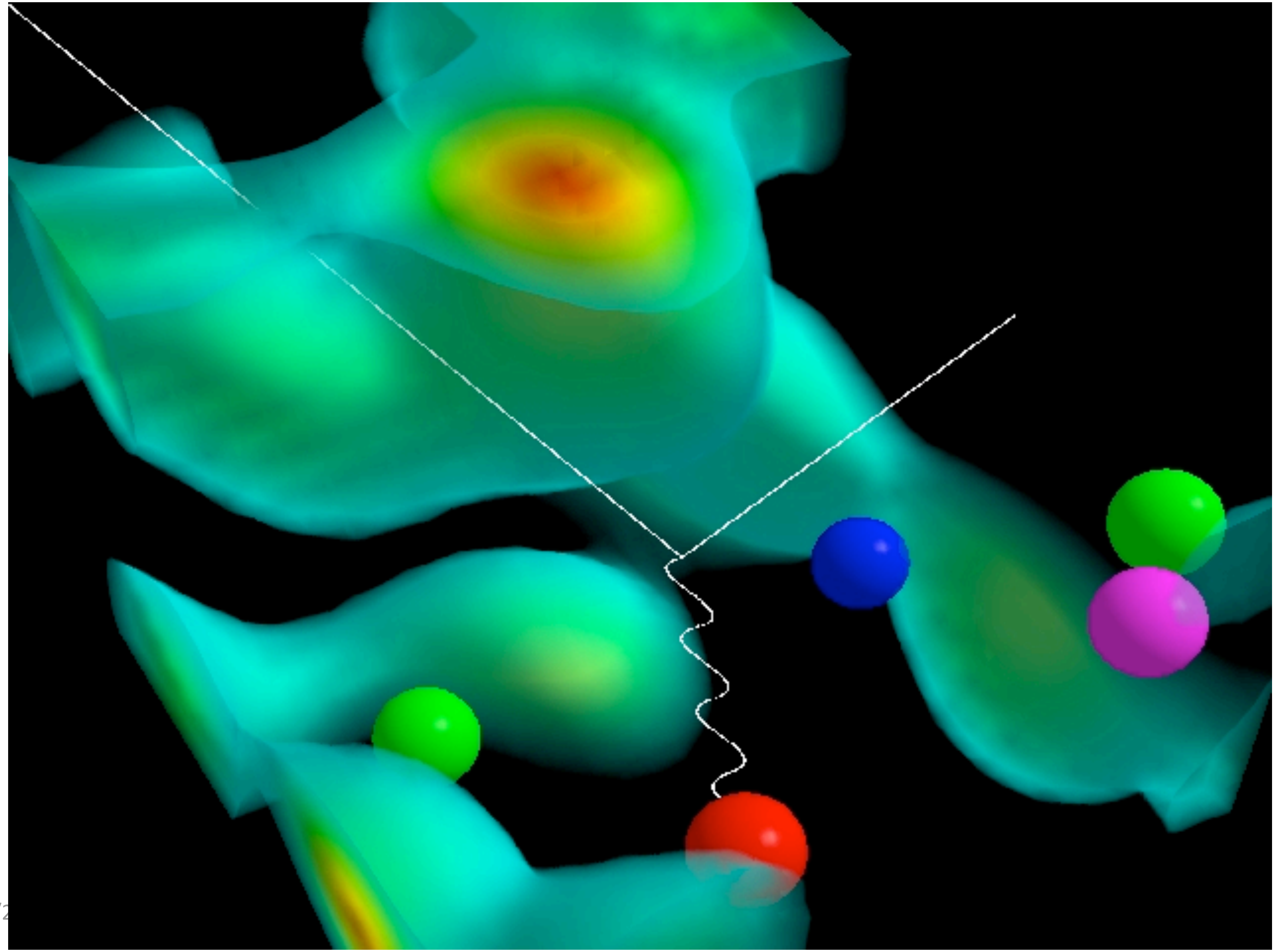

Super-heavy elements

A new regime for QED

Critical- and Super-Critical Fields

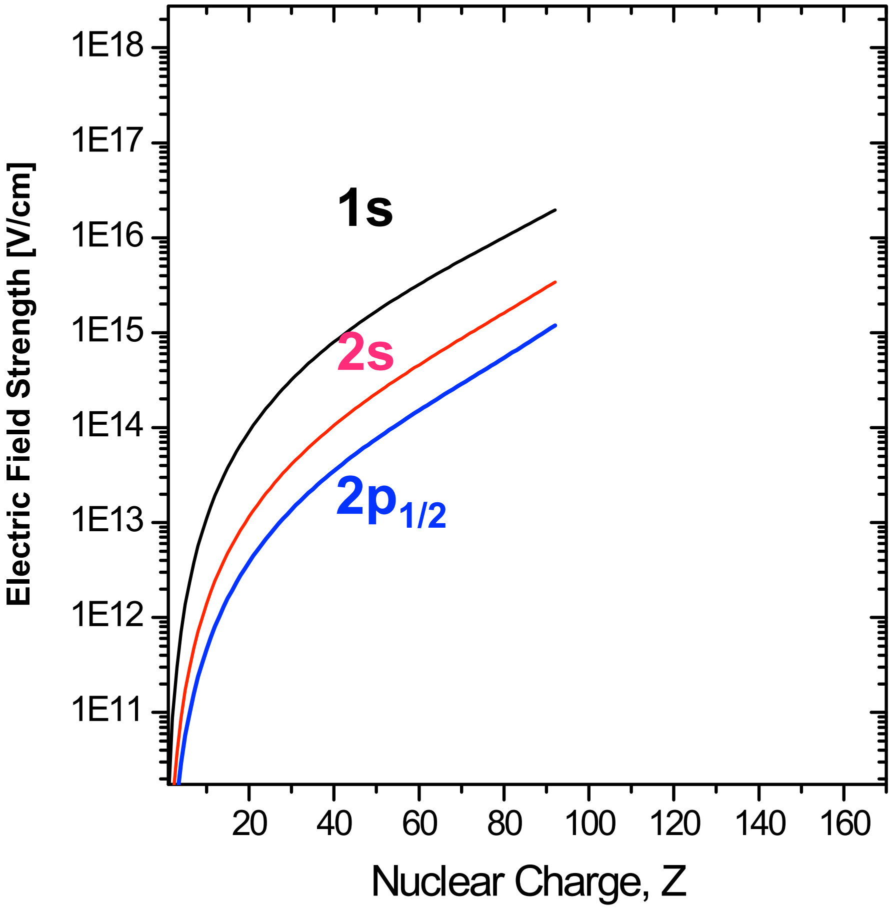

Critical- and Super-Critical Fields

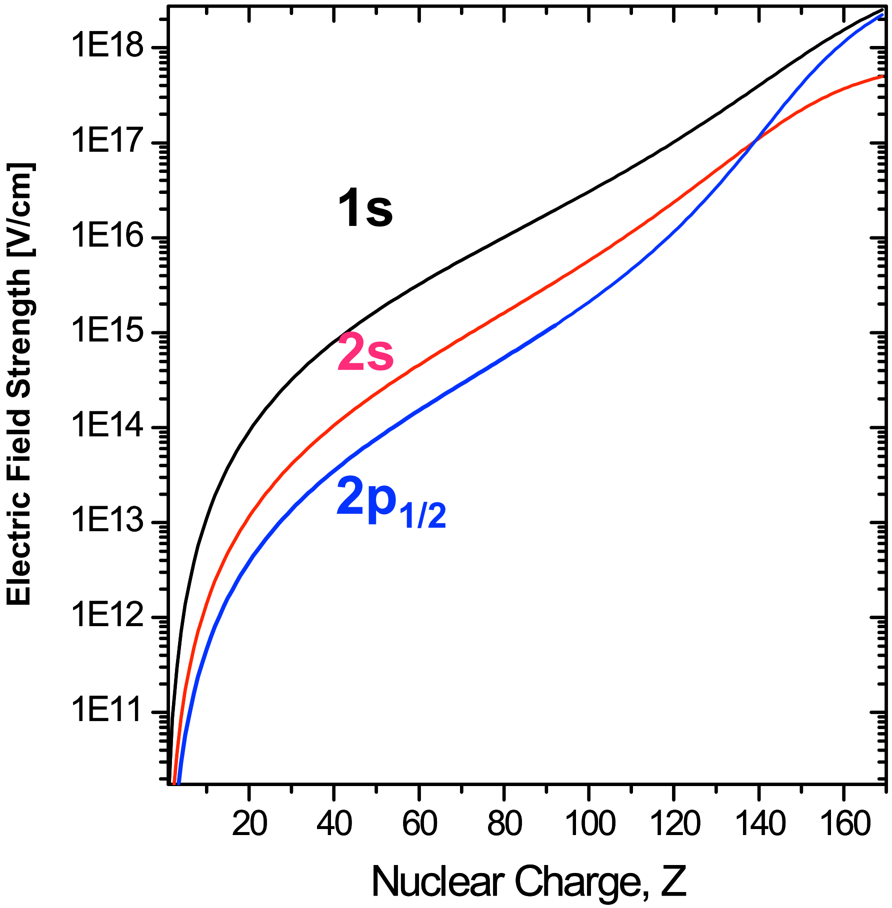

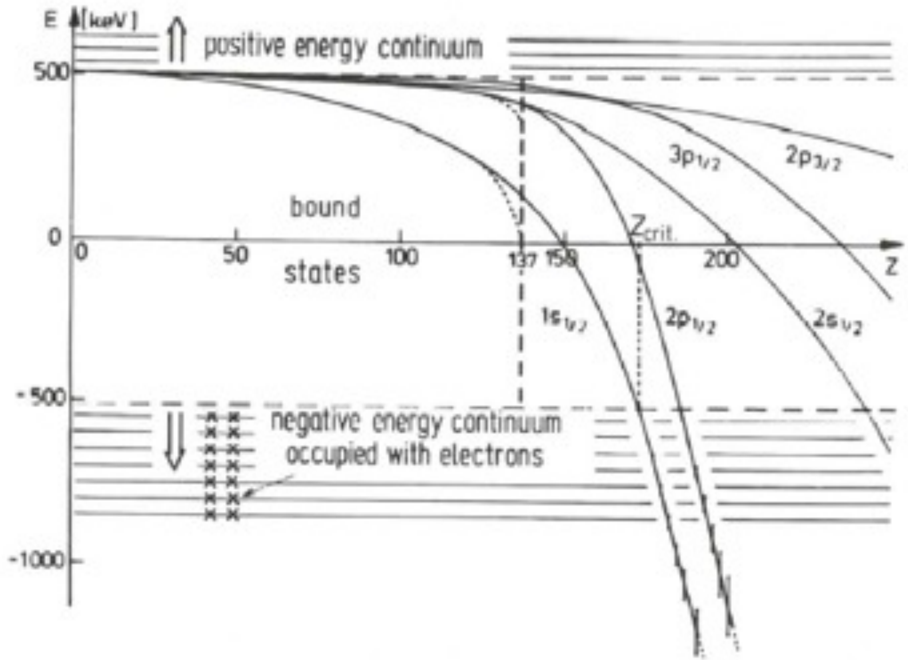

Critical- and Super-Critical Fields

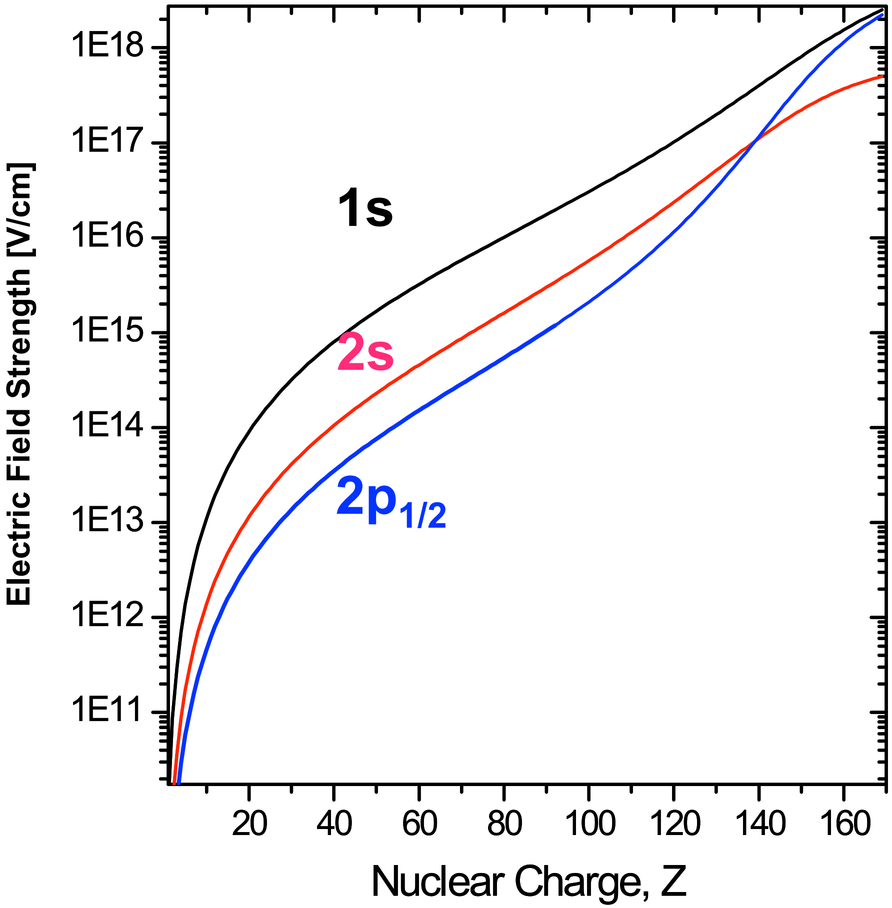

spectroscopy of the inner shells in superheavy quasimolecule systems with energy eigenvalues in the vicinity of the negative continuum

The vacuum decays into a charged vacuum in 10^{-21}s

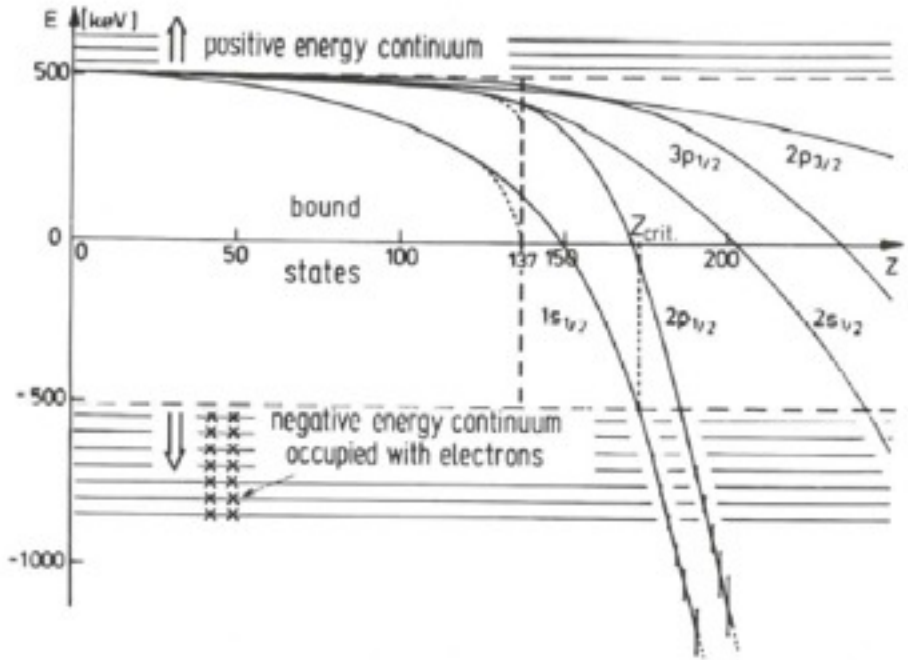

Electromagnetic Phenomena under Extreme & Unusual Conditions

High- γ

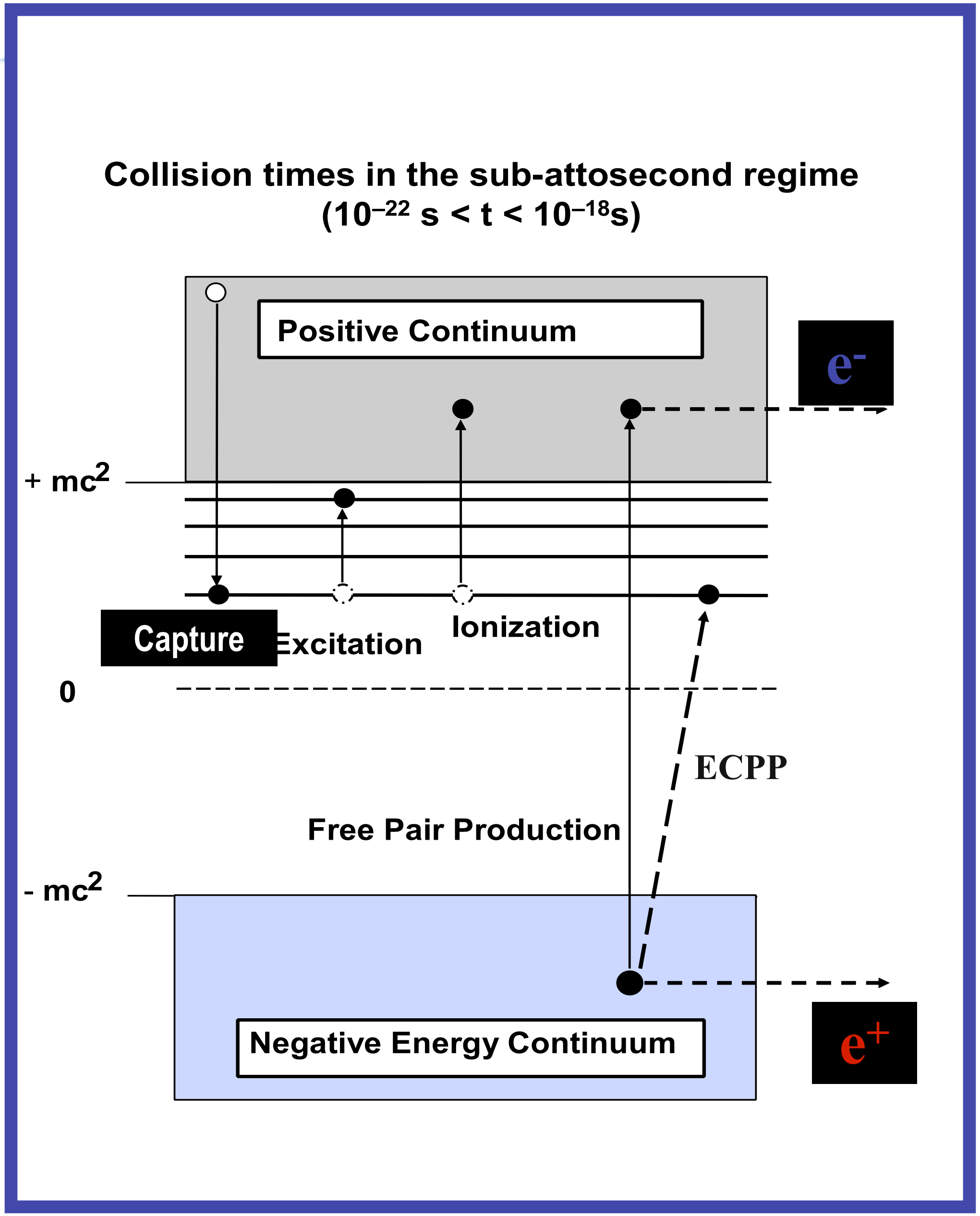

Electromagnetic Phenomena under Extreme & Unusual Conditions

High- γ

Collision times in the sub-attosecond regime
(10^{-22} s < t < 10^{-18}s)

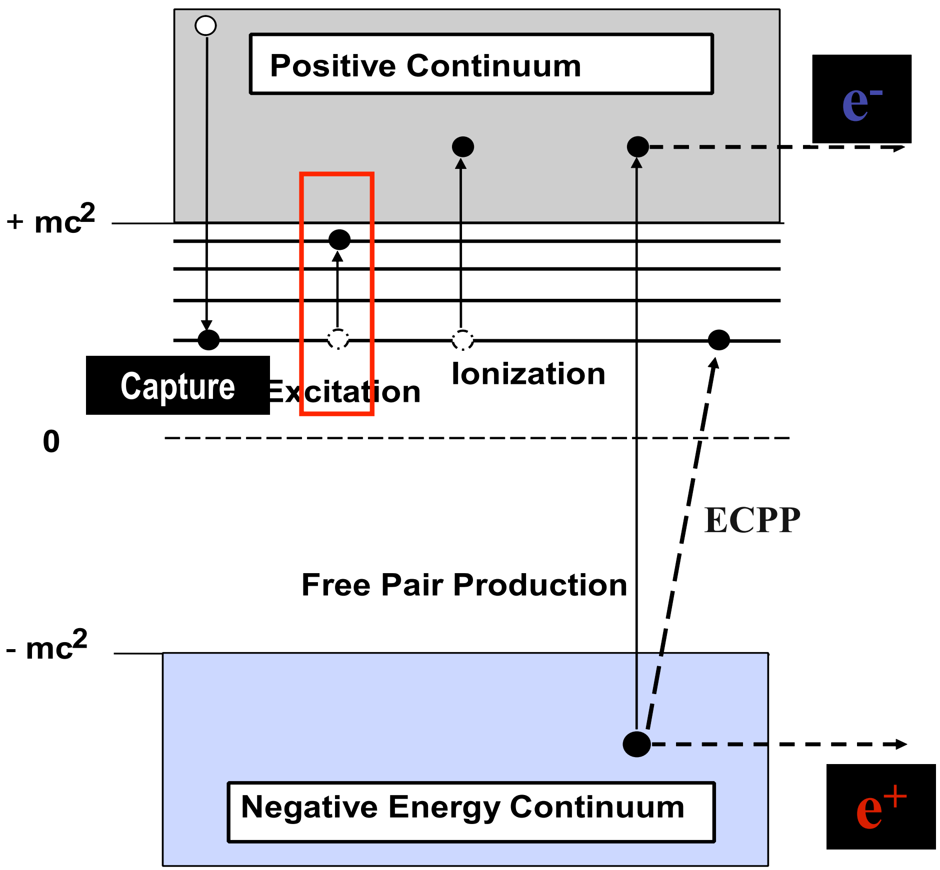

Supercritical fields

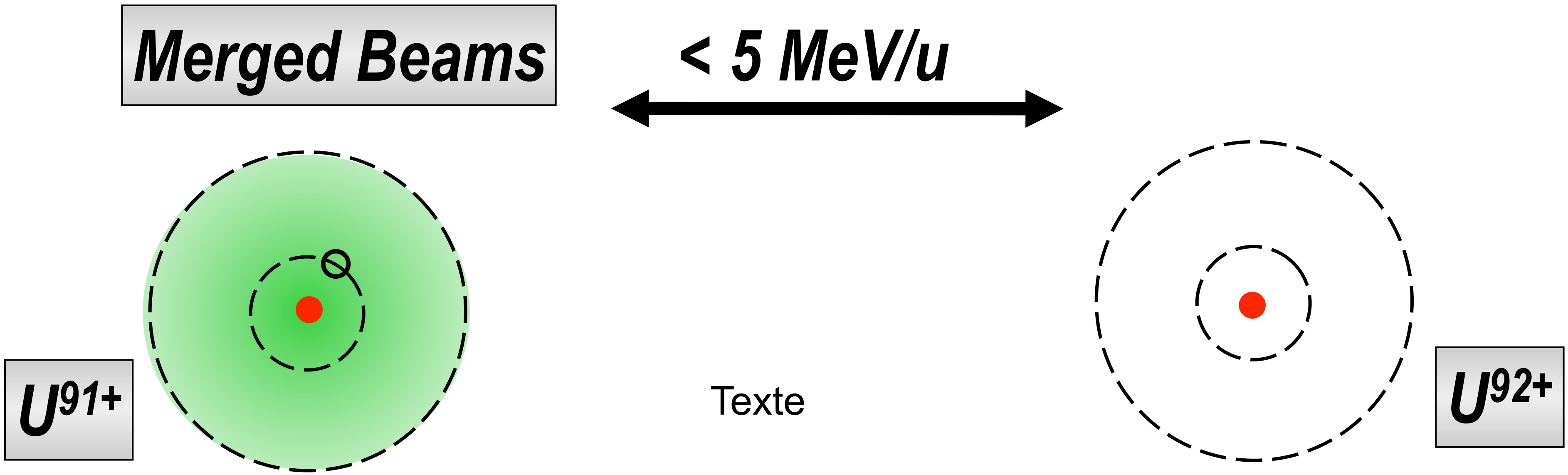

Supercritical fields

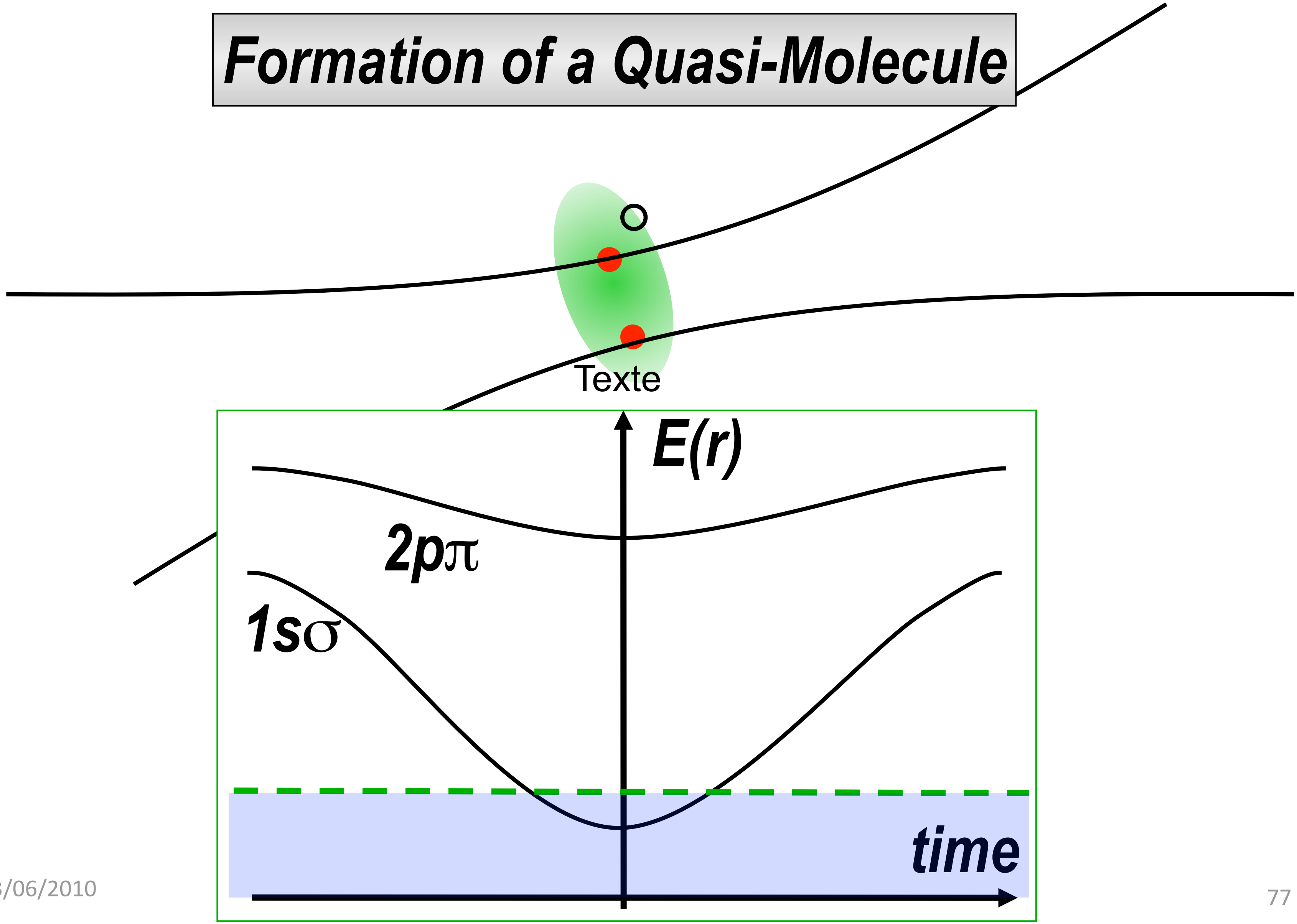

Supercritical fields

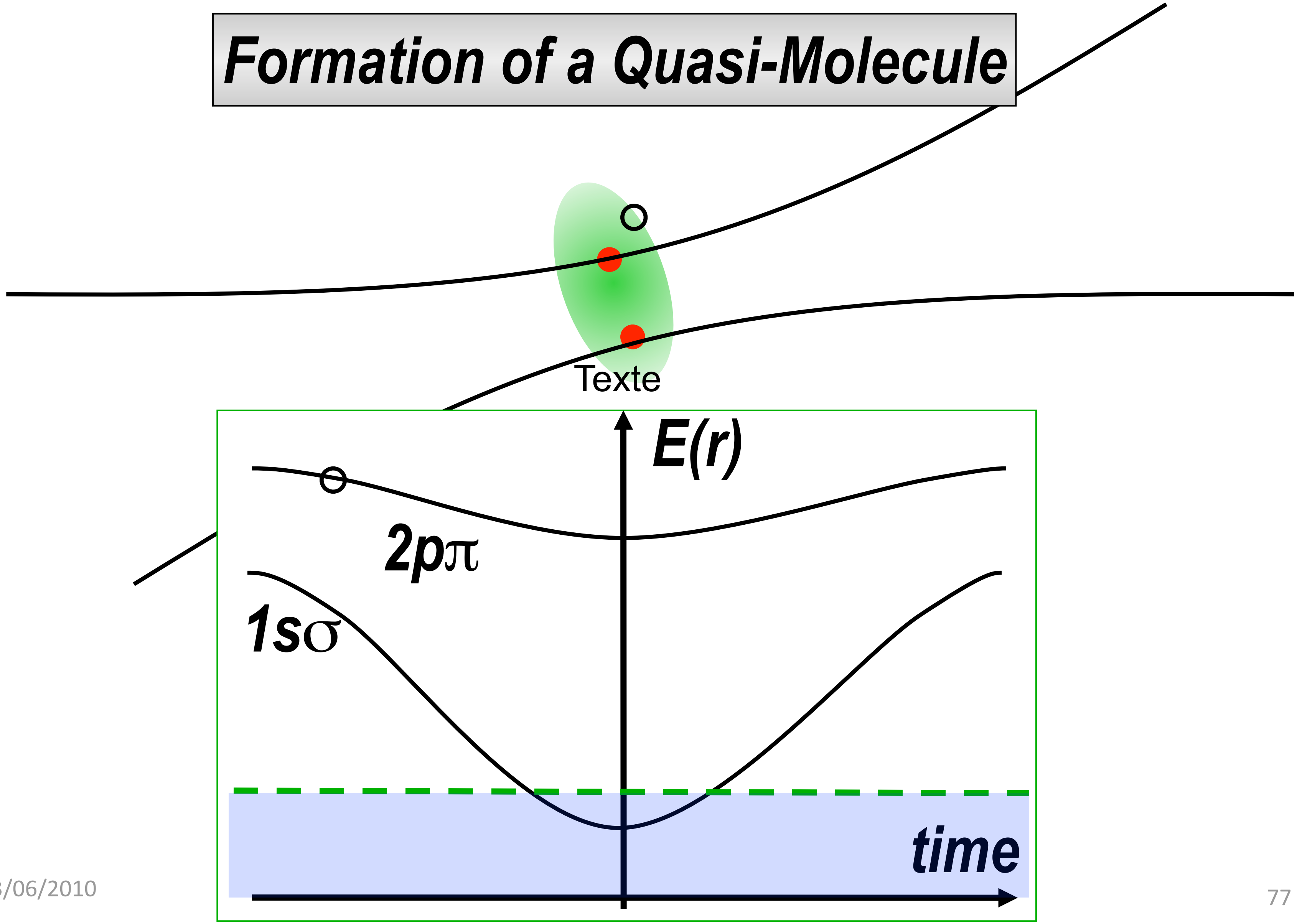

Supercritical fields

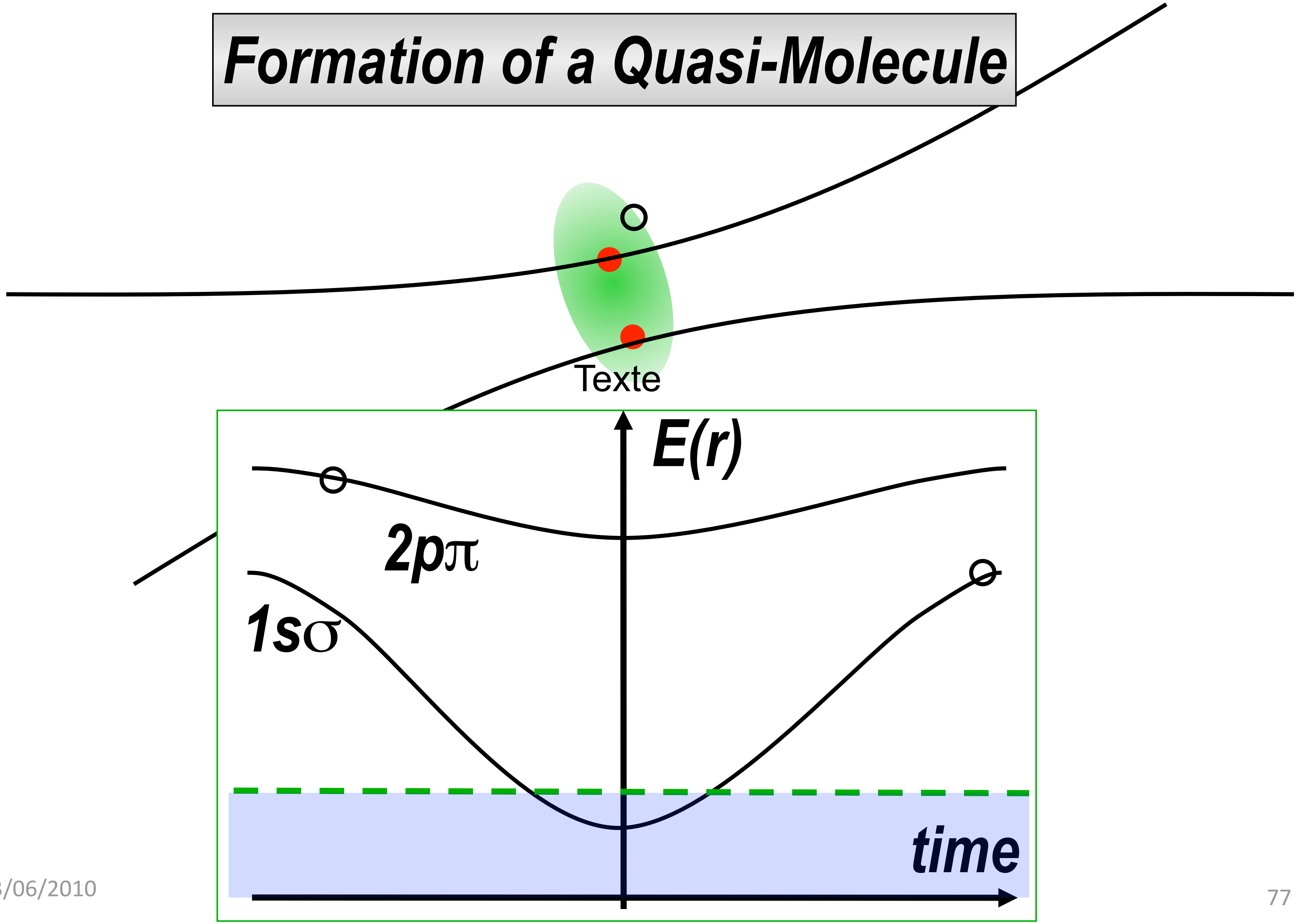

Supercritical fields

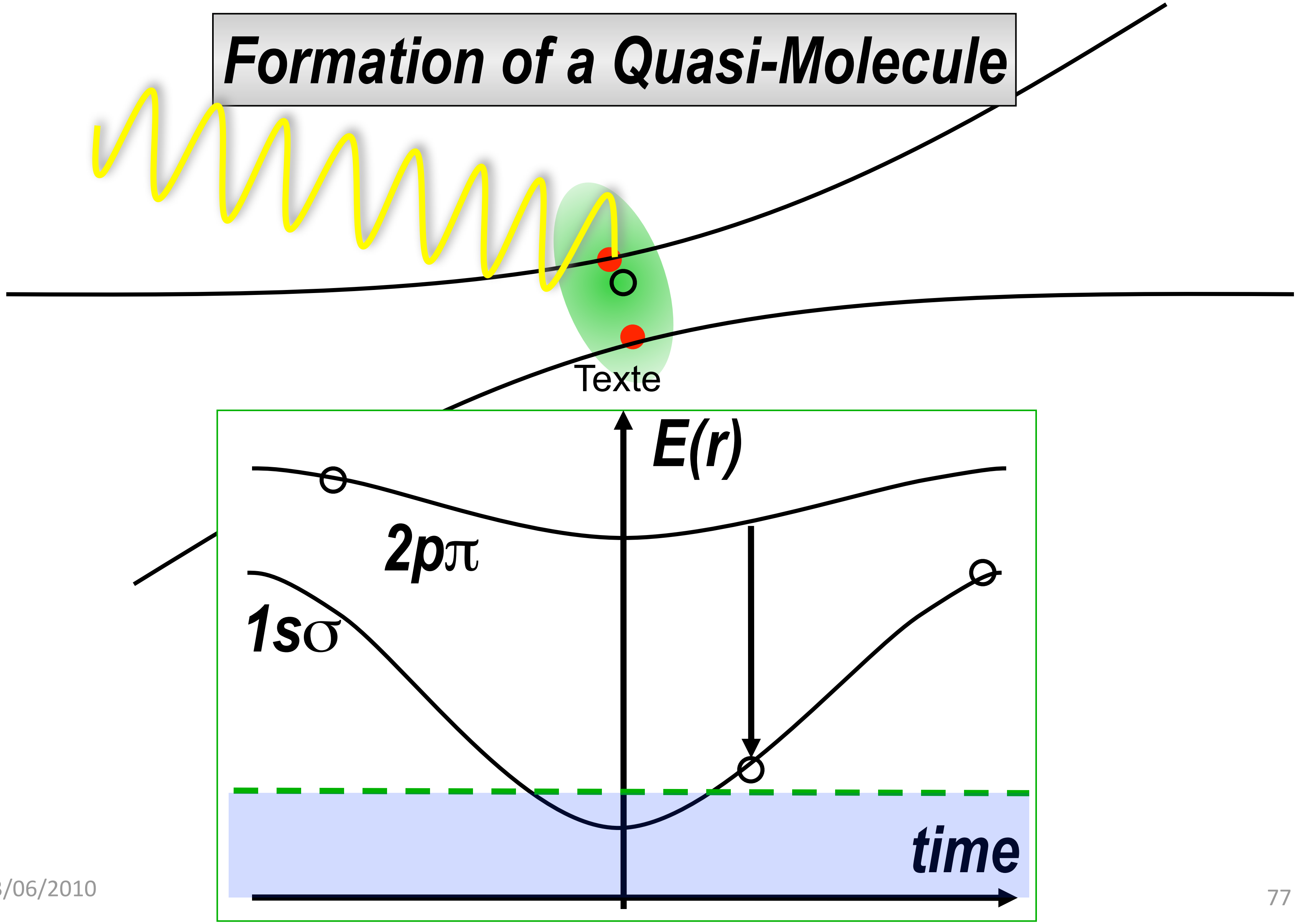

Supercritical fields

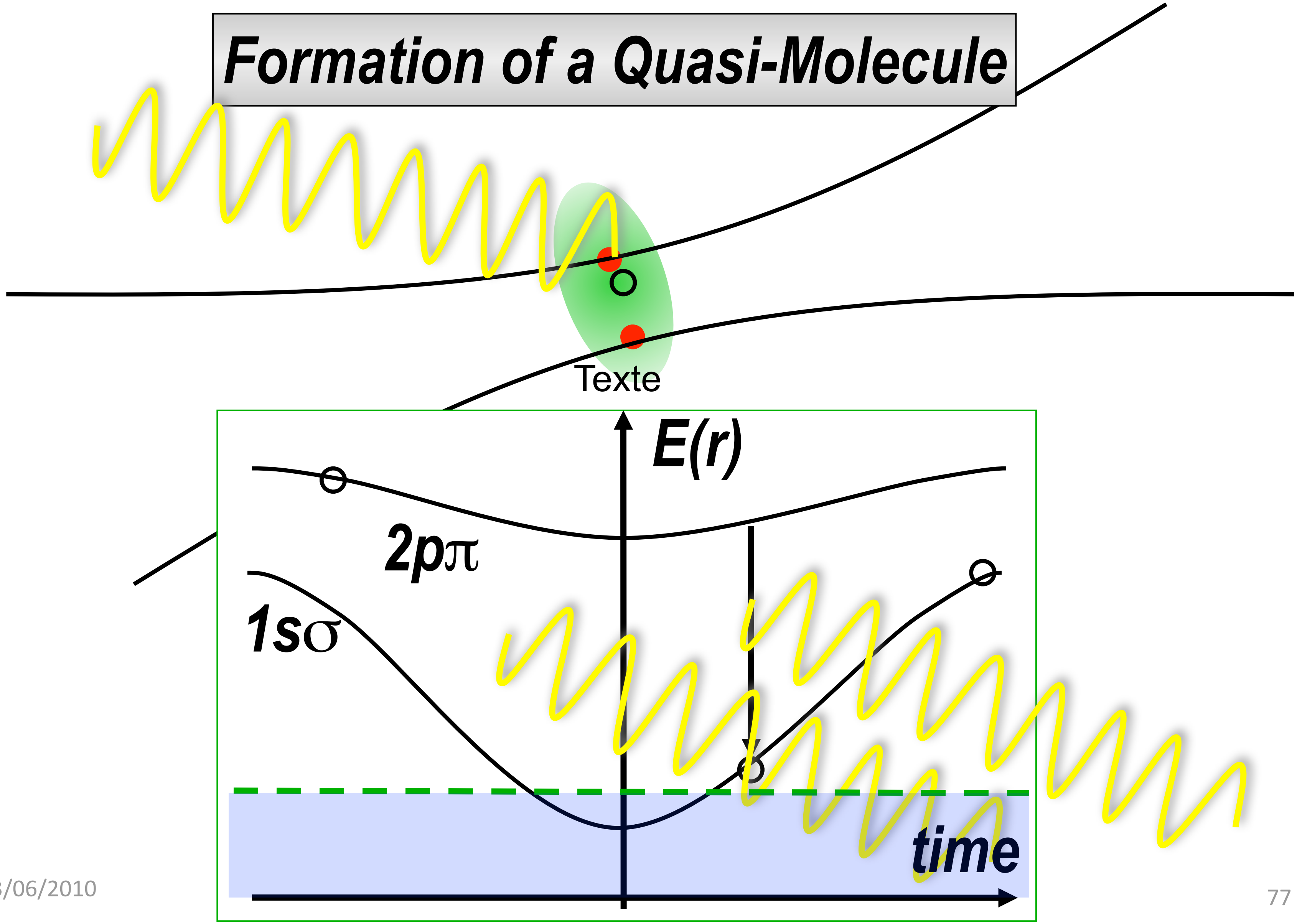

Supercritical fields

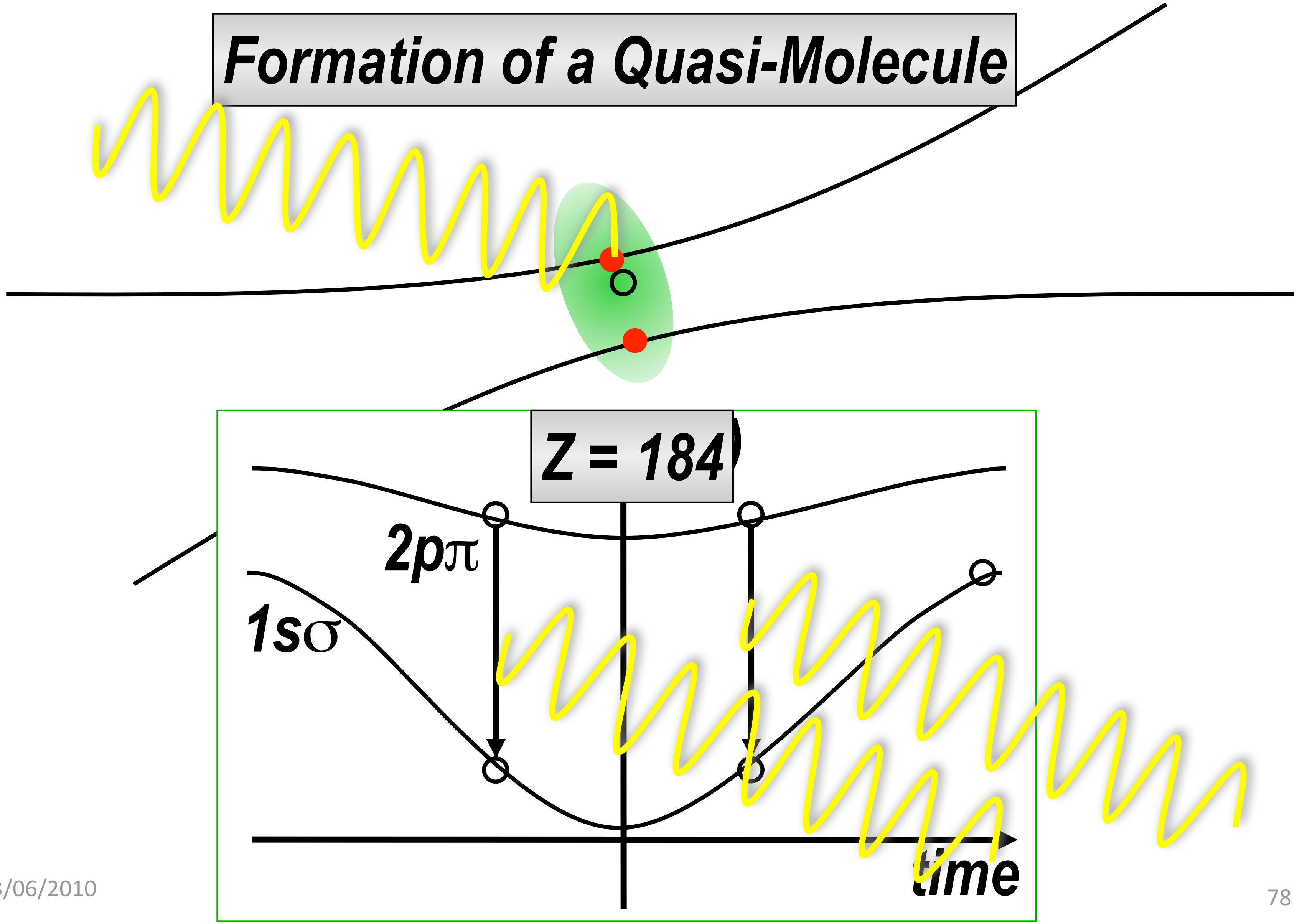

Supercritical fields

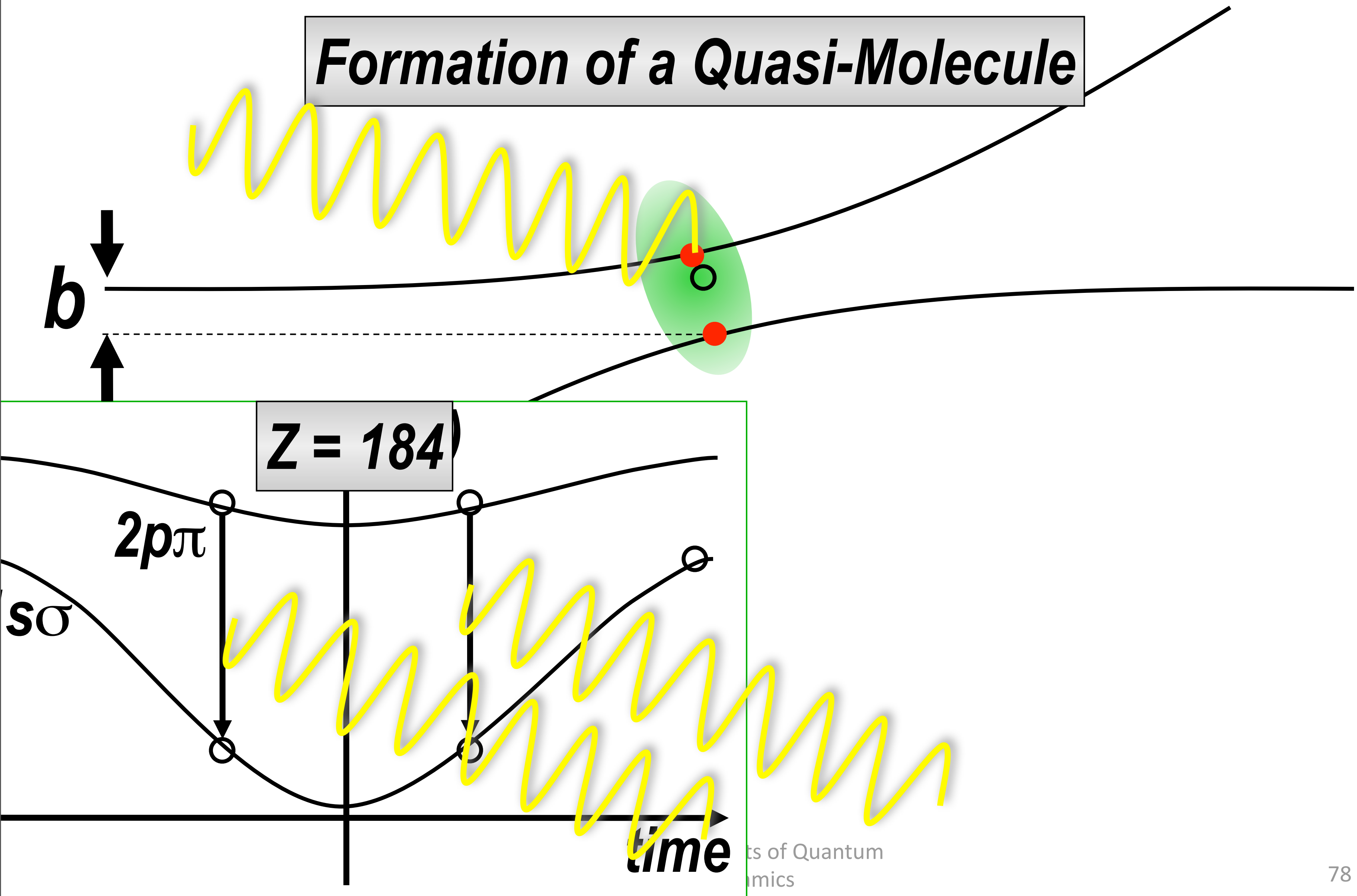

samedi 11 décembre 2010

Supercritical fields

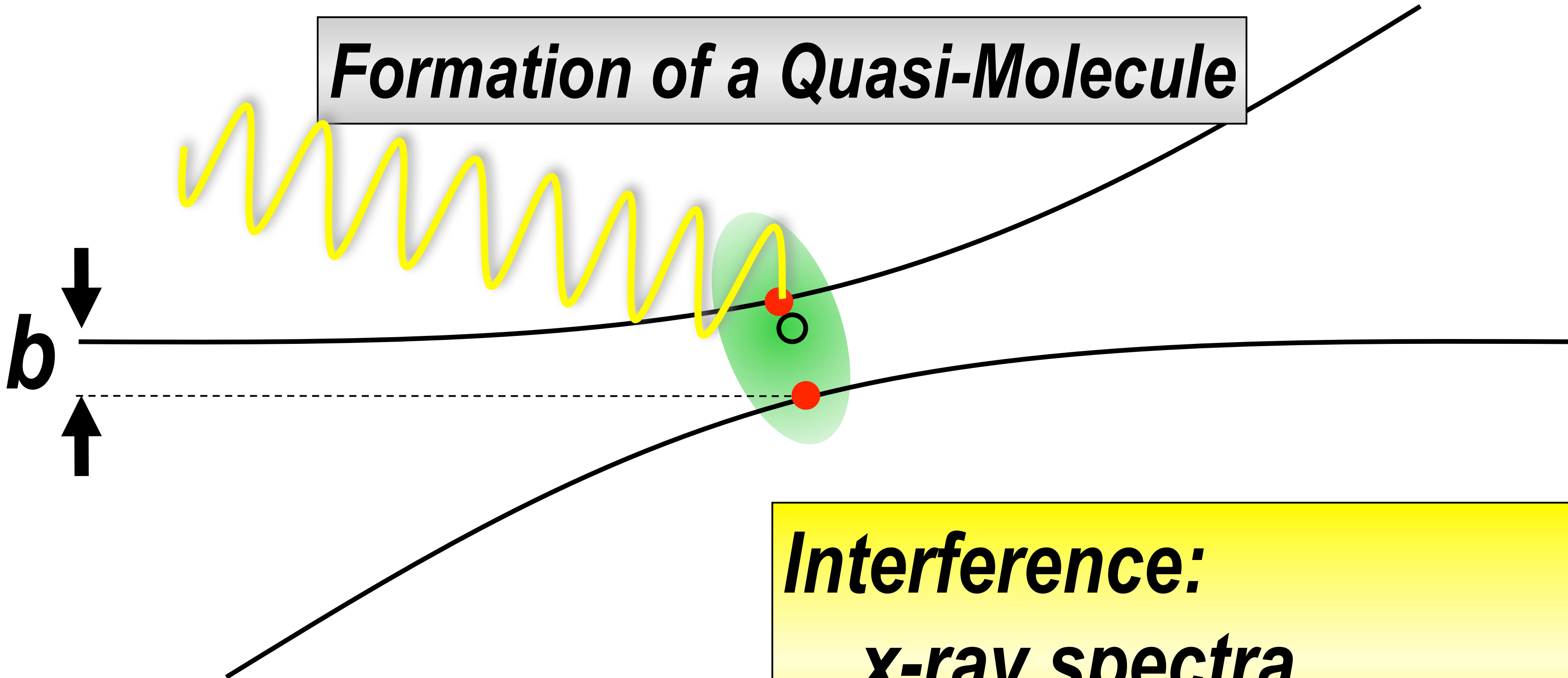

Interference:

x-ray spectra

fixed impact parameter

Supercritical fields

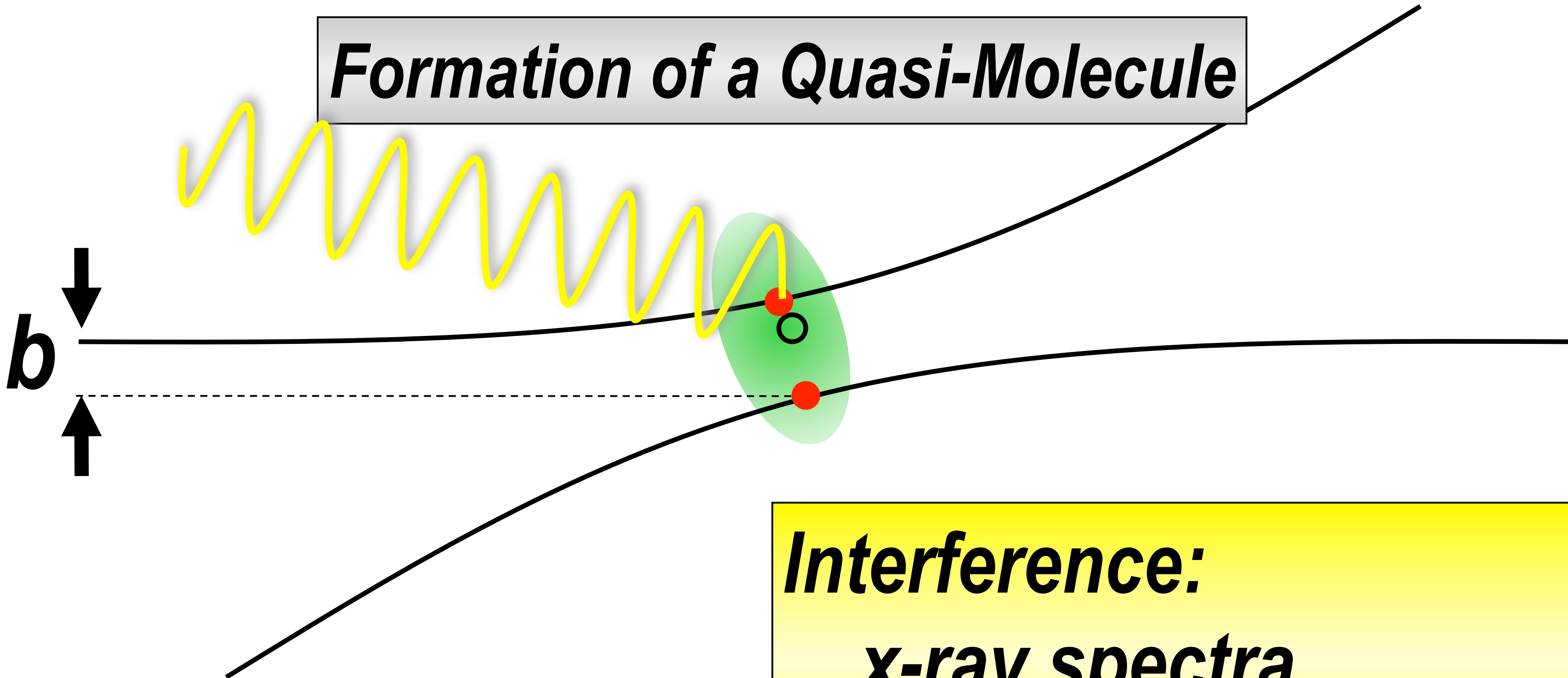

Interference:
- x-ray spectra
- fixed impact parameter

⇒ $E_{1s\sigma}(R)$

QED and other corrections in outer shells

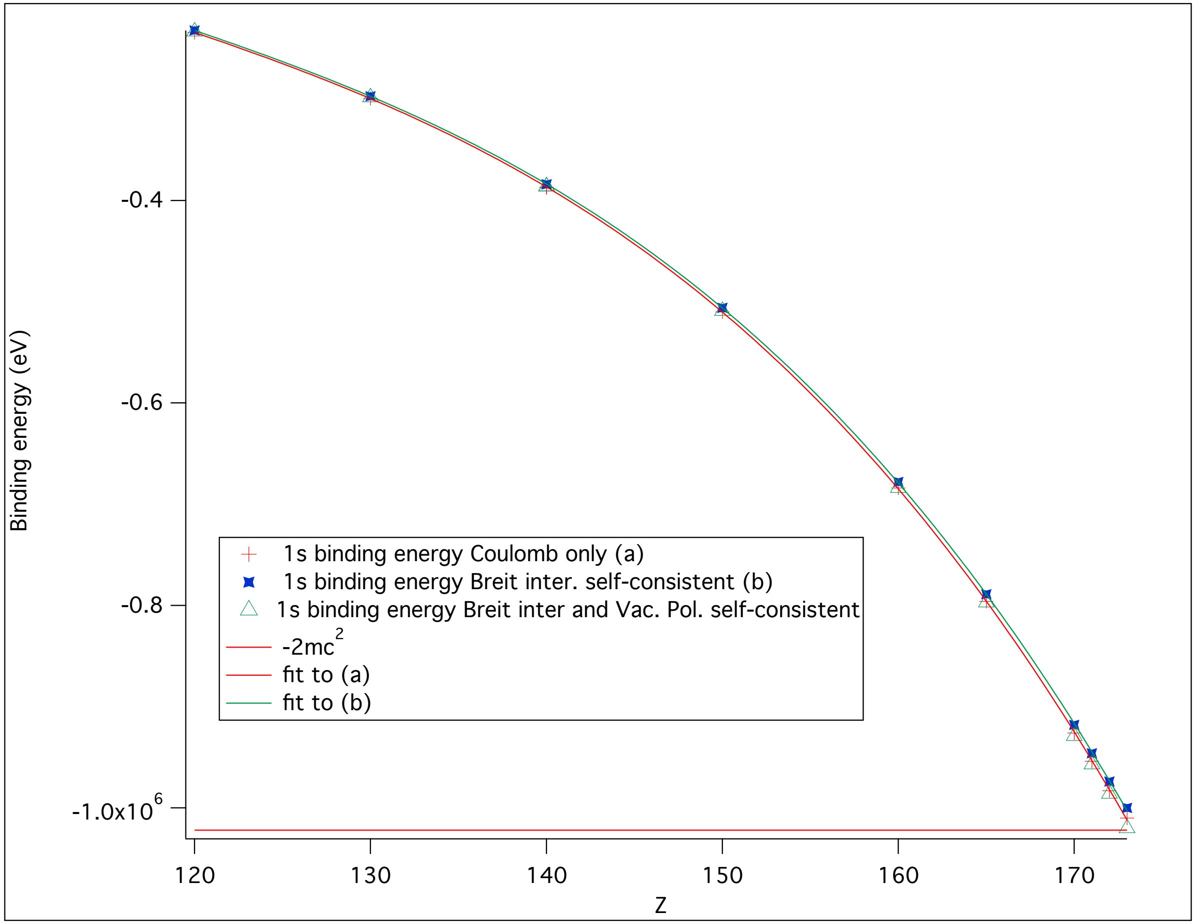

The presence of outer shell electrons does not change critical Z (173)

What would be a neutral atom when the 1s shell is in the continuum

What happens to QED

Quasi-molecular energy

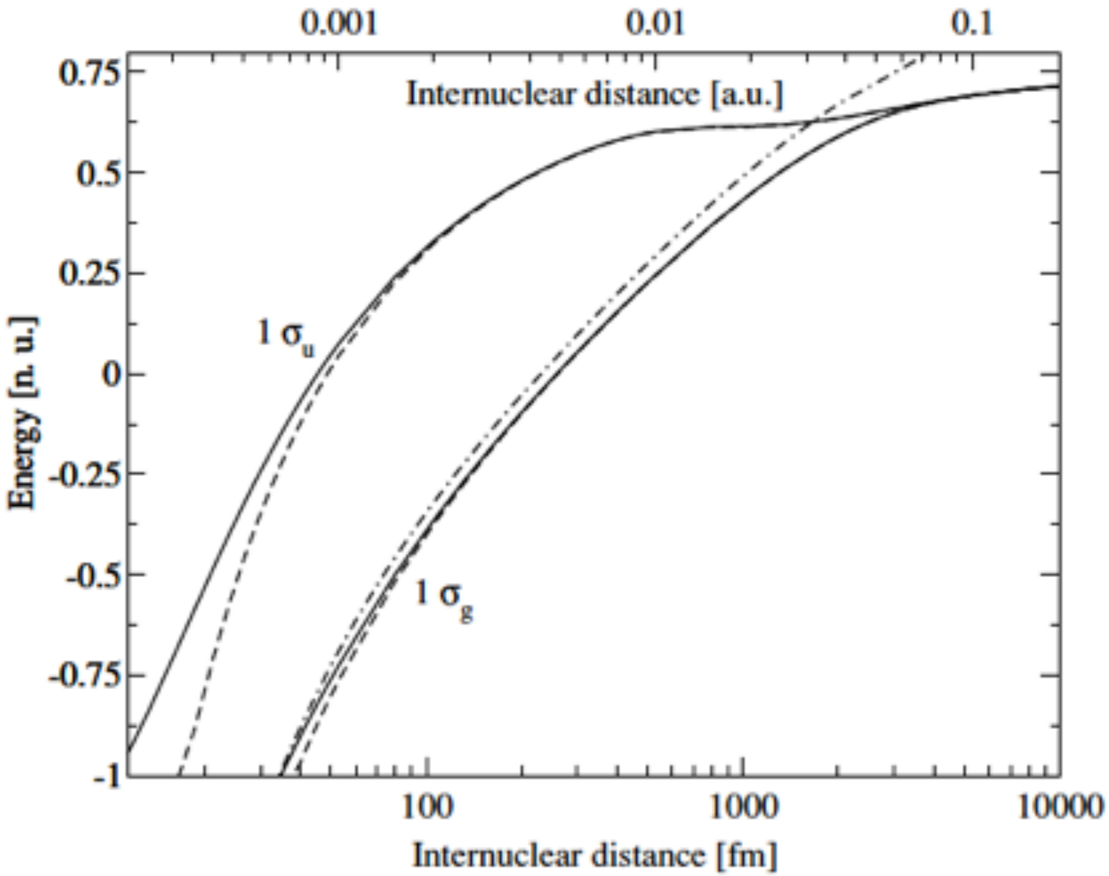

Figure 2. The energy of 1σ states in U_2^{183+} as a function of internuclear distance. The solid and dashed lines correspond to finite-size and point-like nuclei, respectively. The dash-dotted line represents the energy of the 1s state in spherically symmetrical monopole approximation, centred at the middle point of the inter-nuclear axis.

Atoms near critical Z

Z	171	172	173
	total binding energy		
[Rn] $5f^{14}6d^{10}7s^2 7p^6 8s^2 8p^6 7d^{10} 5g^{18} 6f^{14}$	$9s^2 9p$, $J = 1/2$	$9s^2 9p^2$, $J = 2$	$9s^2 9p^3$, $J = 3/2$
Coulomb	-6052798	-6229026	-6409504
Magnetic	24012	24820	25636
Retardation	-1369	-1413	-1459
Higher order ret.	-437	233	284
S.E.&F.N.	28719	29398	30087
Welt. Scr.	-1073	-1093	-1113
Uehling Vac. Pol.	-53303	-55764	-58259
Muon Vac. Pol.	-70	-74	-78
Uelhing corr to elec. Inter.	313	331	350
Wichmann and Kroll VP	4522	4767	5019
Kàllén and Sabry VP	-400	-420	-439
Two-loop SE	-516	-536	-557
SEVP terms	546	579	615
S[VP]E terms	141	150	160
Total	-6051712	-6228047	-6409259

Unsolved problems

- We do not know how to treat in a general and systematic way a 2 or more body problem (recoil in exotic atoms for example)
- Complex atoms (more than 3 electrons or one open shell) cannot be calculated
- Higher-order diagrams are beyond our grasp
- Even the relativistic treatment of few or many electron atoms is beyond what we know how to do (no relativistic hamiltonian...)

LKB

Conclusions and perspectives

- Hydrogen and exotic hydrogen will be again a very intense field of research
- New developments will involve both few-body atomic and nuclear physics (nuclear polarization in muonic D, He...) as well as QCD
- A new generation of experiments are leading to very accurate results at medium and high-Z
- More general techniques for the many-body case needed...
- New methods for the resummation of classes of diagrams to all-orders required